Corrosion Inhibitors in Concrete; Interim Report

PB2002-106407

FHWA-RD-02-002

MARCH 2002

U.S. Department of Transportation
Federal Highway Administration

Research, Development, and Technology
Turner-Fairbank Highway Research Center
6300 Georgetown Pike
McLean, VA 22101-2296

FOREWORD

This investigation focuses on the long-term effectiveness and stability of three commercial corrosion inhibitor admixtures (one nitrite-based and the other two organic) in slowing the initiation and progression of corrosion in steel-reinforced concrete structures for new construction and for repair applications. The investigation examined the ability of inhibitors to remain in place in concrete, and the effectiveness of the inhibitors after chloride contamination of the concrete. The work included tests in liquid solutions, laboratory concrete specimens, and yard and field tests. This interim report documents the progress achieved and preliminary results obtained during the first three years of work. Transport rates in concrete were evaluated for the nitrite-based inhibitor and found to be comparable to those of chloride ions. The nature and extent of binding of this inhibitor in concrete, as well as its effects on pore water chemistry, were also determined. In early testing the calcium nitrite inhibitor tended to show better corrosion mitigating performance than the organic inhibitors.

This report provides insight into the ability of admixed corrosion inhibitors to be effective in controlling corrosion of steel in concrete. It will be of interest to materials and bridge engineers, inspectors, construction contractors who are involved with reinforced concrete structures, and corrosion control specialists.

T. Paul Teng, P.E.
Director, Office of Infrastructure
Research and Development

NOTICE

This document is disseminated under the sponsorship of the United States Department of Transportation in the interest of information exchange. The United States Government or the State of Florida assumes no liability for its content or use thereof. This report does not constitute a standard, specification, or regulation.

The United States Government or the State of Florida does not endorse products or manufacturers. Trade and manufacturers' names appear in this report only because they are considered essential to the object of the document.

Technical Report Documentation Page

1. Report No.	2. Government Accession No.	3. Recipient's Catalog No.
FHWA-RD-02-002		

4. Title and Subtitle	5. Report Date
CORROSION INHIBITORS IN CONCRETE INTERIM REPORT	March 2002
	6. Performing Organization Code

7. Author(s)	8. Performing Organization Report No.
R.G. Powers*, A.A. Sagues**, W.D. Cerlanek*, C.A. Kasper*, Lianfang Li**, Hui Liang**, Noreen Poor**, Rajesh Baskaran**	

9. Performing Organization Name and Address		10. Work Unit No.
Florida Department of Transportation* 2006 NE Waldo Road Gainesville, Florida 32609	University of South Florida** 4202 Fowler Avenue Tampa, Florida 33620	11. Contract or Grant No. WPI No.

12. Sponsoring Agency Name and Address	13. Type of Report and Period Covered
Office of Infrastructure R&D Federal Highway Administration 6300 Georgetown Pike McLean, Virginia 22101-2296	Interim Report July 1996 to June 1999
	14. Sponsoring Agency Code

15. Supplementary Notes

Contracting Officer's Technical Representative (COTR): Y.P. Virmani, HRDI

Acknowledgments: Mario Paredes, Andrew Donn, Todd Hoyle, Tommy Poore, Tom Byron, Pete Vega, Ray Roucher, Ralph Marks, David Williams, Milan Duke, Robert Langley, Matt Duncan, Jeff Zenuch, Joyline Benham, Elizabeth Tuller, Duane Robertson.

16. Abstract

The overall objective of this work in progress is to assess the effectiveness of corrosion inhibitors for steel in concrete. Three commercially available inhibitors, DCI-S (calcium nitrite-based), and FerroGard 901 and Rheocrete 222+ (both based on organic compounds), were selected for detailed examination. To determine the amount of inhibitor remaining in concrete, an accurate method to analyze for calcium nitrite was developed, and analyses for the other two inhibitors are being explored. The ability of calcium nitrite to stay in place was examined by laboratory experiments of inhibitor diffusion in concrete and by examination of available concrete samples exposed for long times to the outdoors environment. Results indicated a nitrite ion diffusivity comparable to that of chloride ions in concrete. Tentative tests with FerroGard 901 suggest similar behavior. Examination of long-term outdoor specimens indicated that a high level of corrosion protection was achieved when the mass of nitrite ion per volume of concrete equaled or exceeded that of chloride ions. Tests with DCI-S also disclosed that typically only a fraction of the inhibitor resides in the pore water of the concrete, but in simulated pore water experiments that fraction was enough to provide substantial protection to chloride-induced corrosion. Although nitrite in the pore water slightly reduced pH, this potentially detrimental effect was amply counteracted by the overall beneficial action of the nitrite ion. During the early phase of tests in progress with laboratory concrete specimens DCI-S was the most effective of the three inhibitors in mitigating corrosion. Under those test conditions the organic inhibitors showed modest or little evidence of effective corrosion protection. In early testing none of the inhibitors evaluated substantially affected the penetration of chloride ions in concrete, or its strength and sulfate resistance. The presence of DCI-S did reduce the resistivity of the concretes tested by about 1/3.

17. Key Words	18. Distribution Statement
Concrete, corrosion, reinforcing steel, macrocell current, corrosion inhibitor, calcium nitrite, rebars, polarization, leaching	No restrictions. This document is available to the Public through the National Information Service, Springfield, VA 22161.

19. Security Classif. (of this report)	20. Security Classif. (of this page)	21. No. of Pages	22. Price
Unclassified	Unclassified	79	

Form DOT F 1700.7

SI* (MODERN METRIC) CONVERSION FACTORS

APPROXIMATE CONVERSIONS TO SI UNITS

Symbol	When You Know	Multiply By	To Find	Symbol
	LENGTH			
in	inches	25.4	millimeters	mm
ft	feet	0.305	meters	m
yd	yards	0.914	meters	m
mi	miles	1.61	kilometers	km
	AREA			
in^2	square inches	645.2	square millimeters	mm^2
ft^2	square feet	0.093	square meters	m^2
yd^2	square yards	0.836	square meters	m^2
ac	acres	0.405	hectares	ha
mi^2	square miles	2.59	square kilometers	km^2
	VOLUME			
fl oz	fluid ounces	29.57	milliliters	mL
gal	gallons	3.785	liters	L
ft^3	cubic feet	0.028	cubic meters	m^3
yd^3	cubic yards	0.765	cubic meters	m^3
NOTE: Volumes greater than 1000 l shall be shown in m^3.				
	MASS			
oz	ounces	28.35	grams	g
lb	pounds	0.454	kilograms	kg
T	short tons (2000 lb)	0.907	megagrams (or "metric ton")	Mg (or "t")
	TEMPERATURE (exact)			
°F	Fahrenheit temperature	5(F-32)/9 or (F-32)/1.8	Celcius temperature	°C
	ILLUMINATION			
fc	foot-candles	10.76	lux	lx
fl	foot-Lamberts	3.426	candela/m^2	cd/m^2
	FORCE and PRESSURE or STRESS			
lbf	poundforce	4.45	newtons	N
lbf/in^2	poundforce per square inch	6.89	kilopascals	kPa

APPROXIMATE CONVERSIONS FROM SI UNITS

Symbol	When You Know	Multiply By	To Find	Symbol
	LENGTH			
mm	millimeters	0.039	inches	in
m	meters	3.28	feet	ft
m	meters	1.09	yards	yd
km	kilometers	0.621	miles	mi
	AREA			
mm^2	square millimeters	0.0016	square inches	in^2
m^2	square meters	10.764	square feet	ft^2
m^2	square meters	1.195	square yards	yd^2
ha	hectares	2.47	acres	ac
km^2	square kilometers	0.386	square miles	mi^2
	VOLUME			
mL	milliliters	0.034	fluid ounces	fl oz
L	liters	0.264	gallons	gal
m^3	cubic meters	35.71	cubic feet	ft^3
m^3	cubic meters	1.307	cubic yards	yd^3
	MASS			
g	grams	0.035	ounces	oz
kg	kilograms	2.202	pounds	lb
Mg (or "t")	megagrams (or "metric ton")	1.103	short tons (2000 lb)	T
	TEMPERATURE (exact)			
°C	Celcius temperature	1.8C + 32	Fahrenheit temperature	°F
	ILLUMINATION			
lx	lux	0.0929	foot-candles	fc
cd/m^2	candela/m^2	0.2919	foot-Lamberts	fl
	FORCE and PRESSURE or STRESS			
N	newtons	0.225	poundforce	lbf
kPa	kilopascals	0.145	poundforce per square inch	lbf/in^2

* SI is the symbol for the International System of Units. Appropriate rounding should be made to comply with Section 4 of ASTM E380.

(Revised September 1993)

EXECUTIVE SUMMARY

This interim report summarizes the findings of the first three years of an ongoing seven-year investigation conducted jointly by the Florida Department of Transportation (FDOT) and the University of South Florida. The overall objective of this work is to assess the effectiveness of corrosion inhibitors for steel in concrete, with emphasis on new construction applications. Both the ability of the inhibitor to remain in place in the concrete for very long times, and the ability to control corrosion even far into the future are evaluated. Three commercially available inhibitors, DCI-S, FerroGard 901, and Rheocrete 222+, have been selected for detailed examination.

The ability of the inhibitor to stay in place was examined by laboratory experiments of inhibitor diffusion and by examination of available concrete samples exposed for long periods of time to the environment. To determine the amount of inhibitor remaining, it was first necessary to develop reliable inhibitor analysis techniques. The work to date has developed an accurate method to analyze for calcium nitrite-containing DCI-S. Tentative analytical procedures have been developed for FerroGard 901.

Experiments with DCI-S have indicated a diffusivity comparable to that of chloride ions in concrete. At the dosages commonly used for this inhibitor, the prognosis is good for remaining in adequate amounts in sound, high-quality concrete for extended periods of time. Examination of test slabs exposed to 17 years weathering supported that conclusion. The slab tests also indicated that a high level of corrosion protection was achieved when the mass of nitrite ion per volume of concrete equaled or exceeded that of chloride ions. Tests with DCI-S have also disclosed that typically only a fraction of the inhibitor resides in the pore water of the concrete. Corrosion tests in simulated pore water indicated that under typical dosage conditions that fraction provides significant protection to steel even when the chloride content in the pore water greatly exceeded the amount that initiates corrosion in concrete without inhibitor. Additional experiments revealed that nitrite in the pore water slightly reduced pH, a potentially detrimental effect. However, the tests also indicated that the effect of pH reduction was amply counteracted by the overall beneficial action of the nitrite ion. Tentative tests with FerroGard 901 suggest that its diffusivity in concrete is also comparable to that of chloride ions.

In open-circuit immersion tests in calcium hydroxide solutions with added chloride ions, DCI-S was found to have the most significant corrosion inhibition effect of the three products examined, while FerroGard 901 and Rheocrete 222+ exhibited little or no inhibiting effect. Tests were also conducted with reinforced concrete specimens partially immersed in salt water. The tests used a variety of concrete mixes, including those using ordinary Portland cement and cement blended with pozzolanic additions (fly ash, microsilica). Although some of the tests are still ongoing, preliminary results indicate that DCI-S was the most effective of the three inhibitors in mitigating corrosion. Tests with FerroGard 901 showed only modest indications of corrosion protection, while under the test conditions used, the Rheocrete 222+ specimens showed little evidence of effective corrosion protection. Longer tests with less acceleration are in progress, both in the laboratory and with test piles in an FDOT coastal test facility, to assess the long-term performance of the inhibitors.

Initial tests have indicated that the protection obtained by DCI-S becomes significantly less when used at half the recommended dosage. No appreciable changes from the full-dosage performance

were observed for the other two inhibitors when the dosage was reduced by 1/2. None of the inhibitors tested appears to strongly affect the extent to which chloride ions penetrate in concrete, or to significantly affect the strength or sulfate resistance of the concrete. However, the presence of DCI-S did reduce the resistivity of the concrete tested by about 1/3. This effect could somewhat increase the severity of corrosion macrocells once chloride contamination becomes strong enough to overcome the protective action of the inhibitor.

This investigation is in progress and the above findings are subject to update as additional results develop.

Table of Contents

INTRODUCTION AND OBJECTIVES **1**

OBJECTIVE 1 - EVALUATE ABILITY OF INHIBITOR TO STAY IN PLACE **3**

1.1 Develop Methodology for Analysis of Inhibitors in Concrete 3

1.1.1 Calcium Nitrite-based Inhibitor (DCI-S) 3

1.1.1.1 Extraction from hardened concrete, powdered 3

1.1.1.2 Determination of nitrite in pore water of hardened concrete 4

1.1.2 Organic Corrosion Inhibitor F (FerroGard 901) 5

1.1.3 Organic Corrosion Inhibitor R (Rheocrete 222+) 6

1.2 Determine the Long-Term Stability of Corrosion Inhibitors in Concrete 7

1.2.1 Calcium Nitrite-based Inhibitor (DCI-S) 7

1.2.1.1 Laboratory investigation of nitrite transport in concrete 7

1.2.1.2 Inhibitor presence in existing long-term specimens 16

1.2.2 Organic Corrosion Inhibitor F (FerroGard 901) 17

1.2.2.1 Inhibitor transport in concrete 17

1.2.3 Organic Corrosion Inhibitor R (Rheocrete 222+) 17

OBJECTIVE 2 - ESTIMATE LONG-TERM EFFECTIVENESS - MECHANISTIC ISSUES **18**

2.1 Examine Inhibitor Degradation Mechanisms 18

2.1.1 Calcium Nitrite-based Inhibitor (DCI-S) 18

2.1.1.1 Inhibitor decomposition in concrete 18

2.1.2 Organic Corrosion Inhibitors F and R (FerroGard 901, Rheocrete 222+) 19

2.2 Binding Effects 19

2.2.1 Definitions and Techniques 19

2.2.1.1 Pore Water Expression (PWE) 19

2.2.1.2 In-situ Leaching Method (ISL) 20

2.2.2 Nitrite Binding in the Absence of Chloride Ions 22

2.2.3 Nitrite Binding in the Presence of Chloride Ions 24

2.2.4 Organic Corrosion Inhibitors F and R (FerroGard 901, Rheocrete 222+) 24

2.3 Other Inhibitor Mechanism Issues - Dosage Needs 24

2.3.1 Calcium Nitrite-based Inhibitor (DCI-S) 24

2.3.1.1 Pitting and repassivation tests 24

2.3.2 Comparison of Effectiveness of the Three Inhibitor Types 27

2.3.2.1 Tests in calcium hydroxide solution 27

OBJECTIVE 3 - DETERMINE POSSIBLE NEGATIVE SIDE EFFECTS - MECHANISTIC ISSUES **30**

3.1 Effect on pH of Pore Solution 30

3.1.1 Calcium Nitrite-based Inhibitor (DCI-S) 30

3.1.2 Organic Corrosion Inhibitors 32

OBJECTIVE 4 - ESTIMATE LONG-TERM EFFECTIVENESS - PERFORMANCE TESTS **32**

4.1 Perform Long-Term Laboratory Tests, Outdoor Sheltered Tests, and Field Tests 32

4.1.1 Approach and Experimental Procedures 32

4.1.2 Test Progression, Laboratory and Sheltered Outdoor Tests 37

4.1.3 Test Progression, Field Test Specimens 37

4.2 Evaluation of Inhibitor Performance 38

4.2.1 Scope of Early Observations 38

4.2.2 Calcium Nitrite-based Inhibitor (DCI-S) 42
4.2.3 Organic Corrosion Inhibitor F (FerroGard 901) 45
4.2.4 Organic Corrosion Inhibitor R (Rheocrete 222+) 45
4.2.5 Additional Comments 45
OBJECTIVE 5 - DETERMINE POSSIBLE NEGATIVE SIDE EFFECTS - PERFORMANCE TESTS ... 46
5.1 Estimated Time to Failure 46
5.2 Determine Effect of Insufficient Dosage on Corrosion Progression 47
5.2.1 Calcium Nitrite-based Inhibitor (DCI-S) 48
5.2.2 Organic Corrosion Inhibitor F (FerroGard 901) 49
5.2.3 Organic Corrosion Inhibitor R (Rheocrete 222+) 49
5.3 Effect of Inhibitor on Chloride Transport 49
5.4 Examine Possible Adverse Effects on Concrete Physical Properties 51
5.4.1 Transport Effects - Rapid Chloride Permeability (RCP) 51
5.4.2 Transport Effects - Wet Surface Resistivity (WSR) 53
5.4.3 Transport Effects - Impressed Current 53
5.4.4 Compressive Strength 54
5.4.5 Sulfate Exposure (Length Change and Mass Change) 56
OBJECTIVE 6 - ESTABLISH SUITABILITY FOR REHABILITATION APPLICATIONS 60
6.1 Evaluate Alternative Repair Strategies 60
6.2 Test Field Repairs and Long-Term Assessment 60
CONCLUSIONS 61
REFERENCES 63
APPENDIX 1 - NITRITE RECOVERY CALCULATION 65
APPENDIX 2 - APPARENT DIFFUSION COEFFICIENT CALCULATIONS 67
APPENDIX 3 - PORE WATER NITRITE CONTENT EXAMPLE CALCULATION 68

LIST OF FIGURES

Figure — Page

1. Calibration curve for FerroGard 901 by UV absorption at 224 nm 6

2. Placement of concrete samples in leaching containers 9

3. CFL as a function of the square root of leaching time ($t^{1/2}$) for concrete specimens of DCI-C1-1.0 and DCI-C2-1.0 in Limewater 11

4. CFL as a function of the square root of leaching time ($t^{1/2}$) for specimens of DCI-P1-1.0 in Limewater, DW, and synthetic seawater (sea) at room temperature 12

5. CFL as a function of the square root of leaching time ($t^{1/2}$) for NR concrete specimens in Limewater, DW, and synthetic seawater (sea) at RT and at ~35° C (HT) 12

6. Schematic of PWE arrangement 20

7. Schematic of ISL arrangement 22

8. Relationship between total admixed nitrite content in concrete (w/c = 0.45, cement content = 500 kg/m^3) and pore solution free nitrite concentration as determined with PWE method. Results from duplicate specimens (for total nitrite 1% = 5 kg/m^3, for free nitrite 4600 ppm = 0.1 M) 23

9. Nitrite binding isotherm in mortar (w/c = 0.45, cement content = 700 kg/m^3) expressed in mass per unit volume of mortar assuming $\varepsilon = 0.1$, as determined by the PWE method 23

10. Effect of chloride content on free nitrite in pore solution from mortar (cement content = 700 kg/m^3) containing 1.46% by weight of cement (10.22 kg/m^3 of mortar) total admixed nitrite from DCI-S (1% total chloride = 7 kg/m^3, 4600 ppm free nitrite in pore water = 0.1 M) 24

11. Effect of nitrite content (from DCI-S) on pitting (Ep) and repassivation (Er) potentials of rebar steel (sandblasted, 60 cm^2 nominal surface area) in simulated pore solution with 1.5 M NaCl addition as determined by cyclic polarization technique with an anodic polarization scan rate = 0.167 mV/s (for nitrite concentration, 4600 ppm = 0.1 M) 25

12. Effect of nitrite content (from DCI-S) on pitting (Ep) and repassivation (Er) potentials of rebar steel (sandblasted, 60 cm^2) in simulated pore solution with 0.8 M NaCl addition as determined by cyclic polarization technique with an anodic polarization scan rate = 0.167 mV/s (for nitrite concentration, 4600 ppm = 0.1 M) 26

13. Effect of nitrite content (from $NaNO_2$) on pitting (Ep) and repassivation (Er) potentials of rebar steel (sandblasted, 60 cm^2) in simulated pore solution with 0.8 M NaCl addition as determined by cyclic polarization technique with an anodic polarization scan rate = 0.167mV/s (for nitrite concentration, 4600 ppm = 0.1 M) 26

Figure Page

14. Effect of nitrite addition (from DCI-S or $NaNO_2$) on pH of simulated concrete pore solution (the simulated pore solution without chloride and nitrite was ~13.6) 27

15. Evolution of Eoc of sandblasted rebar in $Ca(OH)_2$ solution with DCI-S (2.6% v/v, equivalent to 7000 ppm or 0.15 M NO_2^-). Chloride was increased stepwise by adding NaCl into the test solution. D1-D5 indicate replicate specimens 28

16. Evolution of Eoc of sandblasted rebar in $Ca(OH)_2$ solution with FerroGard 901 (7.4% v/v). F1-F5 indicate replicate specimens 29

17. Evolution of Eoc of sandblasted rebar in $Ca(OH)_2$ solution with Rheocrete 222+ (2.5% v/v). R1-R5 indicate replicate specimens 29

18. Nominal corrosion rates from EIS as a function of added chloride content 30

19. Evolution of pH in concrete holes of duplicate specimens using the ISL method (calibrated to 21° C). CCTR: Concrete specimens without NO_2^-, CDCI: with NO_2^-. Mix design listed in Table 11. 31

20. Effect of nitrite dosage (from DCI-S) on the pore solution pH expressed from concrete (w/c = 0.45, cement content = 500 kg/m^3) (1% total nitrite = 5 kg/m^3 of concrete; 4600 ppm free nitrite in pore water = 0.1 M) 31

21. Standard laboratory test method (ASTM G-109) 34

22. Sheltered outdoor specimens 34

23. Field columns 34

24. Location of chloride test specimens from a three-bar column 40

25. C1 group half-cell potentials to a SCE over time for the three-bar column specimens 40

26. C2 group half-cell potentials to a SCE over time for the three-bar column specimens 41

27. P3 group half-cell potentials to a SCE over time for the three-bar column specimens 41

28(a). C1 group average current values over time for the three-bar column specimens 42

28(b). C1 group polarization values over time for a selected three-bar column specimen from each group 42

29(a). C2 group average current values over time for the three-bar column specimens 43

29(b). C2 group polarization values over time for a selected three-bar column specimen from each group 43

Figure Page

30(a). P3 group average current values over time for the three-bar column specimens 44

30(b). P3 group polarization values over time for a selected three-bar column specimen from each group 44

31. Comparison of the Group C1 potential histories of the full-dose DCI-S specimens, the half-dose DCI-S specimens, and the control specimens 47

32. Comparison of the Group C1 potential histories of the full-dose FerroGard 901 specimens, the half-dose FerroGard 901 specimens, and the control specimens 48

33. Comparison of the Group C1 potential histories of the full-dose Rheocrete 222+ specimens, the half-dose Rheocrete 222+ specimens, and the control specimens 48

34. Core locations for chloride testing on blank specimens 50

35. Surface resistivity versus RCP using concrete cylinders from all mix groups at 28 and 360 days 53

36. Comparison of compressive strengths between mix groups measured at 28 and 360 days ... 54

37(a). Length change due to sulfate exposure over time for the C1 group 56

37(b). Mass change due to sulfate exposure over time for the C1 group 56

38(a). Length change due to sulfate exposure over time for the P1 group 57

38(b). Mass change due to sulfate exposure over time for the P1 group 57

39(a). Length change due to sulfate exposure over time for the P2 group 58

39(b). Mass change due to sulfate exposure over time for the P2 group 58

40(a). Length change due to sulfate exposure over time for the G1 group 59

40(b). Mass change due to sulfate exposure over time for the G1 group 59

41. Sheltered outdoor specimens 60

LIST OF TABLES

Table		Page
1.	Mix Design and Concrete Properties of Cylinders C_1 and C_0	4
2.	Nitrite Recovery from Hardened Concrete Cylinder C_1	5
3.	Mix Design and Concrete Properties Used in the Leaching Experiments	8
4.	Specimen Specifications and Testing Conditions Used in the ANSI/ANS Experiments	8
5.	k, D_1, and D_2 Obtained for Specimens of DCI-C1-1.0 and DCI-C2-1.0 Leaching in Limewater at 22° C	13
6.	k and D obtained for slabs of DCI-C1-0.5 Leaching in Limewater	13
7.	Slopes and Apparent Diffusion Coefficients Obtained for DCI-P1-1.0 at 22° C	13
8.	Slopes and Apparent Diffusion Coefficients Obtained for Specimens of NR Concrete	14
9.	Mix Proportions of Concrete Specimens for PWE Tests	21
10.	Nitrite Ion Dosage in Concrete Specimens	21
11.	Concrete Mix Design for ISL Tests	21
12.	Concrete Mix Proportions	33
13.	Concrete Mix Matrix	35
14.	Three-Bar Column Autopsy Description (Intentionally Cracked Specimens are not Included)	39
15.	Average Days to Failure for Three-bar Columns	46
16.	Saltwater Exposure Time and Chloride Concentrations for Three-bar Columns	49
17.	Saltwater Exposure Time and Chloride Concentrations for Intentionally Cracked Three-Bar Columns	50
18.	Saltwater Exposure Time and Chloride Concentrations for Blank Lab Columns	51
19.	Average Chloride Content Ratios of All Specific Inhibitor Mixes versus the Corresponding Control Mixes for Blank Lab Columns	51
20.	Impressed Current, RCP and Surface Resistivity at 28 and 360 Days	52

Table | Page

21. 360 Day RCP and Surface Resistivity Ratio Averages of All Specific Inhibitor Mixes versus Corresponding Control Mixes 54

22. Compressive Strength and Sulfate Exposure Properties of All Mixes 55

INTRODUCTION AND OBJECTIVES

This interim report summarizes the findings of the first three years of an ongoing seven-year investigation conducted jointly by the Florida Department of Transportation (FDOT) and the University of South Florida. The overall objective of this work is to assess the effectiveness of corrosion inhibitors for steel in concrete, with emphasis on new construction applications but also for selected rehabilitation applications.

The effectiveness of a steel corrosion inhibitor in concrete depends first on the ability of the inhibitor to remain in place in the concrete for what may be a very long service life (e.g., 100 years), and second on the ability to control corrosion even far into the future when aggressive substances from the environment finally build up to significant levels at the steel surface. Moreover, an appropriate corrosion inhibitor must not cause negative side effects such as pitting corrosion or degradation of physical properties of the concrete. Finally, use of a suitable corrosion inhibitor should favorably impact the designed life cycle cost of the structure. Rehabilitation applications should satisfy the same general principles, keeping in mind the desired length of service. These considerations led to establishing the following specific project objectives and corresponding tasks:

Objective 1: EVALUATE ABILITY OF INHIBITOR TO STAY IN PLACE
Tasks:

- 1.1 Develop Methodology for Analysis of Inhibitors in Concrete
- 1.2 Determine the Long-Term Stability of Corrosion Inhibitors in Concrete

Objective 2: ESTIMATE LONG-TERM EFFECTIVENESS – MECHANISTIC ISSUES
Tasks:

- 2.1 Examine Inhibitor Degradation Mechanisms
- 2.2 Binding Effects
- 2.3 Other Inhibitor Mechanism Issues - Dosage Needs

Objective 3: DETERMINE POSSIBLE NEGATIVE SIDE EFFECTS – MECHANISTIC ISSUES
Tasks:

- 3.1 Effect on pH of Pore Solution

Objective 4: ESTIMATE LONG-TERM EFFECTIVENESS – PERFORMANCE TESTS
Tasks:

- 4.1 Perform Long-Term Laboratory Tests, Outdoor Sheltered Tests, and Field Tests
- 4.2 Evaluation of Inhibitor Performance

Objective 5: DETERMINE POSSIBLE NEGATIVE SIDE EFFECTS – PERFORMANCE TESTS
Tasks:

- 5.1 Estimated Time to Failure
- 5.2 Determine Effect of Insufficient Dosage on Ccorrosion Progression
- 5.3 Effect of Inhibitor on Chloride Transport
- 5.4 Examine Possible Adverse Effects on Concrete Physical Properties

Objective 6: ESTABLISH SUITABILITY FOR REHABILITATION APPLICATIONS
Tasks:

- 6.1 Evaluate Alternative Repair Strategies
- 6.2 Test Field Repairs and Long-Term Assessment

Two other primary objectives, (7) Establish suitability for new construction applications and (8) Quantitative assessment of durability extension, correspond to a later stage of this investigation and will not be addressed in this interim report.

The investigation was focused on the ability of the inhibitors to control chloride-induced corrosion, a main source of corrosion deterioration in concrete structures in the U.S. The work addressed three inhibitors that were widely commercially available at the start of the investigation. Those inhibitors were already being used in a number of building and highway structures, or considered for future application. These are a calcium nitrite-based product, DCI-S, and two organic inhibitors, F: FerroGard 901 and R: Rheocrete 222+.

The objectives and tasks indicated above were addressed for each of the three inhibitors, to the extent described in the following sections. The experimental approach and corresponding methodologies and findings during the first three years of the project are described in each section, keyed to the objectives listed above.

OBJECTIVE 1 - EVALUATE ABILITY OF INHIBITOR TO STAY IN PLACE

1.1 Develop Methodology for Analysis of Inhibitors in Concrete

1.1.1 Calcium Nitrite-based Inhibitor (DCI-S)

1.1.1.1 Extraction from hardened concrete, powdered

The work on analysis methodology development for DCI-S is essentially completed. Standard methods to determine nitrite content in water were already available.[1] Existing well-established methodology for analysis of nitrite in hardened concrete[2] was examined and then improved to enhance nitrite recovery. The resulting procedure uses two consecutive extractions as described below and exemplified by a sample calculation in Appendix 1.

The concrete sample to be analyzed is first powdered until the entire sample passes through a No. 50 sieve (American Society for Testing and Materials [ASTM] E-11). A 2 g subsample of the homogenized powdered concrete is placed with 200 mL de-ionized distilled water (DDW) and stirred for 30 min. The mixture is settled for 5 min and filtered through a No. 40 qualitative filter by vacuum filtration. The collected filtrate is saved and the solids on the filter were rinsed back into the flask. The solids remaining in the flask are diluted with another 150 mL DDW, stirred for 10 min, settled for 5 min and filtered through the original filter. The step is repeated with an additional 100 mL DDW. The combined filtrates are then filtered through a Gelman 0.45 μm membrane and afterwards diluted with DDW to a final 500 mL. An aliquot of this ("initial") extract is then diluted to obtain a target analytical concentration of 0.3 mg NO_2^-/L and analyzed spectrophotometrically.

Both the original filter and membrane (with residues intact) are diluted with DDW to 500 mL and stored for 10 to 15 days at room temperature. An aliquot of this ("residual") extract is then diluted for spectrophotometric analysis.

Nitrite analysis of both the initial and residual extracts was performed using the spectrophotometric method described by the American Public Health Association (APHA).[3] Light absorbance was measured with a Cary 1 dual-beam spectrophotometer at a wavelength of 543 nm and with a 1-cm path length. Standard solutions were used to obtain a calibration curve that was linear (coefficient of determination R^2=0.9999) for nitrite concentrations from 0 to 0.8 mg NO_2^-/L, so that the NO_2^- concentration (in mg/L) was equal to the absorption divided by a calibration factor of 0.913 L/mg. The detection limit was 0.003 mg NO_2^-/L water. The total nitrite recovered was calculated by summing the recoveries from the initial and residual extractions.

The measurement result is obtained as the mass of nitrite extracted per mass of powdered concrete. An approximate indication of the amount of nitrite extracted per unit volume of concrete can be made by assuming that its specific weight is the same as that of the powdered sample. For more accurate evaluations (for example, to determine how close to 100 percent is the recovery of admixed nitrite), it is desirable to refer the measurements to the mass of oven-dry concrete and then relate that amount to the corresponding mass of fresh concrete. To that effect, the evaporable water was

determined by oven drying a subsample of the powdered concrete and measuring the mass loss. The mass of fresh concrete that would have yielded a given amount of dry, hardened concrete was obtained by knowledge of the initial mix design and water absorption of aggregates, plus assumption of the degree of hydration. Since the amount initially admixed is known in terms of mass of nitrite per mass (or per volume) of fresh concrete, this permits estimating the extent of recovery. An example calculation of this procedure is given in Appendix 1.

The extent of recovery was determined for concrete specimens with mix design and properties as shown in Table 1. The specimens were cured capped in a plastic mold for 84 days at 22° C. The admixed nitrite concentration for Mix C1 was 2.46 mg NO_2^-/g concrete. Mix C0 was a control without admixture. Powdered concrete samples were obtained one week after demolding by drilling with a masonry drill and collecting the powder. Table 2 shows the nitrite recoveries obtained in 6 replicate tests, which yielded an average nitrite recovery of 99 percent with a standard deviation of 1 percent. Nitrite recovery from Mix C0 was similar to the recovery of the method control, equivalent to an apparent addition of about 0.6 percent of the amount admixed to Mix C1.

Table 1. Mix Design and Concrete Properties of Cylinders C_1 and C_0

Specimen	Cylinder C_1	Cylinder C_0
Portland cement Type I, kg/m^3	414	414
Water, kg/m^3	167	186
Fine aggregate, kg/m^3	735	735
Coarse aggregate, kg/m^3	1045	1045
DCI-S,* kg/m^3	29.14	0
Water/cement (w/c) ratio	0.45	0.45
Batch weight, kg	1.844	1.836
Unit weight, kg/m^3	2390	2380

*DCI-S contains about 65 %wt of water. This is taken into consideration when computing w/c ratio. The weight fraction of NO_2^- in the DCI-S used was determined to be 0.202

The results indicated that nitrite can be nearly completely recovered from hardened concrete if sufficient time is allowed for nitrite to diffuse from powdered samples. The initial recovery yields about 91 to 95 percent of the admixed nitrite, while the residue contribution gives an additional 6 to 8 percent. Medford and Leming[4] reported a 94 (±1) percent recovery of theoretical nitrite from laboratory mortar standards, using a procedure corresponding to only the initial step used here. The greater recovery with the present method can be ascribed to the longer leaching time for the residue in the second step. According to previous results from the present program,[5,6] only a fraction (e.g., 1/10 to 1/5) of the admixed nitrite as calcium nitrite is present in the pore solution, with most of the admixed nitrite being bound elsewhere. The present results (Table 2) suggest that the bound nitrite may be in reversible equilibrium with the free nitrite in the pore solution, as essentially all of the nitrite can be extracted at large enough dilution.

1.1.1.2 Determination of nitrite in pore water of hardened concrete.

Technology for determining the amount of nitrite in pore water of hardened concrete ("free nitrite," see Section 2.2) was also developed. The method was an extension of the recently developed in-situ leaching (ISL) method.[7] Hardened concrete samples were allowed to stabilize in a 100 percent

Table 2. Nitrite Recovery from Hardened Concrete Cylinder C_1*

Replicate	Nitrite Recovery %		
	Initial Extract	Residual Extract	Total
1	90.9	7.9	98.9
2	91.5	7.96	99.4
3	91.1	6.6	97.7
4	94.2	6.7	100.9
5	94.0	6.4	100.4
6	91.5	6.5	98.0
Mean	92.2	7.0	99.2
Standard Deviation	1.5	0.7	1.3

*The C_1 cylinder contained 8.47 kg $Ca(NO_2)_2$ per m^3 of concrete.

relative humidity (RH) chamber. A small cavity drilled into the sample was then partially filled with water (typically less than 0.4 cm^3). The water was then allowed to nearly equilibrate with the surrounding cavity water, a process that typically took one or more weeks. Spectrophotometric analysis of the cavity water (using the method and calibration described above in Section 1.1.1.1) after appropriate dilution yielded the nitrite content, which was assumed to approach that of the surrounding pore water. That assumption was confirmed by independent pore water expression (PWE) measurements.[6] The methodology is described in detail in Section 2.2.

1.1.2 Organic Corrosion Inhibitor F (FerroGard 901)

Analysis for this inhibitor is hindered by two basic problems. First, the composition of this inhibitor is proprietary, so that it is difficult to differentiate between the actual inhibiting species and any other component (such as fillers, solubilizers, etc.) of the product. Second, even if the appropriate species were identified, standard analytical techniques with the required sensitivity and accuracy may not be available even for simple liquid solutions. Consequently, no satisfactory methods for analysis of this inhibitor have been reported. Review of the literature revealed primarily qualitative or, at best, semiquantitative methods.[8-13]

Initial efforts under this project for development of a quantitative analytical method consisted of the use of an ammonium sensitive electrode, and of analysis of organic residue by extraction with solvents. Neither approach produced useable results. During the last year, efforts concentrated on the use of ultraviolet absorption. The inhibitor has good solubility in water with little turbidity at both neutral or basic pH. A strong, reproducible absorption peak at 224 nm has been used successfully for construction of a reproducible calibration curve (Figure 1) in the concentration range of 25 to 85 μg of inhibitor per cm^3 of water. The calibration was similar for inhibitor dissolved into neutral distilled water, or into filtered water leachate from powdered or solid concrete. There are, however, indications that stability of the calibration is limited. For example, solutions exposed in an open beaker to room temperature air for 6 hours showed UV absorption losses on the order of 25 percent. As a result, time limits in testing procedures will need to be implemented.

Recovery achievable from hardened samples using UV absorption has been recently examined by casting mortar containing 8 mg/g FerroGard 901. Portions of the mortar sample are pulverized by drilling with a masonry drill. The powder is then leached in water for a period of 12 hours while in a motorized shaker. The leachate is filtered through a 0.45 μm filter and the absorption at 224 nm determined afterwards. By application of the calibration curves determined as above, extraction

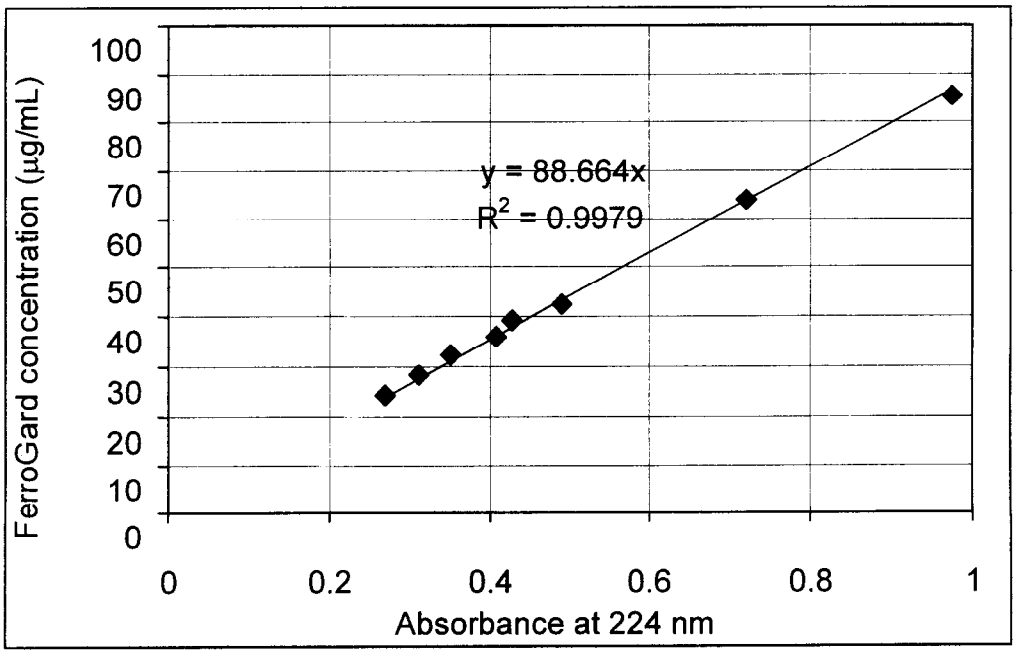

Figure 1. Calibration curve for FerroGard 901 by UV absorption at 224 nm.

recoveries on the order of 70 percent to 80 percent have been obtained. The amount of recovery does not appear to be overly sensitive to thermal aging of the powdered sample. For example, recoveries of 68 percent were obtained after placing the sample in an oven at 50° C for about 100 hours. Recovery was about 73 percent after exposing the concrete powder to air at room temperature for about 50 days.

Applicability of the method for the determination of free (pore water) inhibitor content will be established in the future stages of the project. Another open question is whether the 224 nm peak corresponds to the main inhibiting species or to a non-inhibiting component of the product. Tests with Benzoic acid (one of the inhibiting agents mentioned in the literature)[14] in alkaline solution (NaOH) revealed a strong absorption peak also at 224 nm, suggesting that the chromophore associated with dilution of the product in water is at least one of the inhibiting components in the product.

1.1.3 Organic Corrosion Inhibitor R (Rheocrete 222+)

Determination of the presence and amount of this corrosion inhibitor in hardened concrete has been very challenging and no satisfactory outcome can be reported at this time. Analysis presents all the difficulties indicated for the organic corrosion inhibitor F, plus problems resulting from the low solubility of this product. Upon introduction in water, the product forms a highly turbid colloidal suspension that virtually prevents analysis by UV absorption. The product does dissolve easily in

acetonitrile, forming a limpid solution suitable for UV spectroscopy, where a composite absorption is observed that can be decomposed into two components at 224 nm and 252 nm. Calibration curves (absorption vs. content) for Rheocrete 222+ in acetonitrile have been successfully and consistently obtained using those peaks. Calibration was also feasible for Rheocrete 222+ added to acetonitrile that had been in contact with mortar powder simulating an extraction procedure. However, when acetonitrile was used to extract Rheocrete from powder of mortar with known additions of Rheocrete, the magnitude of the absorption peak recorded was 2 to 4 times greater than that corresponding to the actual addition. The cause for this anomalous extraction result is being investigated. Variations of the extraction procedure (for example, using methanol) to achieve quantitative analysis are being tested, but show no improvement to date over the acetonitrile procedure.

1.2 Determine the Long-Term Stability of Corrosion Inhibitors in Concrete

1.2.1 Calcium Nitrite-based Inhibitor (DCI-S)

1.2.1.1 Laboratory investigation of nitrite transport in concrete

Experimental method - materials

Five different concrete mix proportions were used (see Table 3 for nomenclature and details). Four of those mixes were limited to available specimens made for the long-term test program described under Objective 4. The –0.5 or –1.0 at the end of the designation of those mixes indicates that the inhibitor dosage was either one half or the full amount, respectively, of the 22 L/m^3 specified by FDOT for aggressive marine service applications. The P1 designation indicated 20% Type F fly ash cement replacement. All mixes used Type II cement. One of the mixes (C2 designation) was prepared with a significantly higher w/c ratio than those of the rest. These concretes were cast in cylinders that were demolded one day after casting and then immersed in Limewater for curing for about 100 days. After curing, the cylinders were stored at ~22° C in a plastic enclosure at moderate to high humidity for at least one year before performing the leaching tests. As some inhibitor leaching from those cylinders took place in the initial tank curing, an additional batch of cylinders with proportions approximating those of mix DCI-C1-1.0 was prepared but placed directly in a ~100% RH and ~22° C chamber after one day in the mold. Nitrite loss from leaching during curing was thus expected to be negligible. Specimens from this batch, named NR (Nitrite Recovery), were subject to leach tests after controlled times ranging from 50 to 270 days of curing in the air chamber.

Leaching experiments

The test specimens were whole, as-cast cylinders, or slices cut from the cylinders, with the dimensions indicated in Table 4, which also shows the test solutions and temperatures at which the tests were conducted. The test methodology generally followed the specifications of American National Standards Institute/American Nuclear Society (ANSI/ANS)-16.1-1986.[15] The specimen was placed, supported by a plastic stand, inside a lidded plastic container (Figure 2) with enough solution to maintain a uniform thickness around the specimen and a ratio of liquid solution volume to specimen surface area of at least 10 cm. Some exploratory variations in procedure (e.g., changes in solution renewal interval) were used for specimens of concrete mix DCI-C1-0.5 that were tested early in the program.

Table 3. Mix Design and Concrete Properties Used in the Leaching Experiments

Concrete Type		DCI-C1-0.5	DCI-C1-1.0	DCI-C2-1.0	DCI-P1-1.0	NR
Mix design	Cement, kg/m^3 (lb/yd^3)	390 (657)	390 (657)	390 (657)	310 (525)	382 (643)
	Water, kg/m^3 (lb/yd^3)	160 (270)	160 (270)	195 (329)	160 (270)	139 (235)
	Fine aggregate, kg/m^3 (lb/yd^3)	700 (1179)	694 (1169)	600 (1012)	674 (1135)	679 (1145)
	Coarse aggregate, kg/m^3 (lb/yd^3)	986 (1661)	986 (1661)	986 (1661)	986 (1661)	967 (1629)
	Class F fly ash, kg/m^3 (lb/yd^3)	0	0	0	78 (131.5)	0
	DCI-S, kg/m^3 (lb/yd^3) L/m^3 (gal/yd^3)	14 (23.7) 11 (2.22)	28 (47.5) 22 (4.44)	28 (47.5) 22 (4.44)	28 (47.5) 22 (4.44)	27.7 (46.6) 22 (4.44)
	Water/binder ratio	0.41	0.41	0.50	0.41	0.40
Actual water/binder ratio†		0.41	0.43	0.49	0.40	0.40
Unit weight, kg/m^3 (lb/ft^3)		2237 (139.8)	2235 (139.7)	2178 (136.1)	2216 (138.5)	2195 (137.8)
Cylinder dimensions* cm (in)		10.1x20.3 (4x8)	7.6x15.2 (3x6)	15.2x30.5 (6x12)	7.6x15.2 (3x6)	7.6x15.2 (3x6)
Curing time, days		100	160	60	180	50, 100, 270
Curing medium		Limewater	Limewater	Limewater	Limewater	100%RH

* Cylinder diameter x height

† Adjusted for water in inhibitor and moisture content of aggregates

The test solutions were de-ionized water (DW), Limewater (DW saturated by 2 g/L addition of calcium hydroxide), or synthetic seawater (DW with 41.95 g/L of synthetic "sea-salt" per ASTM D-1141-52). Leaching test temperatures were either ambient (~22° C) or 35 to 37° C achieved by placement of the leaching containers in a temperature-controlled chamber. The solution was sampled and completely replaced by fresh solution at regular intervals during cumulative leaching times

Table 4. Specimen Specifications and Testing Conditions Used in the ANSI/ANS Experiments

	Concrete Type	Specimen Dimensions* cm (in)	Solution Volume (mL)	S/V** (1/cm)	Solution Type	Temperature (°C)
Cylinder	DCI-P1-1.0	7.6x15.2 (3x6)	4558	0.66	Limewater, DW	22
	NR	7.6x15.2 (3x6)	4558	0.66	Limewater, DW, Synthetic Seawater	22
	DCI-C1-1.0	7.6x15.2 (3x6)	4558	0.66	Limewater	22
Slice	DCI-P1-1.0	7.6x2.5 (3x1)	1500	1.31	Synthetic Seawater, DW	22
	NR	7.6x2.5 (3x1)	1500	1.31	Limewater, DW, Synthetic Seawater	22, 35
	DCI-C2-1.0	15.2x4.6 (6x1.8)	5834	0.70	Limewater	22
	DCI-C1-0.5	10.2x2.5 (4x1)	357, 1000	1.18	Limewater	22, 37

* Diameter x height

** Specimen surface area to volume ratio

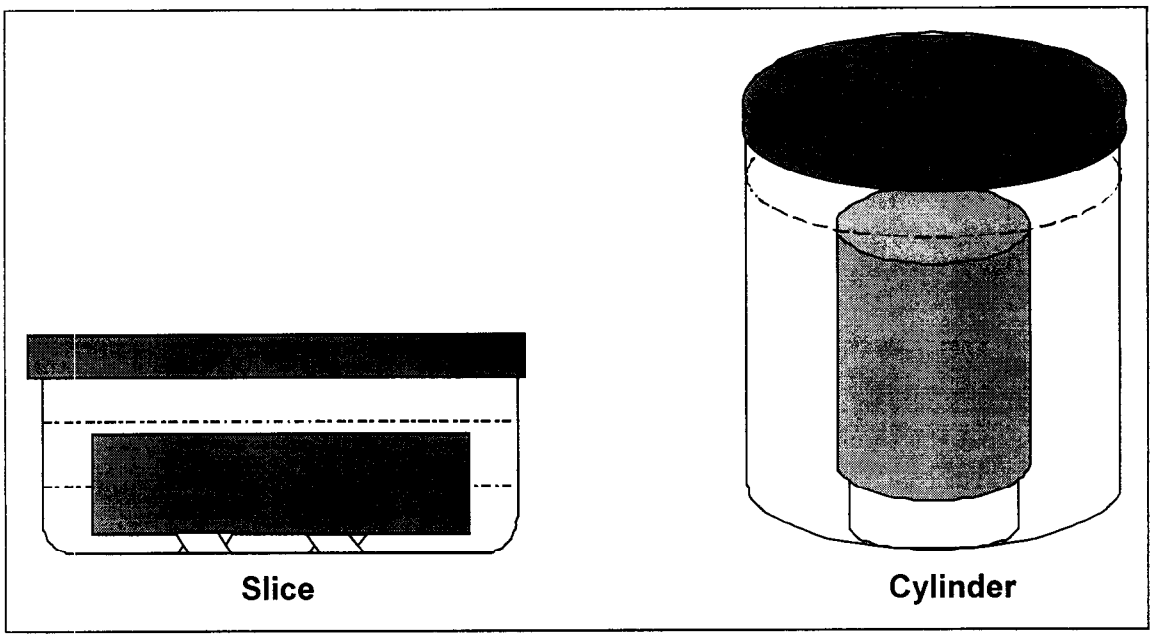

Figure 2. Placement of concrete samples in leaching containers

ranging from 2 to 2160 hours (a total of 90 days). Leaching tests on a few selected specimens were extended for another 90 days. The sampled solution was tested for nitrite with the spectrophotometric method described in Section 1.1.1.1. The apparent diffusivity (D_{app}) of nitrite in water-saturated concrete was calculated from the recorded nitrite concentrations in the leaching solution as function of time, as described below.

Diffusivity estimates

The apparent nitrite diffusion coefficient D_{app} in concrete is defined here as

$$D_{app} = -J\left(\frac{\partial C}{\partial x}\right)^{-1} \qquad (1)$$

where

J = the flux of nitrite ions (mass per cm^2 of concrete per second) along the direction x
C = the concentration of nitrite in concrete (mass of nitrite per cm^3 of concrete)

Internal bulk diffusion of nitrite in concrete is likely to be the rate-determining mechanism during much of the leaching process. Since in the leaching experiments the nitrite concentration in the solution was always kept at a very low level by renewing the solution frequently, a one-dimensional model can approximate the leaching behavior during the early stages of leaching.

From the measured nitrite amount a_n in the solution at the end of the n_{th} liquid renewal interval, a Cumulative Fraction Leached (CFL) can be defined as $CFL = \Sigma a_n / A_o$, where A_o is the total amount of nitrite inside the specimen at the beginning of the leaching experiment. If CFL is plotted against

the square root of the leaching time, a linear correlation with a slope k can be expected during the early stages of leaching (when CFL < ~0.2)[15] so that:

$$D_{app} = \pi(\frac{k}{2})^2(\frac{V}{S})^2 \qquad (2)$$

where

V = Volume of specimen, cm^3

S = geometric surface area of specimen, cm^2

In the following, the D_{app} value so obtained will be called D1 when it is needed to differentiate it from the one obtained with the following equation.

When CFL exceeds ~0.2 significant deviation from one-dimensional behavior takes place.[10] Under those circumstances the apparent diffusion coefficient can be obtained instead by

$$D_{app} = \frac{Gd^2}{t} \qquad (3)$$

where

t = cumulative leaching time since the beginning of the first leaching interval

d = the diameter of the cylinder, cm

G = a dimensionless time factor for the cylinder, which is dependent upon CFL and the specimen height-to-diameter (l/d) ratio.[15]

The D_{app} calculated using Eq.(3) will be designated as D2 if it is necessary to differentiate it from D1. If there was more than one datum with CFL>0.2, then D2 was reported as the average for those points.

Sample calculations of D1 and D2 are presented in Appendix 2.

RESULTS

CFL was calculated for every experiment assuming that the nitrite content of each specimen type was the same as the nominal admixed amount per Table 3. Direct measurements with specimens of DCI-C1-1.0, DCI-C2-1.0, and DCI-P1-1.0 using the procedure described in Section 1.1.1.1 confirmed that the actual nitrite content near the center of the cylinder was close to the nominal nitrite content. Typical behavior during the leaching tests is exemplified in Figure 3, which shows the CFL evolution as a function of $t^{1/2}$ for a specimen of DCI-C1-1.0 concrete (full cylinder, 7.6 cm by 15.2 cm) and two specimens of DCI-C2-1.0 concrete (4.6-cm thick slices with freshly cut faces, sliced from a 15.2-cm diameter cylinder) in Limewater at 22° C. Except for an initial transient region, an approximately linear correlation between CFL and $t^{1/2}$ is evident for each specimen, conforming to the expectation of diffusional leaching control. The CFL-$t^{1/2}$ slopes were smaller at earlier times, especially for the cylinder specimen of DCI-C1-1.0. This phenomenon may be attributed to earlier loss of the nitrite to Limewater during curing, which would cause the nitrite concentration near the concrete surface to be lower than that of the bulk concrete. Since Eq (2) was derived by assuming that the diffusive species are uniformly distributed before the leaching experiment is started, a lower surface concentration should yield a slower leaching rate at the beginning of the test. Compared with the cylinder of DCI-C1-1.0, the slices of DCI-C2-1.0 had 100 days shorter curing time in Limewater and two freshly cut

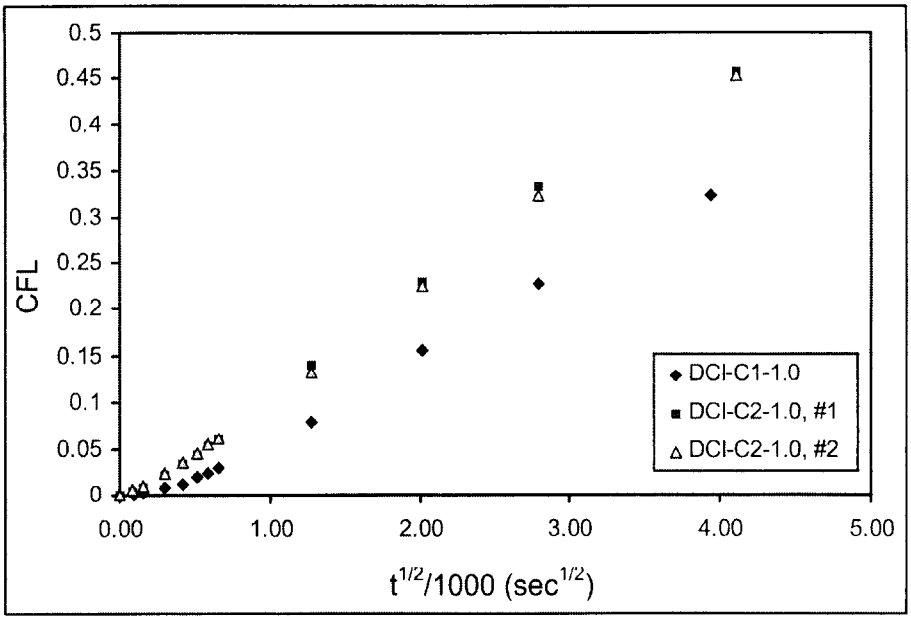

Figure 3. CFL as a function of the square root of leaching time ($t^{1/2}$) for concrete specimens of DCI-C1-1.0 and DCI-C2-1.0 in Limewater.

surfaces. These two freshly cut surfaces should have had a higher nitrite concentration than that of the previously exposed surface, and accounted for more than 70 percent of the total slice surface area. Hence the linearity of the curves for the slices of DCI-C2-1.0 should extend, as observed, to a much earlier leaching time.

Figure 4 illustrates the results of a series of experiments with the same concrete (DCI-P1-1.0) in various leaching media at 22° C, while Figure 5 shows the behavior for the NR concrete specimens in various leaching media and at the two test temperatures. In the latter case, straight line behavior extending to very short times manifested the absence of significant leaching during curing.

As illustrated in Figures 3 through 5, there was generally good reproducibility in the CFL values from duplicate tests with specimens of the same type. Tables 5 through 8 show the slopes and diffusivities calculated from the data from all the experiments, detailing the individual test condition of each specimen. The results showed agreement typically better than within ~20% between the values of D1 and D2 for any given experiment, and between the results of duplicate experiments. However, differences between D1 and D2 values were relatively large in some cases (notably for tests in synthetic seawater, specimens 6 and 7 in Table 7). The D1 values were consistently derived from a larger number of data than for D2, for which sometimes only 1 or 2 data existed and relatively large shape corrections were needed. Consequently, the D2 values were regarded only as supplemental evidence and all quantitative comparisons in the discussion were made based on D1 values only. Tests with specimens of DCI-P1-1.0 under the same conditions but using specimens of different shape (i.e., cylinder vs. slice, Table 7, specimens 3 and 4), yielded similar diffusivity values. The results appeared to be only slightly affected by whether a cut or a cast concrete surface was in contact with the leaching solution.

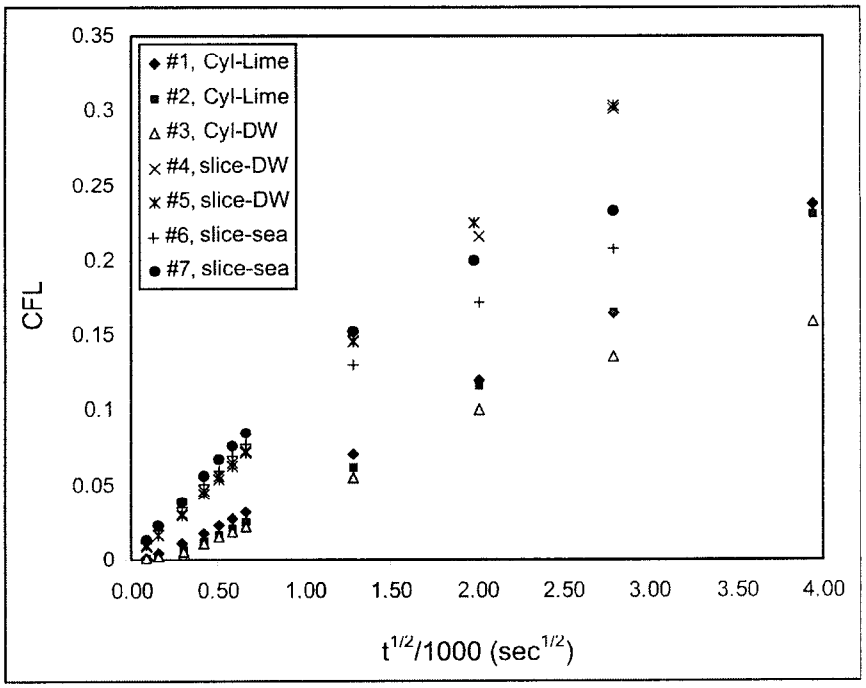

Figure 4. CFL as a function of the square root of leaching time ($t^{1/2}$) for specimens of DCI-P1-1.0 in Limewater, DW, and synthetic seawater (sea) at room temperature.

Measurements of the total amount of remaining nitrite in the concrete specimens were performed in selected specimens using the technique for analysis of nitrite in hardened concrete described in Section 1.1.1.1. The results were in approximate agreement with the amounts leached in the

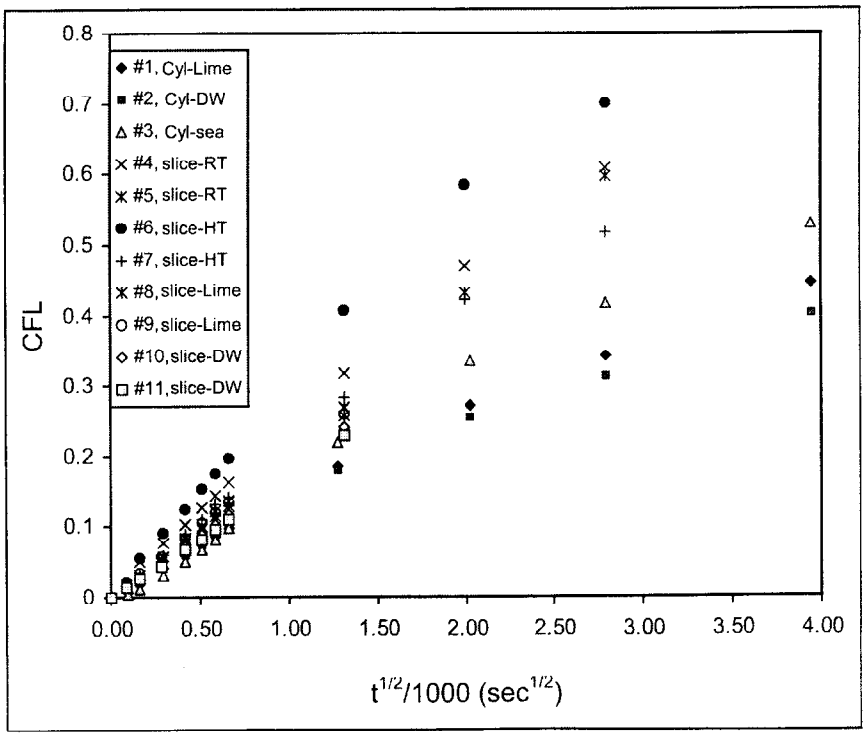

Figure 5. CFL as a function of the square root of leaching time ($t^{1/2}$) for NR concrete specimens in Limewater, DW, and synthetic seawater (sea) at RT and at ~35° C (HT).

Table 5. k, D_1, and D_2 Obtained for Specimens of DCI-C1-1.0 and DCI-C2-1.0 Leaching in Limewater at 22° C.

Concrete Type	Slope k ($s^{-1/2}$)	D_1 (cm^2/s)	D_2 (cm^2/s)
DCI-C1-1.0*	0.91×10^{-4}	1.5×10^{-8}	1.5×10^{-8}
Specimen #1, DCI-C2-1.0†	1.28×10^{-4}	2.6×10^{-8}	2.7×10^{-8}
Specimen #2, DCI-C2-1.0†	1.17×10^{-4}	2.2×10^{-8}	2.6×10^{-8}

* Full cylinder † Slice

Table 6. k and D Obtained for Slabs of DCI-C1-0.5 Leaching in Limewater.

Slice	Slope k ($s^{-1/2}$)	D* (cm^2/s)	Temperature
1	1.76×10^{-4}	1.7×10^{-8}	22°C
2	1.76×10^{-4}	1.7×10^{-8}	22°C
3	1.76×10^{-4}	1.7×10^{-8}	22°C
4	1.65×10^{-4}	1.5×10^{-8}	22°C
5	1.55×10^{-4}	1.4×10^{-8}	22°C
6	2.33×10^{-4}	3.0×10^{-8}	37°C

* No D2 estimates were conducted for these tests.

immersion experiments. Concentration profiles of selected test specimens were also obtained.[16] The profiles showed, as expected, significant nitrite depletion near the surface and higher concentrations inside the specimen. However, the shape of the concentration profiles was not in detailed agreement with that expected from the simplifying assumptions used to calculate D_{app} from concentration of nitrite in the leaching water. It was speculated that the discrepancy was caused by deviation from otherwise nearly linear binding of nitrite in concrete (see Section 2.2).

DISCUSSION

The available data set represents largely exploratory measurements, and as such was limited in coverage of conditions and quantity of specimens. Nevertheless, the results provide useful

Table 7. Slopes and Apparent Diffusion Coefficients Obtained for DCI-P1-1.0 at 22° C

Specimen*	Leaching Solution	Slope k ($s^{-1/2}$)	D_1 (cm^2/sec)	D_2 (cm^2/sec)
1	Limewater	0.612×10^{-4}	6.8×10^{-9}	7.2×10^{-9}
2	Limewater	0.594×10^{-4}	6.4×10^{-9}	7.4×10^{-9}
3	DW	0.575×10^{-4}	6.0×10^{-9}	-
4	DW	1.15×10^{-4}	6.1×10^{-9}	6.5×10^{-9}
5	DW	1.14×10^{-4}	6.0×10^{-9}	6.1×10^{-9}
6	Synthetic Seawater	1.15×10^{-4}	6.1×10^{-9}	2.8×10^{-9}
7	Synthetic Seawater	1.26×10^{-4}	7.3×10^{-9}	4.3×10^{-9}

* Specimens 1 to 3 were cylinders 7.6x15.2 cm; specimens 4 to 7 were slices 7.6x2.5 cm.

Table 8. Slopes and Apparent Diffusion Coefficients Obtained for Specimens of NR Concrete

Specimen*	Curing Time (Days)	Leaching Solution	Slope k ($s^{-1/2}$)	D_1 (cm^2/sec)	D_2 (cm^2/sec)
1	50	Limewater (22° C)	1.47×10^{-4}	3.9×10^{-8}	3.5×10^{-8}
2	50	DW (22° C)	1.40×10^{-4}	3.5×10^{-8}	3.0×10^{-8}
3	50	Synthetic Seawater (22° C)	1.84×10^{-4}	6.1×10^{-8}	4.6×10^{-8}
4	100	Synthetic Seawater (22° C)	2.38×10^{-4}	2.6×10^{-8}	2.9×10^{-8}
5	100	Synthetic Seawater (22° C)	2.15×10^{-4}	2.1×10^{-8}	2.5×10^{-8}
6	100	Synthetic Seawater (35° C)	2.97×10^{-4}	4.0×10^{-8}	3.7×10^{-8}
7	100	Synthetic Seawater (35° C)	2.31×10^{-4}	2.4×10^{-8}	2.8×10^{-8}
8	270	Limewater (22° C)	2.00×10^{-4}	1.8×10^{-8}	2.0×10^{-8}
9	270	Limewater (22° C)	2.03×10^{-4}	1.9×10^{-8}	2.0×10^{-8}
10	270	DW (22° C)	1.78×10^{-4}	1.5×10^{-8}	1.7×10^{-8}
11	270	DW (22° C)	1.67×10^{-4}	1.3×10^{-8}	1.6×10^{-8}

* Specimens 1 to 3 were cylinders 7.6x15.2 cm; specimens 4 to 11 were slices 7.6x2.5 cm.

preliminary information on how diffusivity is affected by key material and exposure variables, and may serve as a guide to detailed future investigations. The trends examined are detailed below.

Magnitude of D_{app}

The experiments yielded nitrite ion values for D_{app} in concrete ranging from ~6×10^{-9} $cm^2 sec^{-1}$ to ~6×10^{-8} $cm^2 sec^{-1}$ (as indicated earlier, all discussion is based on calculations of D1 unless otherwise indicated). These values are on the same order as those reported for chloride ions in concretes comparable to those tested here.[17] This behavior was to be expected as both Cl^- and NO_2^- are anions with the same valence, have comparable diffusivities in water, and experience substantial binding in the concrete matrix (see Section 2.2). It must be emphasized that the D_{app} values calculated from the leaching experiments (and from any other method based on measurement of total species concentration) reflect the assumption of simple diffusional behavior. As indicated by the results from concentration profile measurements, this assumption is only a working simplification. Detailed descriptions of transport processes, including among others the effect of binding, would be required for more accurate evaluation of the distribution of the species in concrete and escape to the external environment.

Dosage

An indication of the influence of nitrite dosage on diffusivity may be obtained by comparing the results from tests in Limewater at 22 °C of specimens of DCI-C1-0.5 (half dosage), with those of the

combined group of the single available specimen of DCI-C1-1.0 and the specimens of the NR mix that had the longest curing period. That combined group had full inhibitor dosage, but approximately the same mix proportions as DCI-C1-0.5 and an extended curing history as well. The average D_{app} for the half- and full-dosage groups were ~1.6 and ~1.7 (10^{-8} $cm^2 sec^{-1}$) respectively, so no significant dosage effect on D_{app} was detected in this limited comparison.

Leaching medium

The DCI-P1-1.0 and the NR concrete were tested in different leaching media under otherwise comparable conditions. The results for DCI-P1-1.0 tested at 22 °C (Table 7) show average D_{app} of 6.6, 6.0, and 6.7 (10^{-9} $cm^2 sec^{-1}$) for tests in Limewater, DW, and synthetic seawater respectively. Tests at 22 °C for NR concrete cured 270 days (Table 8) indicated average D_{app} of 1.9 and 1.4 (10^{-8} $cm^2 sec^{-1}$) for leaching in Limewater and DW respectively. For the same concrete cured 50 days the results (only available for single specimens) were 3.9, 3.5, and 6.1 (10^{-8} $cm^2 sec^{-1}$) for Limewater, DW, and synthetic seawater respectively.

The pH of DW in contact with concrete reaches typically the range ~9 to ~10 after a few days, while that of the Limewater stays at ~12.6. The small difference between the results of DW and Limewater tests suggests that those variations in leachant pH affected little the nitrite transport inside the concrete. The few available comparative data suggest that leaching in synthetic seawater resulted also in similar (but not always close) D_{app} to those obtained with the other two leachants. The synthetic seawater tests with DCI-P1-1.0 showed anomalous behavior at large CFL values, which resulted in significant difference between D1 and D2. Since chloride ions tends to affect the partition between free and bound nitrite (see Section 2.2) in concrete, these observations may be a manifestation of the penetration during the test of chloride ions from the leachant into the concrete. In summary, the present results showed some, but not necessarily dramatic, dependence of D_{app} on the leaching medium. However, the results from synthetic seawater tests underscore the need for further investigation.

Concrete mix proportions and curing

The results of 22° C tests in Limewater of DCI-C1-1.0 and DCI-C1-0.5 (average w/c = 0.42), which may be considered together if the dosage effect is not important, yielded an average D_{app} ~1.6×10^{-8} $cm^2 sec^{-1}$. Mixture DCI-C2-1.0 was comparable to the other two except that it had w/c = 0.49, and the average D_{app} under the same conditions was 2.4×10^{-8} $cm^2 sec^{-1}$, or about half as much more than that of the lower w/c mixes.

The average D_{app} of DCI-P1-1.0 specimens (w/c=0.40, 20% fly ash addition) tested under the same conditions as the DCI-C1-1.0 and DCI-C1-0.5 specimens was 6.4×10^{-9} $cm^2 sec^{-1}$, less than half that of the other concretes, which had only modestly higher w/c but no fly ash.

The 22° C tests with the NR concrete (Table 8) also indicate a consistent reduction of D_{app} with curing time. Assuming that diffusivity is not a strong function of leaching medium, the average of the results for each of the curing times suggest that D_{app} was reduced by about one half by curing from 50 days to 270 days.

The overall results indicate that curing time, w/c ratio and pozzolanic presence influence the D_{app} of nitrite in a manner consistent with the expected effect of those variables on transport of ionic species

in concrete. Similar dependence on those parameters has been well documented for the case of diffusion of chloride ions in concrete.[17]

Temperature

Comparative tests in which temperature was changed from 22° C to 35° C in synthetic seawater (Table 8) increased the average D_{app} in the NR concrete by about 1/2. A roughly comparable increase was indicated by the single available test with DCI-C1-0.5 in Limewater. The change with temperature is consistent with that expected from thermally activated diffusion. Assuming simple Arrhenius dependence, results suggest an activation energy on the order of ~10 kcal/mol, which is comparable with values reported by Goñi et al[18] for leaching of calcium from concrete in DW.

Summary of conclusions from nitrite diffusion experiments.

- The apparent nitrite diffusion coefficient, D_{app}, at 22° C in well-cured concrete with ~390 kg/m^3 of ordinary Portland cement concrete and w/c~0.41 was on the order of 2×10^{-8} cm^2/sec, as determined from leaching experiments. The results showed no strong sensitivity to the leaching medium used, but the effect of seawater needs further investigation.

- An increase in the w/c ratio to 0.49, or an increase in temperature by ~14° C, increased D_{app} by about one half, whereas 20% Type F fly ash addition to the cement reduced the apparent diffusivity by about one half.

- Extended curing of the concrete significantly reduced the D_{app} of nitrite.

- The magnitude of the D_{app} values observed, and the dependence on test parameters, was similar to the values and trends observed for transport of chloride ions in concrete under comparable circumstances.

1.2.1.2 Inhibitor presence in existing long-term specimens

Investigation of 17-Year-Old Slabs from the Federal Highway Administration (FHWA)

Seventeen-year-old reinforced concrete slab specimens prepared for an FHWA investigation of calcium nitrite corrosion inhibitor performance were examined for nitrite content and distribution. Detailed results from this analysis are presented in FHWA Publication No. FHWA-RD-99-145.[5] The following is a summary of those findings.

The slabs were ~15 cm thick and exposed horizontally to natural weathering for most of the 17 years, except for an initial period of 3 months when periodic saltwater ponding was applied to the top surface of the slab. The concrete had w/c=0.53 and a cement factor of 400 kg/m^3, with no pozzolanic additions. The initially admixed nitrite content was ~7.5 kg/m^3 and uniformly distributed through the slab thickness. The upper ~8 cm of the slabs contained various amounts of admixed chloride. Depending on the extent of chloride contamination, some slabs experienced little reinforcement corrosion while others suffered extensive corrosion with consequent deterioration of the concrete in the upper portion of the slab.

Nitrite content determinations of the concrete were made as a function of distance from the top surface of selected slabs, so as to obtain a nitrite concentration profile. Integration of the profile yielded the average nitrite content of the slab, which was then compared with the initially admixed amount. In slabs where deterioration was minor, typically 75 percent of the initially admixed nitrite was still present in the slab after 17 years. However, the concentration profile indicated that the nitrite had redistributed within the slab so that the content at the bottom was sometimes even greater than the initially admixed content. Concurrent chloride analyses indicated that a significant amount of chloride had moved over the same time interval from the upper portion of the slabs into the lower, initially chloride-free region. These findings suggest the possibility of a coupled ionic transport process between nitrite and chloride species. For slabs that had experienced severe deterioration of the top lift, the nitrite and chloride contents there were both much lower than initially. This reduction was attributed to rainfall leaching accelerated by the large surface area created by crumbling.

6-Year-Old Courtney Campbell Causeway Piles

Expansion of the Courtney Campbell Causeway (Tampa Bay) in 1993 used precast piles with a cement factor of 341 kg/m^3, w/c = 0.35, cement replacement of 20 percent fly ash plus 8 percent microsilica (MS), and DCI-S admixture of 22 L/m^3. The piles had been exposed to the bay water service environment for 6 years at the time of core sampling. Analysis of chloride and nitrite content was performed at selected piles at elevations from 0 m to 1 m above the high tide line. The analyses revealed that nitrite content at all elevations was about 85 percent of the admixed amount at depths of 25 mm or more from the concrete surface, slightly higher at about 10 mm from the surface, and slightly lower in the first 6 mm from the surface. Chloride concentration reached a value of 1/2 the surface content at a depth comparable to the maximum in the nitrite profile.

1.2.2 Organic Corrosion Inhibitor F (FerroGard 901)

1.2.2.1 Inhibitor transport in concrete

Only very preliminary results are available for this inhibitor since the reliability of the analysis methods for either hardened concrete or liquid solutions has not yet been confirmed. Leaching experiments were conducted with mortar of w/c=0.4, 800 kg/m^3 cement, and 18 kg/m^3 FerroGard 901 (the recommended FerroGard 901 dosage for concrete is ~9 kg/m^3, but it was doubled here to reflect the cement content per unit volume of the mortar used, which was about twice that of a typical concrete). The initial results indicated an apparent diffusivity of the detectable species on the order of 5×10^{-9} cm^2/sec, which is as in the case of nitrite comparable with the apparent diffusivities expected for chloride ions in the same cementitious medium.

No sources have been identified for analysis of this type of inhibitor in existing long-term specimens.

1.2.3 Organic Corrosion Inhibitor R (Rheocrete 222+)

Because of the difficulties experienced in quantitatively analyzing for this inhibitor, no experiments have been conducted in the first part of this project to determine transport characteristics in the laboratory or in field specimens should any become available.

OBJECTIVE 2 - ESTIMATE LONG-TERM EFFECTIVENESS - MECHANISTIC ISSUES

2.1 Examine Inhibitor Degradation Mechanisms

2.1.1 Calcium Nitrite-based Inhibitor (DCI-S)

2.1.1.1 Inhibitor decomposition in concrete

The available literature on nitrite stability was examined and simplified calculations of rates of decomposition were conducted. The alkali and alkaline earth nitrites in the solid state are very stable but can be thermally decomposed. Calcium nitrite decomposes above 250° C, well above the temperature for normal concrete service.[19] In the aqueous phases, nitrite protonates to nitrous acid according to

$$NO_2^- + H^+ \leftrightarrow HNO_2\,(aq) \leftrightarrow HNO_2\,(g) \qquad (4)$$

Nitrous acid is a weak acid and at 25° C has an equilibrium constant $k = [NO_2^-][H^+] / [HNO_2] = 5.1\times10^{-4}$ M.[20] The effective Henry's law coefficient for nitrous acid at pH 13 (typical of concrete pore solution) is $[HNO_2]/P_{HNO2} = 2.5\times10^{11}$ M/atm[20], strongly favoring the aqueous phase over the gas phase, and nitrite (NO_2^-) as the predominant aqueous species.

Aqueous nitrous acid is not stable and can decompose to nitrate and nitrogen oxide as shown by:

$$3HNO_2 \leftrightarrow H_3O^+ + NO_3^- + 2NO\uparrow \qquad (5)$$

At 25° C, this reaction has a thermodynamic equilibrium constant of 29.4 atm^2/M^2 [19]. The decomposition rate of nitrous acid can be estimated from

$$-d[HNO_2] / dt = k_1 \cdot [HNO_2]^4 / P^2_{NO} - k_2 \cdot [HNO_2] \cdot [H^+] \cdot [NO_3] \qquad (6)$$

where $k_1 = 46$ and $k_2 = 1.6$ at 25°C with concentrations in M, pressure in atm, and time in min.[21] Equation 6 indicates that at pH 13, less than 10^{-10} M of nitrous acid can be formed for a nitrite dosage of 6 kg/m^3, assuming a nitrite pore solution concentration of 0.2 M.[22] Commercial inhibitors may contain 5 percent nitrate[23] and 5 ppb is a reasonable atmospheric concentration of nitrogen oxide.[20] As a result, the net nitrite decomposition rate is expected to be about 10^{-23} moles/L per minute and if so, can be neglected.

The stability expected from those theoretical arguments was supported by the detection after 17 years of a sizable fraction of the admixed nitrite in the FHWA slabs (Section 1.2.1.2) with sound concrete. Under those exposure conditions the missing nitrite is best explained by leaching losses. The nitrite content deep into the concrete of the 6-year-old Courtney Campbell piles (Section 1.2.1.2) was smaller than but close to the reported admixed amount. Although the shortage could be ascribed to chemical instability of the nitrite, other simpler explanations (misreported admixture levels, less efficient extraction of nitrite by the testing procedure in the lower permeability concrete used in the piles) may be equally or more plausible. Other reports in the literature show high recovery from other field structures. Overall the evidence available has not provided any conclusive indication that nitrite spontaneously decomposes in the concrete over the time frame investigated.

2.1.2 Organic Corrosion Inhibitors F and R (FerroGard 901, Rheocrete 222+)

Except for the initial results on aging of FerroGard 901 indicated in Section 1.1, the stability of these inhibitors has not yet been examined in detail, pending development of more quantitative analytical methods.

2.2 Binding Effects

2.2.1 Definitions and Techniques

An extensive series of tests was conducted to determine which fraction of the nitrite was present in the pore water of the concrete. The amount of nitrite that could be extracted with the procedure indicated in Section 1.1.1.1 will be designated as the *total nitrite* and expressed in units of mass per unit mass, or unit volume, of concrete. The nitrite present in the pore water will be designated as *free nitrite*. The free nitrite can be expressed as well in units of mass per unit mass, or unit volume, of concrete, but it is usually obtained by analysis first as mass per unit mass, or unit volume, of pore water. Free nitrite analysis procedures have been implemented only for concrete equilibrated with 100% RH air and assuming that only the capillary pores of the concrete are filled with water, so free nitrite is reported for that condition only. In that condition the volume of water in the pores is equal to the concrete volume multiplied by the concrete capillary porosity ε. Therefore the free nitrite content measured as mass per unit volume of capillary water can be converted, by multiplying by ε, into free nitrite as mass per unit volume of concrete. When both the total nitrite and the free nitrite are expressed in that manner, the *bound nitrite* can be defined as the difference between total and free nitrite.

Two techniques were implemented in this project to measure free nitrite. The first was the well established Pore Water Expression (PWE) method, suitable for cement paste, mortar, and to some extent for concrete where sample yields may not be sufficient for analysis. The second method was In-Situ Leaching (ISL), less limited when sampling concrete. These techniques are described in the following sections.

2.2.1.1 Pore Water Expression (PWE)

PWE procedures were performed as described in Reference (6), using a custom-made hydraulic press with a 20 mm bore expression piston and a nominal pressure of ~650 MPa applied in gradual steps over ~5 minutes (Figure 6). Depending on the quantity and the water/cement ratio of the sample, each test usually yielded from 0.5 to 1 ml of pore solution. The pore water was collected with a syringe and then weighed on an analytical balance. The pore solutions were immediately analyzed for pH, chloride, and nitrite.

The concrete and mortar samples for PWE were prepared as follows. The materials were manually mixed inside a plastic container and then cast into PVC pipes (17 mm I.D. and 150 mm long), with both ends sealed with rubber stoppers. The diameter of the mold was chosen so that the cast cylinder could fit into the pore expression bore without being further crushed. The pipes were rolled periodically during the first few hours after casting to minimize possible segregation. The specimens were demolded after 24 hours and then transferred into airtight PVC bottles. Nearly 100% RH was maintained in the bottles by spraying a small amount of distilled water mist when necessary.

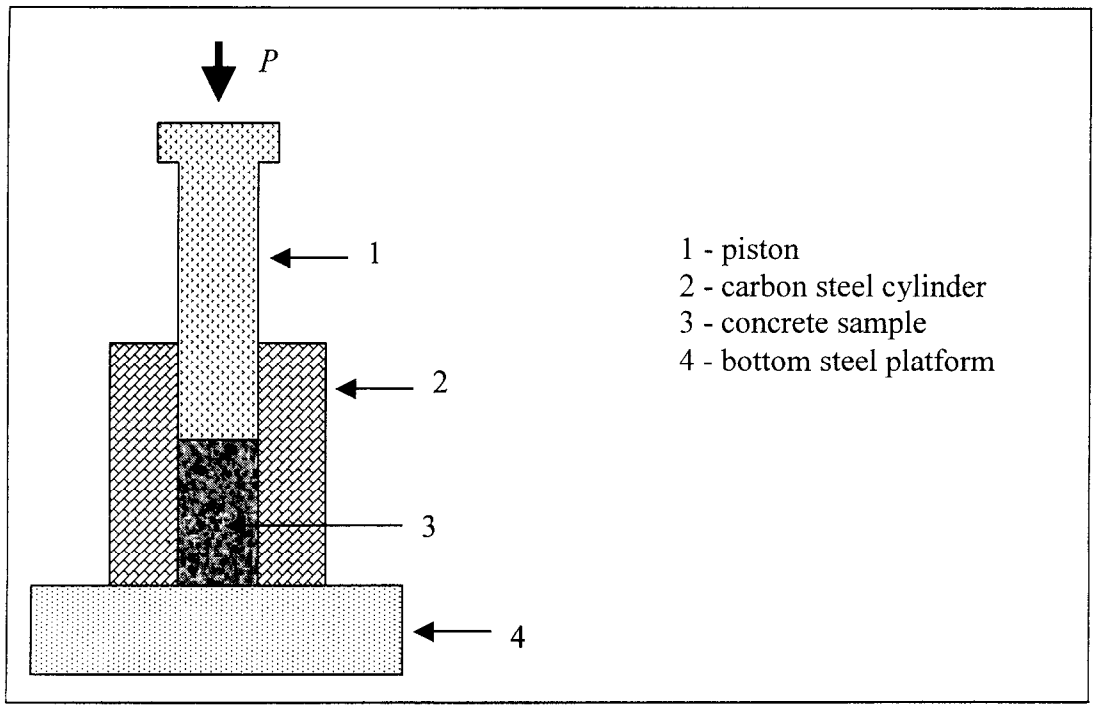

Figure 6. Schematic of PWE Arrangement

To study the binding properties of DCI-S in concrete, concrete samples with a w/c ratio of 0.45 and various inhibitor additions were prepared according to the mix proportions shown in Tables 9 and 10. To reveal possible differences in the nitrite binding behavior between calcium nitrite and sodium nitrite, additional mortar specimens with w/c = 0.45 and sodium nitrite additions were prepared. The purpose of using mortar samples instead of concrete samples was to achieve a higher yield of pore solution from each test. The nitrite contents in those specimens (either from DCI-S or 99.1% pure crystalline $NaNO_2$) are given in Table 10. To investigate the interaction between chloride ions and nitrite ions, mortar specimens (w/c = 0.35, 0.45, and 0.55) containing 1.46 percent nitrite (from DCI-S) and various amounts of chloride (0.5 percent, 1 percent, 2 percent, and 4 percent from NaCl) were also prepared. The cement content in all the mortar specimens was 700 kg/m^3. PWE was usually performed after two weeks of curing, when the pore water composition was found to be stabilized.

2.2.1.2 In-situ Leaching Method (ISL)

The ISL method was developed recently in this laboratory.[7] Cylindrical specimens (100 mm×200 mm) with and without DCI-S were cast as part of large mix batches (>0.26 m^3 ea.) per mix design in Table 11. The specimens were cast in plastic molds, demolded after 24 hours, and then cured in Limewater for 160 days. One cylinder from each mix was then cut transversely in half with a diamond saw. Three holes ~5 mm diameter and ~30 mm deep were drilled perpendicular to each of the freshly cut surfaces with a masonry drill bit. The holes were equidistant to the center of the cylinder and ~30 mm apart from each other. The holes were carefully cleaned after being drilled to remove all traces of dust. An acrylic washer was then attached to the rim of each hole with a fast-curing epoxy. Immediately after that, 0.4 mL of distilled water was injected into each hole with a syringe, and rubber stoppers were pushed into the acrylic washers. The solution inside the hole was thus completely separated from the outside environment. The prepared specimens (Figure 7) were then placed inside a closed ~100% RH chamber so that the concrete remained saturated with water (the preparation procedure was performed quickly to minimize evaporation). A tray filled with

Table 9. Mix Proportions of Concrete Specimens for PWE Tests.

Material	Pore Expression
Cement content (kg/m^3)	504
Alkali (as Na_2O) in cement (%wt)	0.37
Water (kg/m^3)	227
F.A. (Ottawa 50-70 sand) (kg/m^3)	835
C. A. (limestone) (kg/m^3)	735
Max. aggregate size (cm)	0.6
NO_2^-	Per Table 10
W/c ratio	0.45

Table 10. Nitrite Ion Dosage in Concrete Specimens.

Mix Designation	Admixed nitrite (NO_2^-)* (as %wt. of cement)
DCI0	0
DCI1	0.18
DCI2	0.37
DCI3	0.73
DCI4	1.46
DCI5	2.92

*Obtained by addition of DCI-S assuming that it contained 30.0 %wt $Ca(NO_2)_2$ (or 20.9 %wt NO_2^-), or by addition of the appropriate amount of solid $NaNO_2$.

saturated calcium hydroxide solution was placed inside the chamber to act as a CO_2 trap to avoid carbonation.

The pH of the solution in the holes was measured in-situ by means of a MI-405 micro-pH glass electrode and a silver-silver chloride reference electrode. Before and after each pH measurement, the electrodes were calibrated in standard pH 10, pH 12 and pH 13 buffer solutions. A small pipette was

Table 11. Concrete Mix Design for ISL Tests.

	Concrete Control (CCTR)	Concrete with Inhibitor (CDCI)
Cement type	II	II
Cement content (kg/m^3)	391	391
Alkali (as Na_2O) in cement (%wt)	0.51	0.51
Water (kg/m^3)	149	160
Fine agg. (sand) (kg/m^3) (SSD)	709	696
Coarse agg. (kg/m^3) (SSD) (Limestone, max. agg. size 1 cm)	957	948
Inhibitor (L/m^3)	0	22
w/c ratio	0.38	0.41

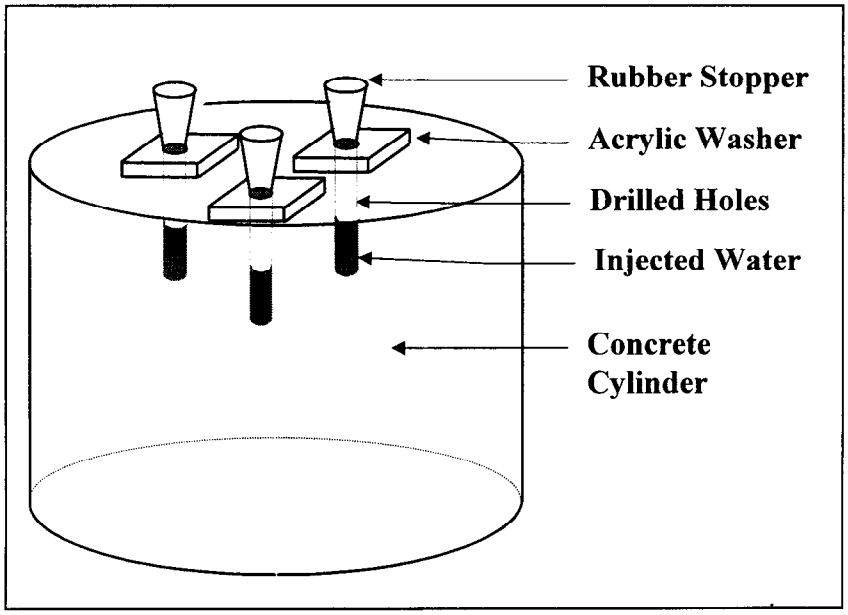

Figure 7. Schematic of ISL arrangement

used to extract ~10 μL of the solution from the holes at various times after the initiation of the experiment. The amount of extracted solution was determined to an accuracy of 0.1 mg while transferred into a 100 mL volumetric flask bottle placed on an analytical balance. The flask was then filled to 100 mL with distilled water. Further dilution was made when necessary. The nitrite content in the diluted sample was then analyzed spectrophotometrically as described in Section 1.1.1. The results from multiple holes in a sample were averaged.

2.2.2 Nitrite Binding in the Absence of Chloride Ions

For chloride-free specimens in which nitrite was introduced as calcium nitrite, the free nitrite in the pore water was found to be present in a concentration approximately proportional to the total nitrite content of the concrete (Tables 9 and 10), as exemplified in Figure 8. All tests were performed at 21±2° C. The proportionality was such that for a total nitrite content of 5.8 kg per m^3 of concrete (a typical specified admixed dosage) the free nitrite had a pore water concentration of about 0.2 M. If the concrete capillary porosity had a typical value of $\varepsilon = 0.1$, then 0.2 M pore water nitrite would correspond to about 1/6 of the total nitrite (see Appendix 3). This behavior was typical of all the chloride-free specimens investigated. The results indicate that much of the admixed nitrite is bound in some manner in the concrete matrix. Figure 9 shows the same results for calcium nitrite but expressed in the form of a binding isotherm where bound nitrite is given as a function of free nitrite, assuming $\varepsilon = 0.1$. The near linear nature of the binding in the concentration range examined can be appreciated; the results can be approximated by a straight line with slope ~7. The binding process itself has not been identified, but it appears to be nearly completely reversible since the water extraction technique detailed in Section 1.1.1.1 is able to approach 100 percent extraction by simple leaching in a large enough amount of water.

Figure 9 compares the binding isotherms obtained when admixing calcium or sodium nitrite (assuming $\varepsilon = 0.1$ in both cases). When nitrite was introduced as sodium nitrite, binding was still present but to a lower extent than in the case of calcium nitrite. At the higher dosage levels the nitrite introduced as sodium nitrite was present in the free and bound forms in roughly the same amounts,

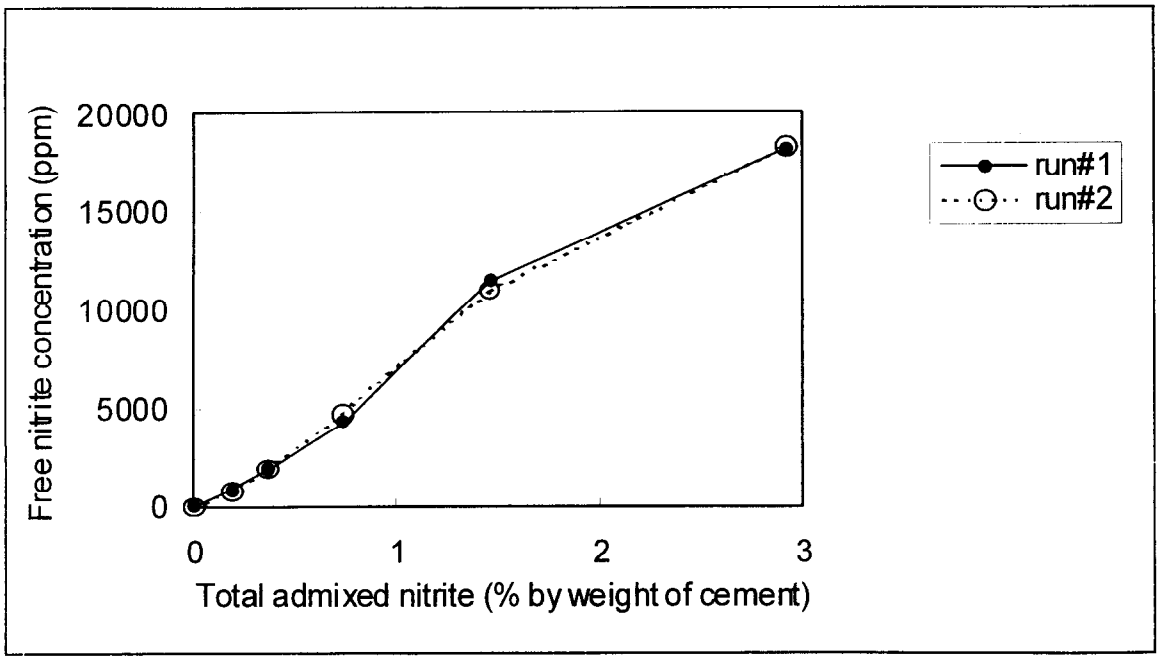

Figure 8. Relationship between total admixed nitrite content in concrete (w/c = 0.45, cement content = 500 kg/m^3) and pore solution free nitrite concentration as determined with PWE method. Results from duplicate specimens (for total nitrite 1% = 5 kg/m^3, for free nitrite 4,600 ppm = 0.1 M).

while the bound form was predominant in the case of calcium nitrite. The relationship between the bound and free contents was noticeably less linear for sodium nitrite than that for calcium nitrite.

Tests with the ISL method were used extensively to investigate effect of nitrite on pore water pH (Section 3.1), and provided independent confirmation of selected PWE results described above.

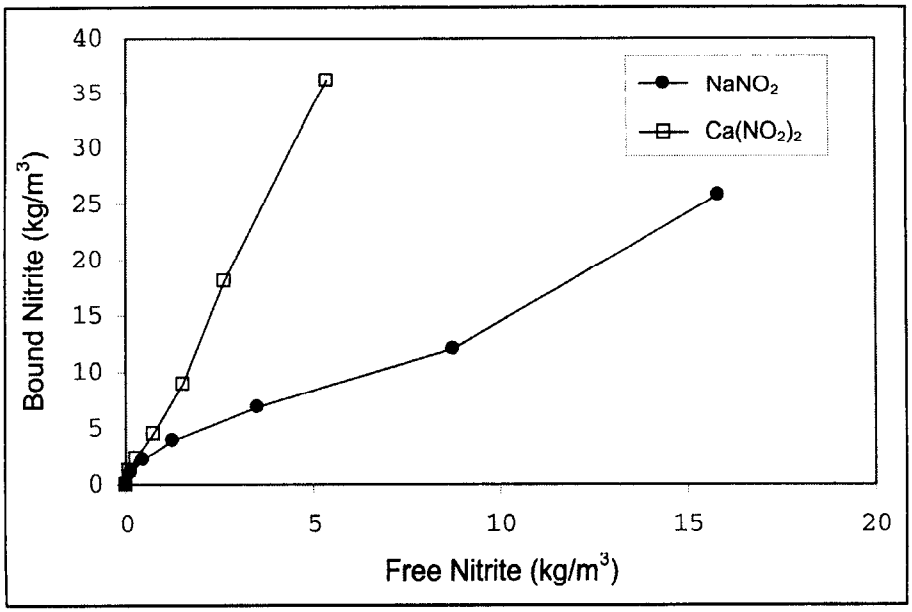

Figure 9. Nitrite binding isotherm in mortar (w/c = 0.45, cement content = 700 kg/m^3) expressed in mass per unit volume of mortar assuming $\varepsilon = 0.1$, as determined by the PWE method.

2.2.3 Nitrite Binding in the Presence of Chloride Ions

Introduction of chloride ions (admixed as sodium chloride) decreased the extent of nitrite binding in mortar admixed as calcium nitrite and released more nitrite into the pore water, as shown in Figure 10 for a series of PWE tests. With enough sodium chloride addition, the binding of nitrite admixed as either calcium or sodium nitrite was essentially the same as in the case of sodium nitrite without chlorides. Admixing sodium chloride did not significantly alter the extent of binding of nitrite admixed as sodium nitrite. The decrease in nitrite binding upon introduction of chlorides in concrete admixed with calcium chloride is a potentially beneficial effect. If the same were to take place when chloride penetrates from the outside (for example in a marine environment), the reduction in binding would lead to an increase in the local free nitrite content coincident with chloride arrival.

2.2.4 Organic Corrosion Inhibitors F and R (FerroGard 901, Rheocrete 222+)

The possible concrete binding characteristics of these inhibitors have not been yet examined, pending development of more reliable analytical methods.

2.3 Other Inhibitor Mechanism Issues - Dosage Needs

2.3.1 Calcium Nitrite-based Inhibitor (DCI-S)

2.3.1.1 Pitting and repassivation tests

Evidence that nitrite concentrations in excess of the chloride concentration suppress initiation of pitting in simulated concrete pore solutions is already well documented in the literature.[5] Tests in this project were conducted to determine the effect of nitrite when chloride contents are significantly

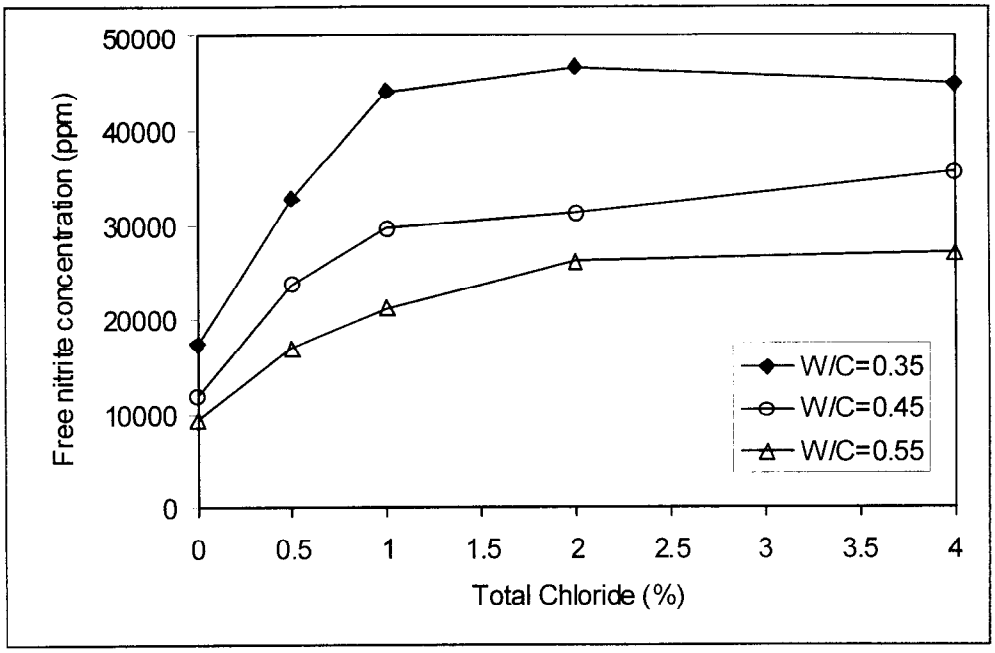

Figure 10. Effect of chloride content on free nitrite in pore solution from mortar (cement content = 700 kg/m^3) containing 1.46% by weight of cement (10.22 kg/m^3 of mortar) total admixed nitrite from DCI-S (1% total chloride = 7 kg/m^3, 4600 ppm free nitrite in pore water = 0.1 M).

in excess. Electrochemical tests of steel were conducted in simulated concrete pore solution ($[K^+]$~0.36 M + $[Na^+]$~0.2 M (balance OH^-); pH~13.6; saturated with $Ca(OH)_2$) with additions of 0.8 M or 1.5 M NaCl and various amounts of nitrite (added as calcium or sodium nitrite). The $[NO_2^-]$ was between 0 M and 0.26 M to represent levels comparable to those encountered in the pore water analyses of concrete with admixed calcium nitrite (Section 2.2.3). Steel specimens with ~60 cm^2 nominal surface area were cut from ordinary reinforcing steel bar and sandblasted before each test. The cyclic polarization technique was employed to determine the pitting and repassivation potential of steel in each specific solution. An anodic scan rate of 0.167 mV/s as specified in the ASTM standard test practice G-61 was used throughout the tests. All tests were performed at 21±2° C. Earlier laboratory experiments indicated that a scan rate of 0.167 mV/s used in the experiments was reasonably away from a domain of large scan rate dependence of the pitting potential.[24]

Results of the tests with calcium nitrite (introduced as DCI-S) are shown in Figures 11 and 12. For both levels of chloride contamination there was a small, gradual increase in the average value of the pitting potential, as well as the repassivation potential, as $[NO_2^-]$ increased from 0 M to 0.26 M. The increase was more notable for the 0.8 M Cl^- solution, for which Ep was about +0.2 V SCE after 0.04 M NO_2^- addition. Since the open-circuit potential of passive steel in concrete tends to be on the order of 0.0 V SCE, it is possible that even this low amount of NO_2^- could have a significant beneficial effect in preventing corrosion initiation (but not propagation, as Er was about 400 mV more negative than Ep in both cases). Observation of the surface of the specimens after completion of each test revealed another possible beneficial effect: without NO_2^- addition, the corrosion on the surface of the specimens involved usually few but large pitted spots, where corrosion propagated easily. In contrast, with NO_2^- the pits tended to be numerous but generally small and with no evidence of fast propagation.

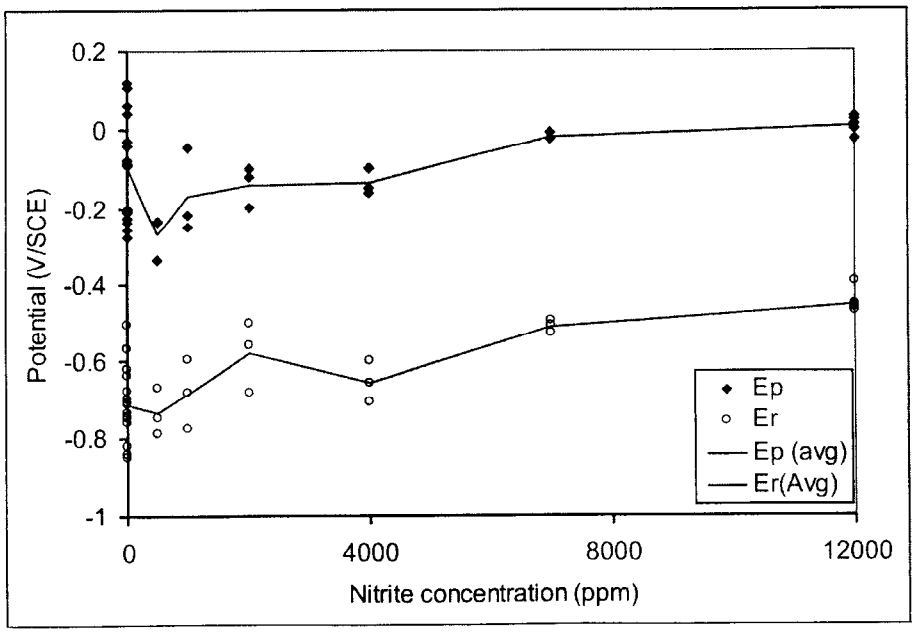

Figure 11. Effect of nitrite content (from DCI-S) on pitting (Ep) and repassivation (Er) potentials of rebar steel (sandblasted, 60 cm^2 nominal surface area) in simulated pore solution with 1.5 M NaCl addition as determined by cyclic polarization technique with an anodic polarization scan rate = 0.167 mV/s (for nitrite concentration, 4600 ppm = 0.1M).

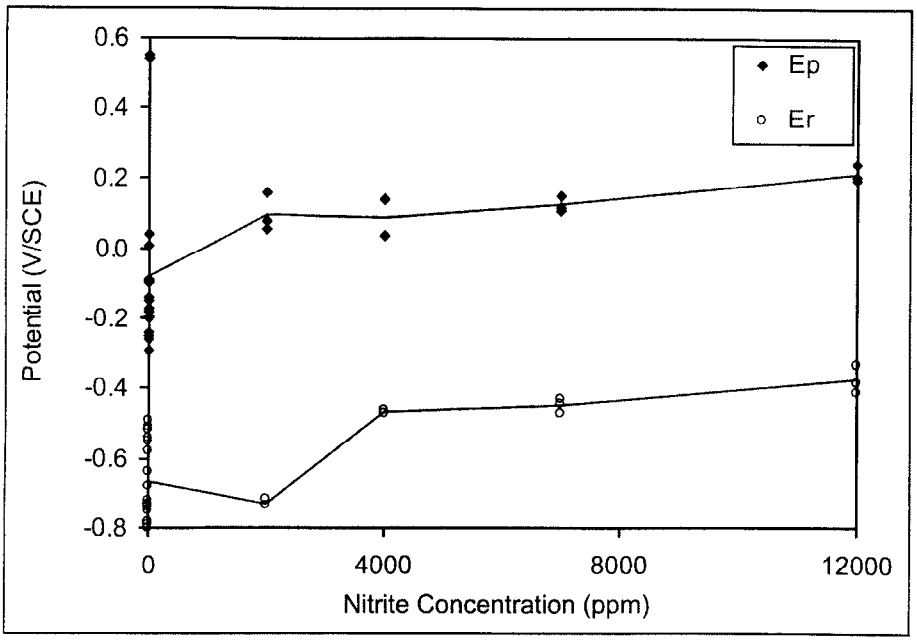

Figure 12. Effect of nitrite content (from DCI-S) on pitting (Ep) and repassivation (Er) potentials of rebar steel (sandblasted, 60 cm^2) in simulated pore solution with 0.8 M NaCl addition as determined by cyclic polarization technique with an anodic polarization scan rate = 0.167 mV/s (for nitrite concentration, 4600 ppm = 0.1 M).

Results of tests with sodium nitrite are presented in Figure 13. For the same amount of nitrite addition, the pitting potential of sandblasted rebar steel in the $NaNO_2$-containing solution was generally ~300 mV higher than that obtained in the $Ca(NO_2)_2$-containing solution. The difference in pitting potentials may be explained by differences in the way in which calcium and sodium nitrite affect the solution pH. As shown in Figure 14, both species lower pH but calcium nitrite does so to a greater extent (discussed further in Section 3.1) and results in a less favorable $[OH^-]$ to $[Cl^-]$ ratio

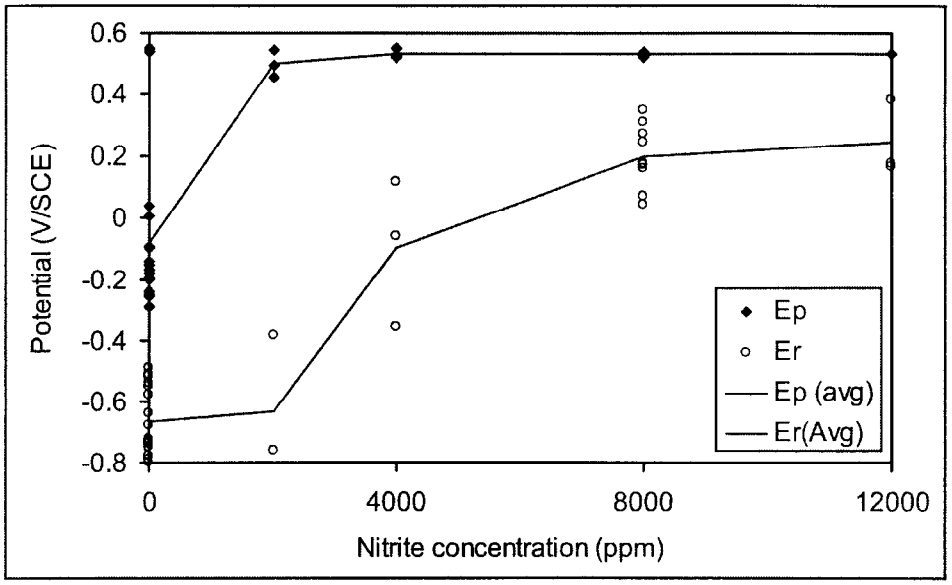

Figure 13. Effect of nitrite content (from $NaNO_2$) on pitting (Ep) and repassivation (Er) potentials of rebar steel (sandblasted, 60 cm^2) in simulated pore solution with 0.8 M NaCl addition as determined by cyclic polarization technique with an anodic polarization scan rate = 0.167 mV/s (for nitrite concentration, 4600 ppm = 0.1 M).

with consequently lower pitting potential. Passivity was promoted whenever either the NO_2^- or the OH^- ion concentration was increased, suggesting that both ions have comparable beneficial roles.

2.3.2 Comparison of Effectiveness of the Three Inhibitor Types

2.3.2.1 Tests in calcium hydroxide solution

Sandblasted rebar steel specimens (nominal area = 60 cm^2) were immersed at the open-circuit potential (E_{oc}) in saturated $Ca(OH)_2$ solutions containing corrosion inhibitors with the following volumetric dosages: 2.6 percent DCI-S, 2.5 percent Rheocrete 222+, and 7.4 percent FerroGard 901. The 2.6 percent DCI-S addition corresponds to 7000 ppm (0.15 M) [NO_2^-] in the solution, an amount comparable to those expected in the pore solution when typical dosages are used (see Section 2.2). Since binding isotherms are not yet available for the other two inhibitors, their concentrations were chosen by assuming provisionally that concrete had a capillary porosity $\varepsilon = 0.1$, and that one half of the total admixed inhibitor goes into the pore solution. The steel specimens were first allowed to passivate in each solution in the absence of any chloride addition. After that, the chloride concentration was raised by adding NaCl in consecutive steps over a period of several months. In the solution containing DCI-S, [Cl^-] was increased in steps to 0.5 M, 1.0 M, 1.5 M, and 2.0 M. In the solutions containing Rheocrete 222+ or FerroGard 901, [Cl^-] was increased in steps to 0.1 M, 0.2 M, and 0.4 M (preliminary tests had indicated that corrosion mode transitions in the organic inhibitor solutions took place at relatively low [Cl^-] levels). The open-circuit potential (E_{oc}) of the steel specimens was monitored throughout the process. Electrochemical Impedance Spectroscopy (EIS) tests were conducted periodically in selected specimens to obtain an estimate of the polarization resistance (Rp), using data in the frequency range ~0.1 Hz to ~0.001 Hz. Nominal corrosion current density (i_{corr}) values were obtained by using the Stearn-Geary equation, $i_{corr} = B/Rp$, with Rp = 0.026

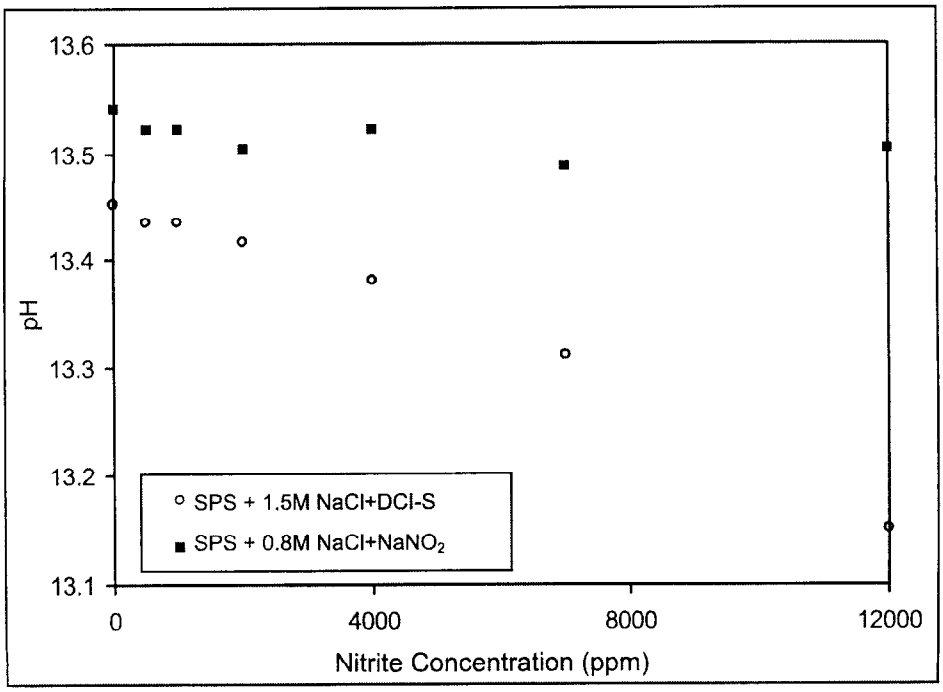

Figure 14. Effect of nitrite addition (from DCI-S or $NaNO_2$) on pH of simulated concrete pore solution (the simulated pore solution without chloride and nitrite was ~13.6).

V.[25] At the end of the immersion tests, each specimen was examined for corrosion morphology and tested for weight loss.

The E_{oc} results as a function of time and chloride addition are shown in Figures 15 through 17. Figure 18 summarizes the i_{corr} measurements as a function of chloride addition. Under the test conditions, DCI-S was the most effective in corrosion inhibition. For this inhibitor, occasional downward fluctuations of E_{oc}, suggestive of unstable passivity breakdown, were observed only when $[Cl^-] > 1$ M. This value is more than one order of magnitude higher than the chloride corrosion threshold reported for steel tested under similar circumstances, but in the absence of inhibitor[25] The nominal corrosion current density was ≤ 0.01 $\mu A/cm^2$, a value normally not associated with .significant corrosion, even when $[Cl^-]$ reached 2 M. Small-sized corrosion pits were found on each specimen upon final inspection, but overall weight loss was negligible.

In the solutions with Rheocrete 222+ or FerroGard 901, potentials indicative of steady active corrosion of steel (about –500 mV/SCE) were detected when $[Cl^-] > 0.2$ M. As $[Cl^-]$ increased toward 0.4 M, the nominal corrosion current density reached top values that were over one order of magnitude higher than in the DCI-S tests. Weight loss measurements at the end of the exposure period were in agreement with the electrochemical observations. The weight loss of the steel (average of 5 specimens) in the DCI-S test solution was 0.019 g, while the loss was 0.19 g and 0.35 g in the Rheocrete 222+ and the FerroGard 901 tests respectively. The difference in behavior between the calcium nitrite and the other inhibitors is notable considering that the terminal chloride concentration was much greater in the DCI-S test solution than in the others.

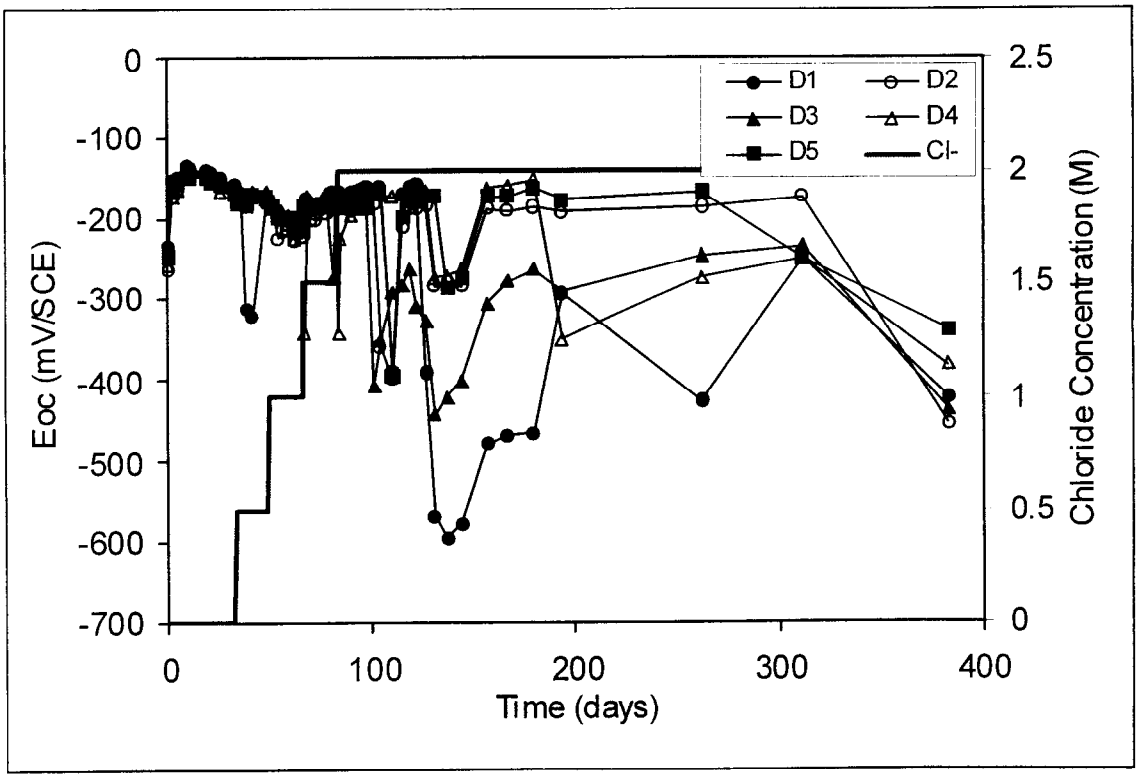

Figure 15. Evolution of Eoc of sandblasted rebar in $Ca(OH)_2$ solution with DCI-S (2.6% v/v, equivalent to 7000 ppm or 0.15 M NO_2^-). Chloride was increased stepwise by adding NaCl into the test solution. D1-D5 indicate replicate specimens.

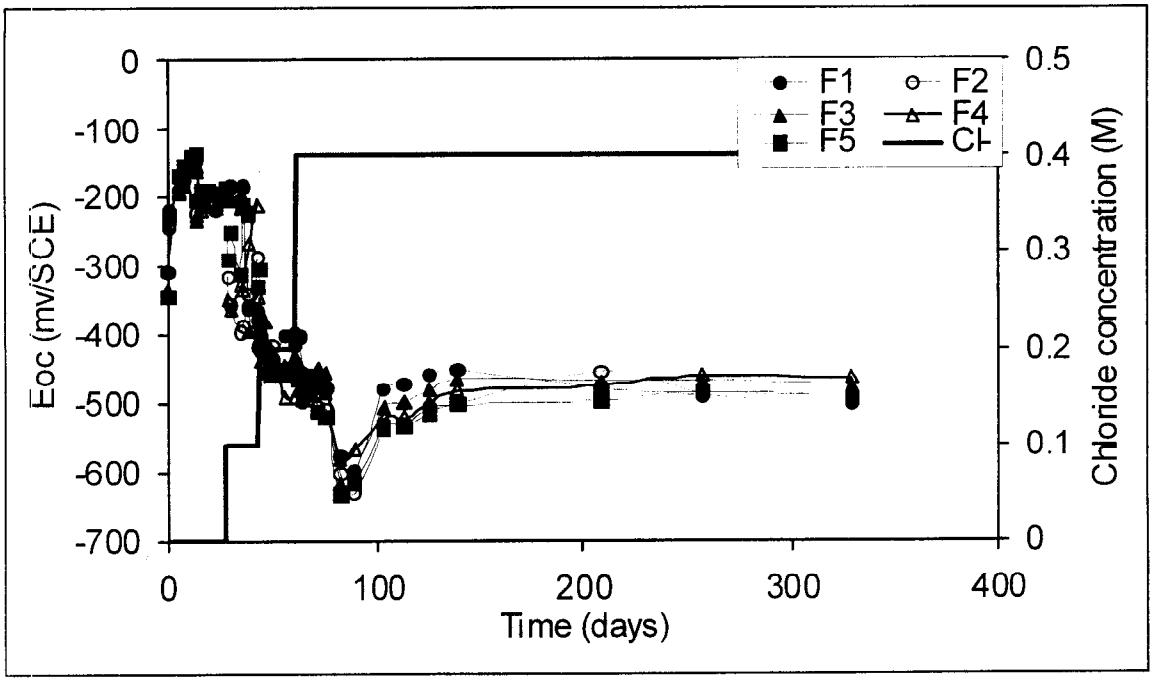

Figure 16. Evolution of Eoc of sandblasted rebar in $Ca(OH)_2$ solution with FerroGard 901 (7.4% v/v). F1-F5 indicate replicate specimens.

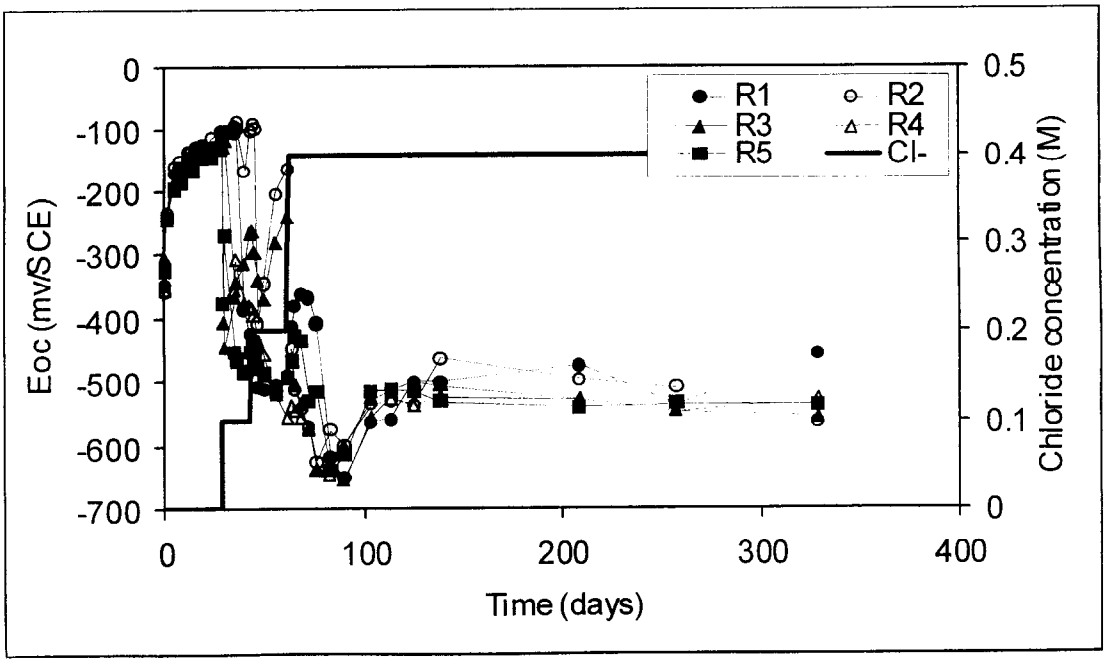

Figure 17. Evolution of Eoc of sandblasted rebar in $Ca(OH)_2$ solution with Rheocrete 222+ (2.5% v/v). R1-R5 indicate replicate specimens.

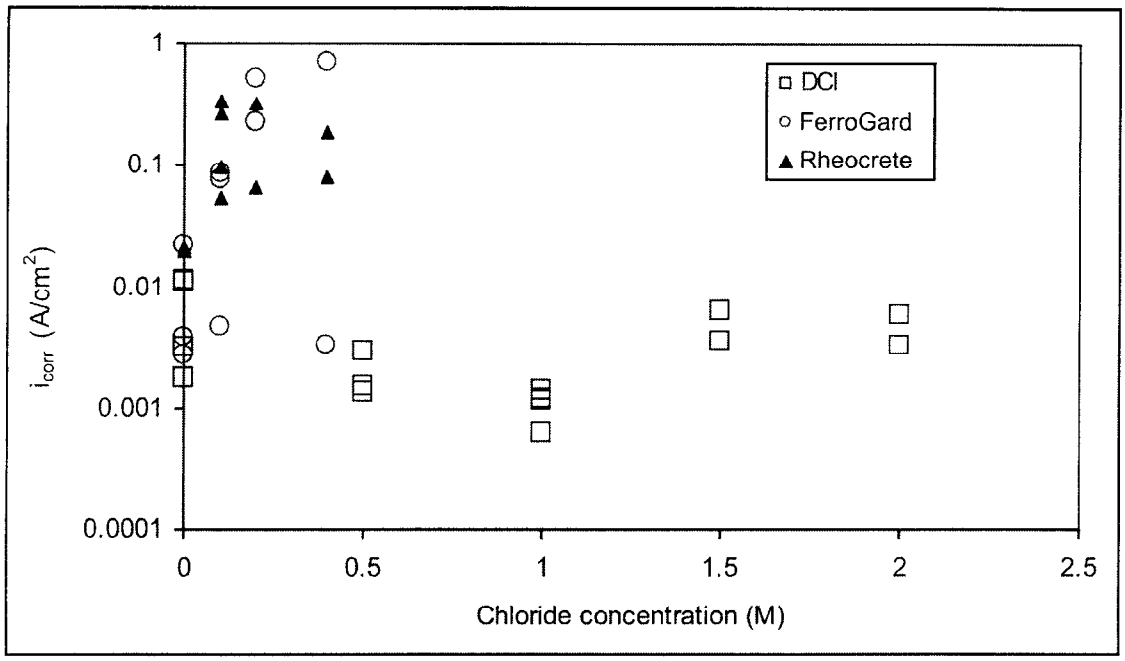

Figure 18. Nominal corrosion rates from EIS as a function of added chloride content.

OBJECTIVE 3 - DETERMINE POSSIBLE NEGATIVE SIDE EFFECTS – MECHANISTIC ISSUES

3.1 Effect on pH of Pore Solution

3.1.1 Calcium Nitrite-based Inhibitor (DCI-S)

The presence of DCI-S had a significant effect on pore solution pH, as shown by tests using the ISL method (Section 2.2.1.2) performed on concrete with and without admixed DCI-S (mixtures CDCI and CCTR respectively, Table 11). Addition of 22 L/m^3 DCI-S in concrete decreased the pore solution pH by about 0.3 units (Figure 19). The pH drop was proportional to the total nitrite dosage in concrete (Figure 20). Although the presence of NO_2^- ions in the pore solution is beneficial to the pitting resistance of reinforcing steel in concrete, the decrease of pore solution pH upon introduction of calcium nitrite could lessen its inhibition effect as compared with sodium nitrite. This issue has been discussed in Section 2.3 when documenting this effect in simulated pore water solutions.

The pH drop can be interpreted as a result of the limited solubility of Ca^{2+} ions. Calcium nitrite is highly soluble in neutral water (46 g at 0°C and 89 g at 91°C in 100 mL of water for $Ca(NO_2)_2{\cdot}2H_2O$).[26] However, in solutions of very high pH value the concentration of Ca^{2+} ions is strongly limited by the solubility product of $Ca(OH)_2$ ($K_{sp}=1.3\times10^{-6}$ at 25° C).[27] For example, in a solution of pH 13 at 25 °C the solubility of Ca^{2+} is $\sim8\times10^{-5}$ M, which is about 1/200 of the concentration of a pH 12.6 solution containing only saturated $Ca(OH)_2$ at the same temperature. Since the concrete pore solution without corrosion inhibitor had pH ~13.4, the equilibrium amount of Ca^{2+} ions was very small. The presence of calcium nitrite in the pore solution causes part of its Ca^{2+} ions to react with the OH^- ions in the solution to precipitate calcium hydroxide as follows:

$$Ca^{2+} + 2OH^- \rightarrow Ca(OH)_2\ (s) \qquad (7)$$

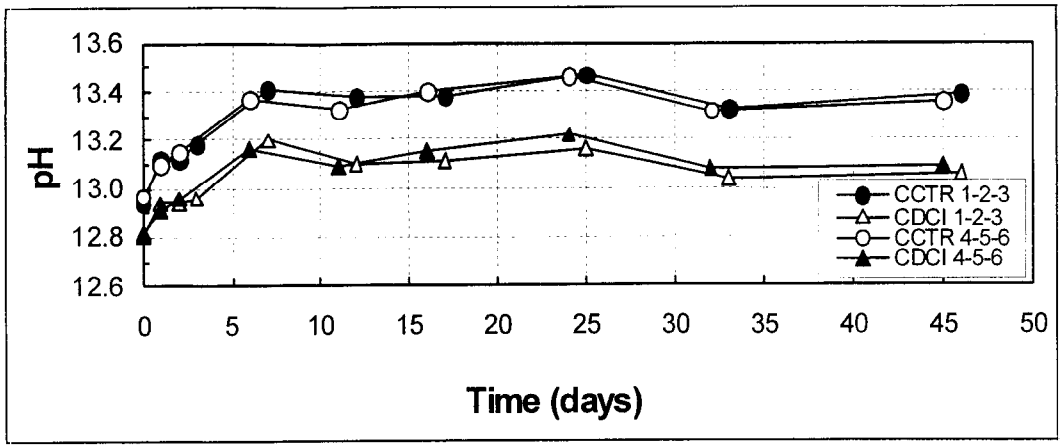

Figure 19. Evolution of pH in concrete holes of duplicate specimens using the ISL method (calibrated to 21° C). CCTR: Concrete specimens without NO_2^-, CDCI: with NO_2^-. Mix design listed in Table 11.

The precipitation of $Ca(OH)_2$ (and consequent reduction in pH) takes place until a new equilibrium is reached in accordance with the value of the solubility product. Charge neutrality has to be maintained by replacing OH^- ions with an equal amount of NO_2^- ions if the total alkali content in the pore solution is assumed to be unaffected by the introduction of calcium nitrite. The NO_2^- concentration in the pore solution (8,000 ppm, or 0.17 M, measured in the CDCI concrete specimens by ISL) greatly exceeds that of Ca^{2+} in the pH range of interest. The pH depression due to the presence of the inhibitor can then be simply estimated from

$$[OH^-]_n - [OH^-]_i = [NO_2^-] \qquad (8)$$

where the subscripts i and n correspond to the conditions with inhibitor and without inhibitor respectively. As an independent check, the nitrite concentration in the pore solution could be

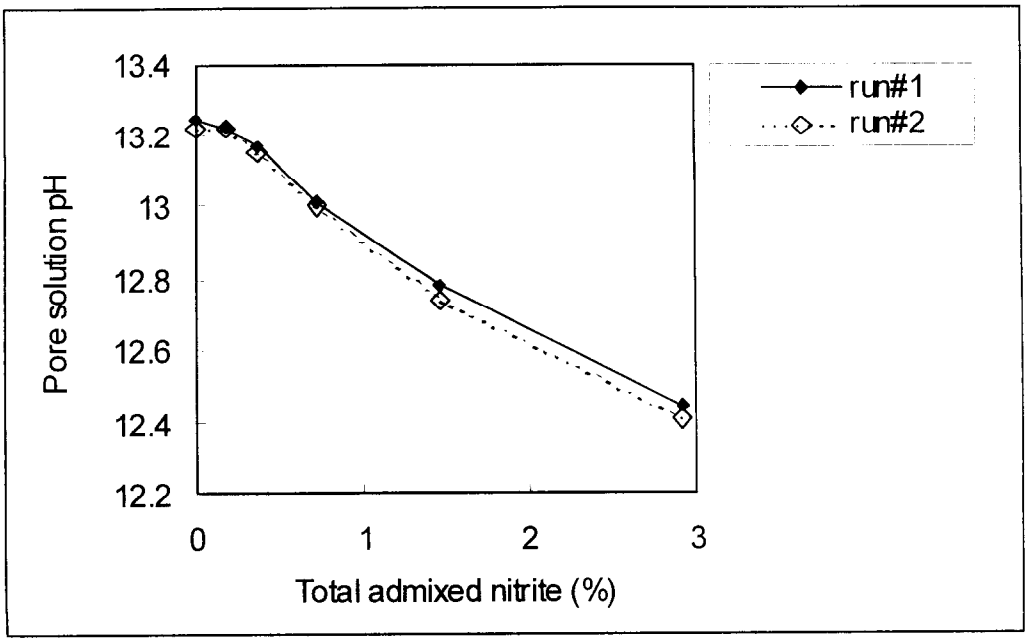

Figure 20. Effect of nitrite dosage (from DCI-S) on the pore solution pH expressed from concrete (w/c = 0.45, cement content = 500 kg/m^3) (1% total nitrite = 5 kg/m^3 of concrete; 4600 ppm free nitrite in pore water = 0.1 M).

estimated from the pH measurements according to:

$$[NO_2^-] = \frac{10^{(pH_n - X)}}{\gamma_n} - \frac{10^{(pH_i - X)}}{\gamma_i} \qquad (9)$$

where X is the logarithm of the dissociation constant of water, pH_i and pH_n are the pH, and γ_i and γ_n are the activity coefficients, of OH^- ions in pore solution in concrete and mortar with and without inhibitor respectively. Using the approximations X = -14, $\gamma_i = 1$, and $\gamma_n = 1$, application of Eq (9) to the example in Figure 19 ($pH_n \sim 13.4$; $pH_i \sim 13.1$) yields $[NO_2^-] \sim 0.12$ M, which is on the order of the directly measured value of 0.17 M. More detailed examples using this approach are given in Reference (6).

3.1.2 Organic Corrosion Inhibitors

Preliminary tests with Rheocrete 222+ and FerroGard 901 did not reveal any significant effect of the presence of these inhibitors on the pH of the concrete pore solution.

OBJECTIVE 4 - ESTIMATE LONG-TERM EFFECTIVENESS – PERFORMANCE TESTS

4.1 Perform Long-Term Laboratory Tests, Outdoor Sheltered Tests, and Field Tests

4.1.1 Approach and Experimental Procedures

The purpose of these tests was to evaluate the effect of the presence of each type of inhibitor and its dosage on the onset and progression of corrosion in concrete. Special emphasis was given to establishing the critical chloride concentrations for corrosion initiation for each inhibitor, as a function of concrete mix parameters. The tests are designed to obtain critical chloride concentrations by incorporating information from nondestructive electrochemical testing, periodic sampling for chloride content, and detailed autopsy analysis. The variables examined included type of concrete (Type II cement concrete, concrete admixed with microsilica, and concrete admixed with both fly ash and microsilica), type of inhibitor (each of the three commercial products plus blank controls), and extent of inhibitor addition (full dosage and half dosage).

A summary of the mix proportions used is given in Table 12. All mixes used 985 kg/m^3 coarse aggregate with a maximum diameter of 10 mm. The coarse aggregate was oolitic limestone unless otherwise indicated. The fine aggregate was silica sand with a fineness module of 2.16. The cementitious factor was 7 bags (390 kg/m^3), with either 20% Type F fly ash and/or 8% silica fume replacement of cementitous material. Examples of typical mix designs used are listed in Table 3.

The concrete was batched in a 27-ft^3 central mixer, which is located in a warehouse environment. During extreme conditions, batching was conducted with a portable mixer in a temperature-controlled room. To maintain control of the w/c ratio, all components were carefully measured and aggregate moisture adjustments were made according to standards. All aggregate was obtained from FDOT approved sources, and tests were conducted to determine proper gradation before batching. The bagged aggregate was submerged in water and completely saturated prior to mixing. One hour before mixing began the aggregate was removed from the tanks and placed on grating. This was done to drain excess moisture from the aggregate and to ensure a more accurate w/c ratio was

Table 12. Concrete Mix Proportions

	7-BAG STD MIX	WATER/CEMENT RATIO	20% FLY ASH	8% SILICA FUME	GRANITE
C1	X	0.41			
C2	X	0.50			
P1	X	0.41	X		
P2	X	0.41	X	X	
P3	X	0.50	X		
P4	X	0.41		X	
G1	X	0.41			X

achieved. The concrete was placed into the forms in two lifts using ordinary hand tools. A table vibrator was used to consolidate the laboratory specimens. For each lift, the concrete was vibrated for 45 seconds. Specimens for field testing were externally vibrated after each lift. After the specimens were cast, they were given a light trowel finish and covered with polyethylene film for 24 hours. Next, the forms were stripped and specimens for G-109 tests (see below) were transported to a moisture room where they remained for 28 days. Upon removal from the moisture chamber, the G-109 specimens were sealed in polyethylene bags to prevent carbonation. The specimens remained in the bags until they were 90 days old to ensure that some degree of maturity developed before testing commenced. All other specimens were cured in 100% humidity conditions for 72 hours and also cured for at least 90 days before testing. Other differences in typical fabrication of the G-109 specimens include: Specimens were cast upside down to minimize subsidence cracking over the top rebar (anode), and the specimen face to be ponded was not wire-brushed since it was a form face rather than a floated surface.

Three basic types of reinforced concrete specimens were used: Specimens manufactured and tested in accordance with a standard laboratory test method (ASTM G-109; Figure 21(a)); sheltered, outdoor specimens designed to provide relatively short-term results (three-bar columns - uncracked, cracked, and blank, Figure 22(a)); and specimens that will provide long-term test results (field columns, Figure 23(a)). The dimensions and physical arrangement of each type of specimen are detailed in Figures 21(b), 22(b), and 23b). The nomenclature used to designate each combination of specimen type, mix design, and inhibitor dosage is indicated in Table 13. Control specimens without inhibitor addition are indicated by CTRL. Examples of specific mix designs are given in Table 3. Inhibitor dosages are indicated by either 1.0 (full recommended dosage per manufacturer guidelines) or 0.5 (half dosage). Specimens with 0.24 kg/m^3 Cl^- addition are indicated by Cl. The nomenclature is self-explanatory for the rest of the cases. The number of specimen replicates made for each combination is indicated in the table.

Triplicate specimens of selected three-bar specimens had cracks deliberately introduced. The purpose of cracking these specimens was to determine if the corrosion inhibitors could slow or prevent the formation of corrosion, even in the presence of cracks. The procedure for introducing the cracks was as follows: a groove 6 mm wide and 13 mm deep was cut 178 mm from the bottom of the

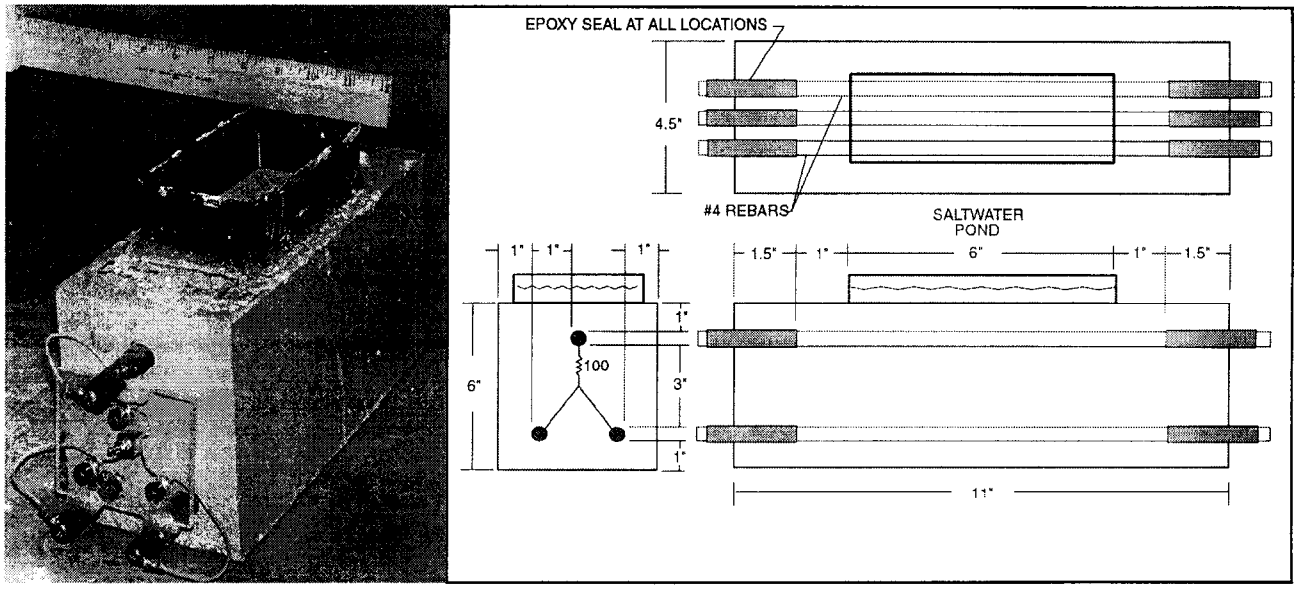

(a) (b)

Figure 21. Standard laboratory test method (ASTM G-109).

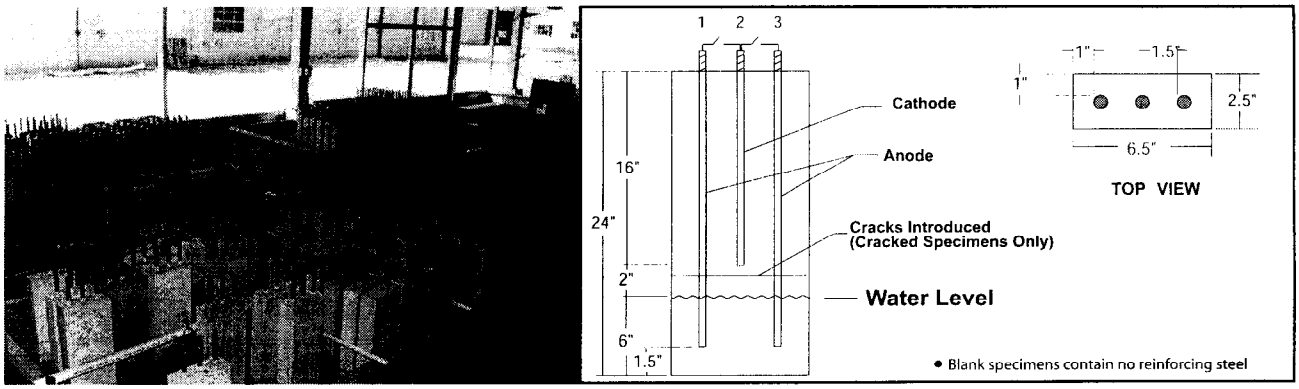

(a) (b)

Figure 22. Sheltered outdoor specimens.

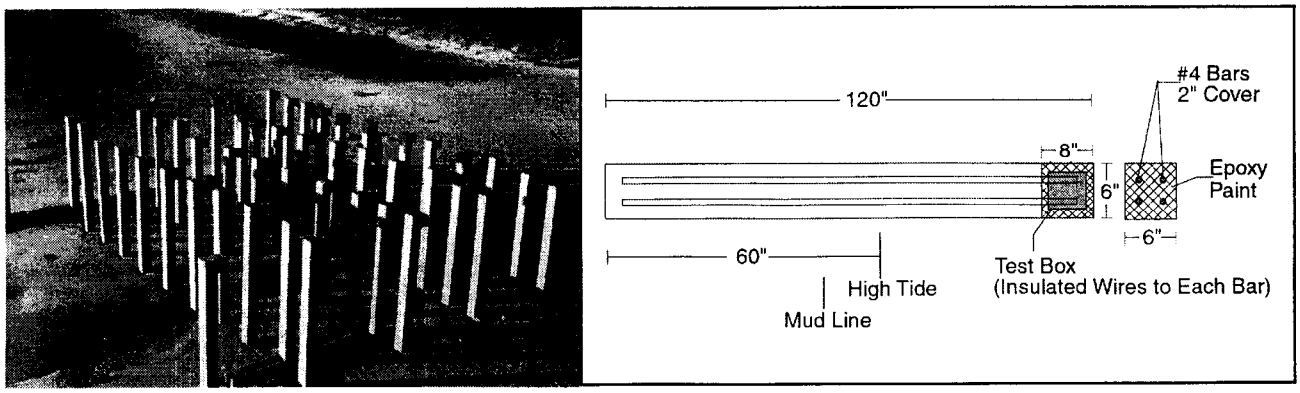

(a) (b)

Figure 23. Field columns.

Table 13. Concrete Mix Matrix.

MIX GROUP C1: w/c = 0.41													
MIX NAME	3-BAR COLUMN	3-BAR CRK COLUMN	BLANK COLUMN	G109	FIELD COLUMN	4X8 CYL RCP & WP*	6X12 CYL BREAKS	C490 LNTH CHNG	REPAIR	IMPRESS CURRENT	3X6 CYL LEACH	REINF PRISM	Total/Mix
CTRL-C1-1	6	3	2	3	0	4	7	6	12	3	6	0	52
CTRL-C1-2	0	0	0	0	3	0	0	0	0	0	0	0	3
FER-C1-0.5	6	0	2	3	0	0	0	0	0	0	0	0	11
FER-C1-1.0	6	3	2	3	3	4	7	6	0	3	6	0	43
DCI-C1-0.5	6	0	2	3	0	0	0	0	0	0	0	0	11
DCI-C1-1.0	6	3	2	3	3	4	7	6	0	3	6	0	43
REO-C1-0.5	6	0	2	3	0	0	0	0	0	0	0	0	11
REO-C1-1.0	6	3	2	3	3	4	7	6	0	3	6	0	43
TOTAL	42	12	14	21	12	16	28	24	12	12	24	0	217
MIX GROUP C2: w/c = 0.50													
MIX NAME	3-BAR COLUMN	3-BAR CRK COLUMN	BLANK COLUMN	G109	FIELD COLUMN	4X8 CYL RCP & WP	6X12 CYL BREAKS	C490 LNTH CHNG	REPAIR	IMPRESS CURRENT	3X6 CYL LEACH	REINF PRISM	Total/Mix
CTRL-C2	6	0	2	3	0	4	6	0	0	3	0	0	24
FER-C2-1.0	6	0	2	3	0	4	6	0	0	3	0	0	24
DCI-C2-1.0	6	0	2	3	0	4	6	0	0	3	0	0	24
REO-C2-1.0	6	0	2	3	0	4	6	0	0	3	0	0	24
TOTAL	24	0	8	12	0	16	24	0	0	12	0	0	96
MIX GROUP P1: w/c = 0.41, 20% FA													
MIX NAME	3-BAR COLUMN	3-BAR CRK COLUMN	BLANK COLUMN	G109	FIELD COLUMN	4X8 CYL RCP & WP	6X12 CYL BREAKS	C490 LNTH CHNG	REPAIR	IMPRESS CURRENT	3X6 CYL LEACH	REINF PRISM	Total/Mix
CTRL-P1-1	6	3	2	6	0	4	8	6	12	3	0	12	62
CTRL-P1-2	0	0	0	0	3	0	0	0	0	0	0	0	3
CTRL-P1+Cl	0	0	0	0	0	0	1	0	0	0	0	0	1
FER-P1-0.5	6	0	2	3	0	0	0	0	0	0	0	0	11
FER-P1-1.0	6	3	2	6	3	4	8	6	0	3	6	12	59
FER-P1+Cl	0	0	0	0	0	0	1	0	0	0	0	0	1
DCI-P1-0.5	6	0	2	3	0	0	0	0	0	0	0	0	11
DCI-P1-1.0	6	3	2	6	3	4	8	6	0	3	6	12	59
DCI-P1+Cl	0	0	0	0	0	0	1	0	0	0	0	0	1
REO-P1-0.5	6	0	2	3	0	0	0	0	0	0	0	0	11
REO-P1-1.0	6	3	2	6	3	4	8	6	0	3	6	12	59
REO-P1+Cl	0	0	0	0	0	0	1	0	0	0	0	0	1
TOTAL	42	12	14	33	12	16	36	24	12	12	18	48	279
MIX GROUP P2: w/c = 0.41, 20% FA, 8% SF.													
MIX NAME	3-BAR COLUMN	3-BAR CRK COLUMN	BLANK COLUMN	G109	FIELD COLUMN	4X8 CYL RCP & WP	6X12 CYL BREAKS	C490 LNTH CHNG	REPAIR	IMPRESS CURRENT	3X6 CYL LEACH	REINF PRISM	Total/Mix
CTRL-P2-1	6	3	2	6	3	8	10	6	0	3	0	0	47
CTRL-P2+Cl	0	0	0	0	0	0	1	0	0	0	0	0	1
FER-P2-0.5	6	0	2	3	0	0	0	0	0	0	0	0	11
FER-P2-1.0	6	3	2	6	3	8	10	6	0	3	6	0	53
FER-P2+Cl	0	0	0	0	0	0	1	0	0	0	0	0	1
DCI-P2-0.5	6	0	2	3	0	0	0	0	0	0	0	0	11
DCI-P2-1.0	6	3	2	6	3	8	10	6	0	3	6	0	53
DCI-P2+Cl	0	0	0	0	0	0	1	0	0	0	0	0	1
REO-P2-0.5	6	0	2	3	0	0	0	0	0	0	0	0	11
REO-P2-1.0	6	3	2	6	3	8	10	6	0	3	6	0	53
REO-P1+Cl	0	0	0	0	0	0	1	0	0	0	0	0	1
TOTAL	42	12	14	33	12	32	44	24	0	12	18	0	243

Table 13. Concrete Mix Matrix - continued

MIX GROUP P3: w/c = 0.50, 20% FA													
MIX NAME	3-BAR COLUMN	3-BAR CRK COLUMN	BLANK COLUMN	G109	FIELD COLUMN	4X8 CYL RCP & WP*	6X12 CYL BREAKS	C490 LNTH CHNG	REPAIR	IMPRESS CURRENT	3X6 CYL LEACH	REINF PRISM	Total/Mix
CTRL-P3	6	0	2	6	0	8	9	0	12	3	0	0	46
FER-P3-1.0	6	0	2	6	0	8	9	0	0	3	6	0	40
DCI-P3-1.0	6	0	2	6	0	8	9	0	0	3	6	0	40
REO-P3-1.0	6	0	2	6	0	8	9	0	0	3	6	0	40
TOTAL	24	0	8	24	0	32	36	0	12	12	18	0	166
MIX GROUP P4: w/c = 0.41, 8% SF													
MIX NAME	3-BAR COLUMN	3-BAR CRK COLUMN	BLANK COLUMN	G109	FIELD COLUMN	4X8 CYL RCP & WP	6X12 CYL BREAKS	C490 LNTH CHNG	REPAIR	IMPRESS CURRENT	3X6 CYL LEACH	REINF PRISM	Total/Mix
CTRL-P4	6	3	2	3	0	8	8	0	0	3	0	0	33
FER-P4-1.0	6	3	2	3	0	8	8	0	0	3	0	0	33
DCI-P4-1.0	6	3	2	3	0	8	8	0	0	3	0	0	33
REO-P4-1.0	6	3	2	3	0	8	8	0	0	3	0	0	33
TOTAL	24	12	8	12	0	32	32	0	0	12	0	0	132
MIX GROUP G1: w/c = 0.41													
MIX NAME	3-BAR COLUMN	3-BAR CRK COLUMN	BLANK COLUMN	G109	FIELD COLUMN	4X8 CYL RCP & WP	6X12 CYL BREAKS	C490 LNTH CHNG	REPAIR	IMPRESS CURRENT	3X6 CYL LEACH	REINF PRISM	Total/Mix
CTRL-G1-1	6	3	2	3	0	8	9	6	12	3	0	0	52
CTRL-G1-2	0	0	0	0	3	0	0	0	0	0	0	0	3
FER-G1-1.0	6	3	2	3	3	8	9	6	0	3	0	0	43
DCI-G1-1.0	6	3	2	3	3	8	9	6	0	3	0	0	43
REO-G1-1.0	6	3	2	3	3	8	9	6	0	3	0	0	43
TOTAL	24	12	8	12	12	32	36	24	12	12	0	0	184
TOTAL NUMBER OF SAMPLES/SAMPLE TYPE													
SAMPLE TYPE	3-BAR COLUMN	3-BAR CRK COLUMN	BLANK COLUMN	G109	FIELD COLUMN	4X8 CYL RCP & WP	6X12 CYL BREAKS	C490 LNTH CHNG	REPAIR	IMPRESS CURRENT	3X6 CYL LEACH	REINF PRISM	Total/Mix
TOTAL	222	60	74	147	48	176	236	96	48	84	78	48	1317

* RCP - Rapid chloride permeability
WP - Water permeability

specimen. The groove was cut into three sides of the specimen and steel collars were placed 6 mm from each side of the groove. The steel collars were designed to prevent the concrete from being crushed and control the position of the crack. Each specimen was placed in a compression machine under three-point loading; pressure was slowly applied until a visible crack developed. The deflection of the rebar maintained the crack width between 0.01 mm and 0.08 mm, with an average width of 0.04 mm.

4.1.2 Test Progression, Laboratory and Outdoor Sheltered Tests

Concrete preparation in batches for this project began on December 16, 1996, and continued until the last mix was completed on June 19, 1997. Initial testing of ASTM G-109 specimens commenced in March 1997, and for the three-bar specimens it began in October 1997. The G-109 specimens are housed in a constant temperature, constant humidity chamber per ASTM G-109. This testing schedule requires a two week dry cycle followed by a two week wet cycle, with all tests conducted in the middle of the wet cycle. The specimens are ponded in a 3 percent NaCl solution and the ponds are covered to reduce evaporation. At the end of the two week wet cycle the solution is removed, and the lids remain off to allow the concrete to fully dry. Exposure conditions for the outdoor sheltered specimens consisted of continuous partial immersion, as indicated in Figure 22(b), in a solution of 3 percent NaCl, at temperatures corresponding to the daily cycle encountered in Gainesville, Florida, starting October 1997. The four tanks are interconnected and two pumps are used to circulate the water. The water is circulated twice per day to obtain full water aeration and uniform chloride content in the four tanks. The water depth is measured weekly and water is added to compensate for evaporation. Salt is added as necessary to maintain the desired concentration. Periodic specimen tests included half-cell potentials (using a saturated calomel electrode, [SCE]), macrocell current, interelectrode resistance, resistance to an external electrode, EIS, polarization resistance, and wet surface resistivity.

4.1.3 Test Progression, Field Test Specimens

The field specimens were constructed during Spring 1997. Field installation of these specimens was delayed due to environmental permit difficulties. Installation of the forty-eight specimens at the FDOT Crescent Beach outdoor field test facility in Florida began on February 23, 1999, and was completed on March 3, 1999. Initial testing began 8 days after the onset of saltwater exposure. Three sets of corrosion measurements have been collected for these field specimens. Concrete resistance measurements (increasing resistance) indicate that the specimens are continuing to cure and as yet no corrosion activity is apparent. Four field specimens to be studied simultaneously were already in place at Matanzas Inlet in Florida. Two of those specimens (all with a 0.41 w/c ratio) are control mixes and two specimens contain calcium nitrite (5.4 gal/yd^3). The specimens were cast in Spring 1986 and installed in Spring 1987.

Routine monitoring of the experimental test piles is in progress. Tests include half-cell potentials vs. a saturated copper-copper sulfate electrode, macrocell current, interelectrode resistance, resistance to an external titanium electrode, EIS, polarization resistance, and surface resistivity. The half-cell potentials vs. an SCE at the soil level indicate uncertain corrosion activity of the rebar in that area for the control specimens, but generally passive behavior for the specimens containing calcium nitrite.

In November 1992 two lanes were added to Bridge #150138 on State Road 60 over Tampa Bay, Florida. Four experimental piles and caps were included in this construction project. The

experimental piles and caps contain Type II cement with low w/c ratios (0.30 and 0.33 respectively). The mix design specified that the cementitious material be replaced with 8% silica fume and 20% Type F fly ash, and that the mix also contain 22 L/m^3 of DCI-S. The experimental piles/caps are located well above the high tide mark with exposure to salt water limited to extreme storm surges. In April 1997 FDOT personnel performed an in-depth corrosion survey of these four piles/caps. Electrochemical tests revealed no corrosion activity, consistent with the relatively moderate exposure conditions of these piles. Monitoring of this test site continues.

4.2 Evaluation of Inhibitor Performance

4.2.1 Scope of Early Observations

This report covers test results obtained until mid-late 1999. Within this period, most of the test specimens remained inactive. Significant manifestations of corrosion were observed only in some of the three-bar column groups and reporting will be limited to those categories.

Each three-bar column specimen was monitored until visual indications of corrosion-induced cracking were observed on the surface of the specimen. That event was designated as specimen failure and the failed specimen was removed from the test tank for autopsy. Testing on the unfailed replicates continued.

Upon later examination, some specimens were found to contain bars that had shifted out of position during casting. Those specimens and their corresponding time-to-failure and electrochemical data were removed from consideration when computing average properties or statistical analyses of the peer group (however, some of the discarded specimens were used to evaluate chloride penetration). The number of remaining specimens in each group is indicated as "TOTAL" in Table 15.

The pre-cracked three-bar specimens experienced very early failures. In June 1998 one third of those specimens were removed from the tanks, and in November 1999 the last cracked specimens were removed. Because of the early development of failure there was little differentiation in behavior between the various categories of pre-cracked specimens, and analysis of those results has been suspended. Of the remaining three-bar columns, three groups experienced significant deterioration through June 1999 and will be discussed in detail. The mixes for those groups were C1 (no pozzolans, 0.41 w/c ratio), C2 (no pozzolans, 0.50 w/c ratio), and P3 (20 percent fly ash replacement, 0.50 w/c ratio). Autopsy information obtained from failed specimens is listed in Table 14. Chloride contents were measured from concrete removed from the failed specimen as indicated in Figure 24. In this section, only the results for the specimens with full inhibitor dose will be considered; the effect of dosage reduction will be discussed in Section 5.1.

Figures 25, 26, and 27 show the evolution of half-cell potentials for mix groups C1, C2, and P3, respectively. A nominal threshold of -280 mV/SCE (which would indicate greater than 90 percent probability of corrosion activity per ASTM C-876) was adopted for comparison purposes. The potentials shown are the average of the specimens of a given type remaining in the tank at the indicated time. Charting is discontinued after 50 percent of the initial specimens in the group failed.

The sum of the currents flowing between the center bar and the side bars (indicative of corrosion macrocell activity) was averaged for all the specimens in these groups and is plotted as a function of exposure time in Figures 28(a), 29(a), and 30(a). Polarization resistance histories for selected

Table 14. Three-Bar Column Autopsy Description
(Intentionally cracked specimens are not included).

SAMPLE NAME	SAMPLE ID	DAYS TO FAILURE	CRACK LOCATION	BAR	CRACK WIDTH	CRACK LENGTH
CTRL-C1	A	250	FRONT	2	N/A	N/A
	D	346	RIGHT FACE	3	0.08 mm	60.26 mm
FER-C1-0.5	A	390	FRONT	3	0.08 mm	35.12 mm
	B	390	FRONT, BACK	3	max. 0.40 mm	max. 81.92 mm
	C	476	LEFT FACE	1	max. 0.10 mm	max. 98.10 mm
	D	530	RIGHT FACE	3	0.10 mm	49.84 mm
	E	390	RIGHT FACE, BOTTOM	3	max. 0.20 mm	max. 68.11 mm
	F	390	LEFT FACE	1	0.10 mm	156.55 mm
FER-C1-1.0	A	390	FRONT, RIGHT FACE	3	max. 0.15 mm	max. 62.47 mm
	B	390	FRONT, RIGHT FACE	3	max. 0.20 mm	max. 141.96 mm
	D	306	N/A	3	N/A	N/A
	F	390	LEFT FACE	1	0.20 mm	101.14 mm
DCI-C1-0.5	F	390	FRONT, RIGHT FACE	3	max. 0.25 mm	max. 119.11 mm
DCI-C1-1.0	B	530	FRONT	1	0.10 mm	191.78 mm
	E	476	RIGHT FACE	3	0.25 mm	115.37 mm
REO-C1-0.5	A	390	RIGHT FACE	3	0.30 mm	58.55 mm
	C	390	FRONT	3	max. 0.08 mm	max. 20.45 mm
	F	306	FRONT, R FACE, BACK	3	max. 0.25 mm	max. 96.69 mm
REO-C1-1.0	A	390	FRONT, LEFT FACE	1	max. 0.25 mm	max. 104.35 mm
	C	167	RIGHT FACE	3	0.10 mm	84.74 mm
CTRL-C2	C	138	FRONT, RIGHT FACE	3	max. 0.30 mm	max. 198.08 mm
	D	138	FRONT, LEFT FACE	1	max. 0.25 mm	max. 128.18 mm
	E	306	FRONT, RF, LF, BOTTOM	1,3	max. 0.40 mm	max. 151.32 mm
	F	167	FRONT, R FACE, L FACE	1,3	max. 0.50 mm	max. 97.51 mm
FER-C2-1.0	B	476	RIGHT FACE, LEFT FACE	1,3	max. 0.20 mm	max. 106.66 mm
	D	167	LEFT FACE	1	0.50 mm	203.92 mm
	E	250	FRONT, RIGHT FACE	3	max. 0.20 mm	max. 111.53 mm
	F	224	FRONT, RIGHT FACE	3	max. 0.15 mm	max. 140.24 mm
DCI-C2-1.0	A	306	FRONT, LEFT FACE	1	max. 0.5 mm	max. 187.96 mm
	B	306	FRONT, LEFT FACE	1	max. 0.20 mm	max. 191.03 mm
	C	306	RIGHT FACE	3	0.15 mm	130.09 mm
	E	306	RIGHT FACE	3	max. 0.10 mm	max. 78.67 mm
	F	306	FRONT	3	0.08 mm	102.22 mm
REO-C2-1.0	A	306	RIGHT FACE	3	max. 0.20 mm	max. 115.13 mm
	B	306	FRONT	3	0.15 mm	148.73 mm
	C	390	FRONT, R FACE, L FACE	1,3	max. 0.33 mm	max. 209.70 mm
	D	194	FRONT, LF, BOTTOM	1	max. 0.40 mm	max. 228.64 mm
	E	390	FRONT, RIGHT FACE	1,3	max. 0.20 mm	max. 173.52 mm

SAMPLE NAME	SAMPLE ID	DAYS TO FAILURE	CRACK LOCATION	BAR	CRACK WIDTH	CRACK LENGTH
CTRL-P1	D	530	FRONT	3	0.10 mm	19.18 mm
	F	530	FRONT	3	0.08 mm	43.28 mm
FER-P1-0.5	D	306	FRONT, RIGHT FACE	3	max. 0.08 mm	max. 60.35 mm
	E	530	FRONT, BOTTOM	3	max. 0.10 mm	max. 101.16 mm
REO-P1-0.5	E	530	FRONT	1	0.08 mm	32.95 mm
	F	449	FRONT, BOTTOM	3	max. 0.10 mm	max. 101.16 mm
REO-P1-1.0	C	530	LEFT FACE	1	0.15 mm	21.34 mm
	D	530	FRONT	3	0.08 mm	34.44 mm
CTRL-P2	C	449	RIGHT FACE	3	0.15 mm	119.71 mm
CTRL-P3	B	390	LEFT FACE	1	0.25 mm	109.42 mm
	C	530	FRONT, LF, BOTTOM	1,3	max. 0.20 mm	max. 67.98 mm
	E	306	FRONT, LF, BOTTOM	1	max. 0.10 mm	max. 64.79 mm
	F	390	LEFT FACE	1	0.08 mm	79.01 mm
FER-P3-1.0	A	194	LEFT FACE, BOTTOM	1	max. 0.15 mm	max. 84.07 mm
	B	306	FRONT	3	0.08 mm	21.25 mm
	E	390	RIGHT FACE, BOTTOM	3	max. 0.33 mm	max. 169.07 mm
	F	306	FRONT, BOTTOM	1	max. 0.10 mm	max. 60.31 mm
DCI-P3-1.0	A	390	RIGHT FACE	3	0.10 mm	142.74 mm
	F	306	FRONT	3	0.10 mm	92.49 mm
REO-P3-1.0	B	306	FRONT	1	0.10 mm	69.50 mm
	C	390	RIGHT FACE	3	0.40 mm	183.46 mm
	E	390	FRONT, LF, BOTTOM	1,3	max. 0.40 mm	max. 141.35 mm
	F	390	FRONT, RIGHT FACE	3	max. 0.10 mm	max. 170.15 mm
CTRL-G1	A	361	LEFT FACE	1	0.30 mm	191.05 mm
	B	361	RIGHT FACE	3	0.15 mm	152.65 mm
	C	361	RIGHT FACE	3	0.08 mm	86.61 mm
	D	361	FRONT, LEFT FACE	1	max. 0.15 mm	max. 104.46 mm
	E	449	FRONT, LEFT FACE	1	max. 0.15 mm	max. 186.73 mm
	F	361	RIGHT FACE, BOTTOM	3	max. 0.25 mm	max. 279.58 mm
FER-G1-1.0	B	449	RIGHT FACE	3	0.10 mm	66.34 mm
	C	449	FRONT	1	max. 0.15 mm	max. 99.35 mm
	D	449	FRONT, LEFT FACE	1	0.15 mm	118.40 mm
	E	449	FRONT, RIGHT FACE	3	0.10 mm	83.07 mm
	F	361	RIGHT FACE	3	0.08 mm	136.90 mm
REO-G1-1.0	F	537	FRONT, RIGHT FACE	1,3	0.10 mm	156.45

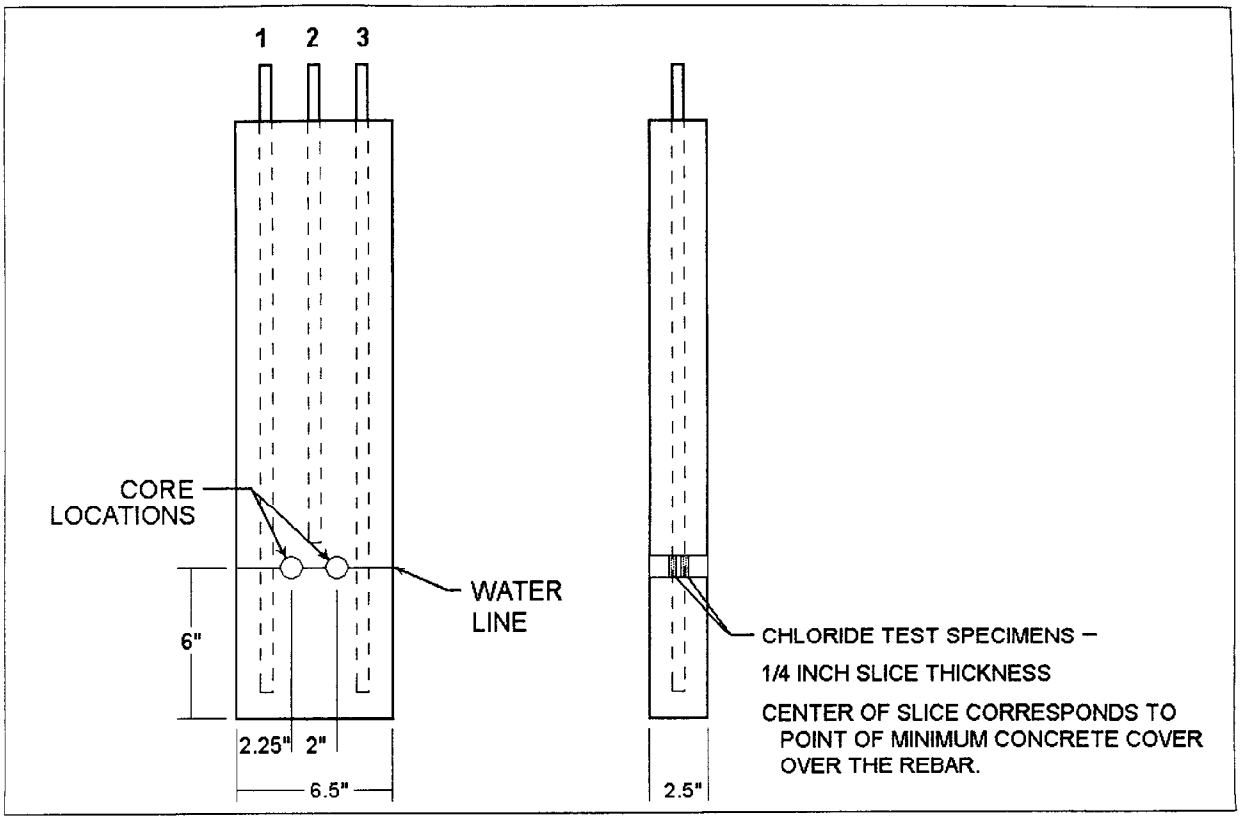

Figure 24. Location of chloride test specimens from a three-bar column.

specimens in these mix groups are likewise displayed in Figures 28(b), 29(b), and 30(b). Discussion of these results is given below for each inhibitor separately. Comparisons between the behavior with and without inhibitors are only relative, and cover a time frame of only about one year. It must be

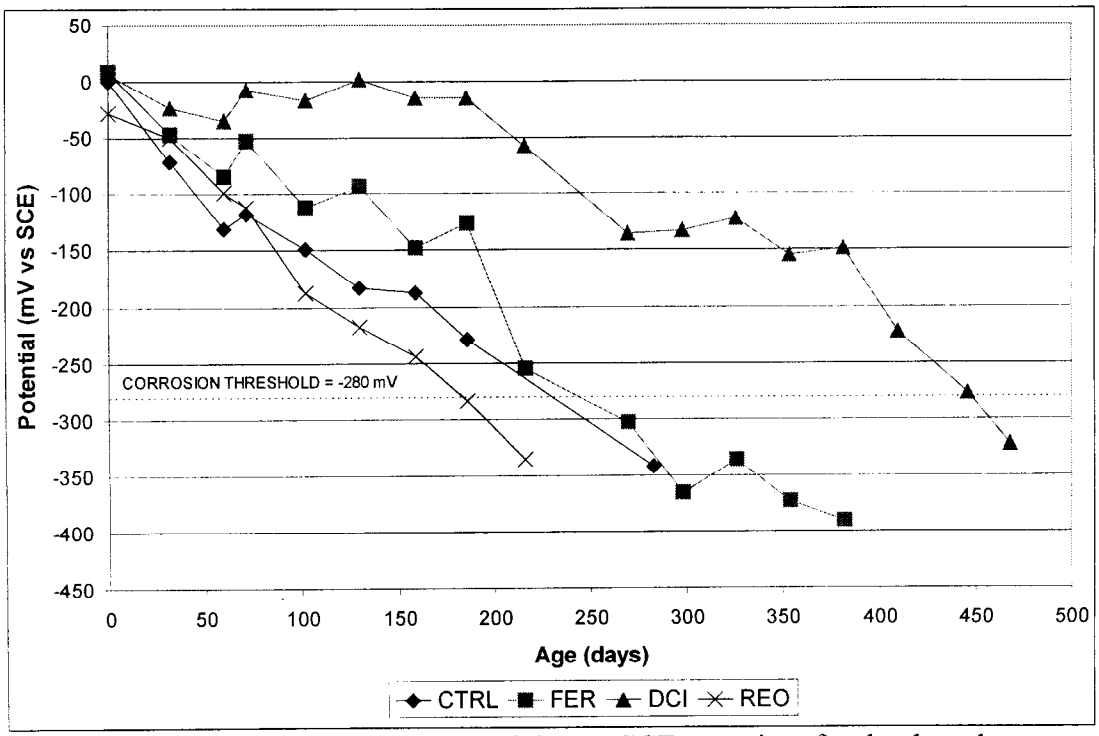

Figure 25. C1 group half-cell potentials to a SCE over time for the three-bar column specimens.

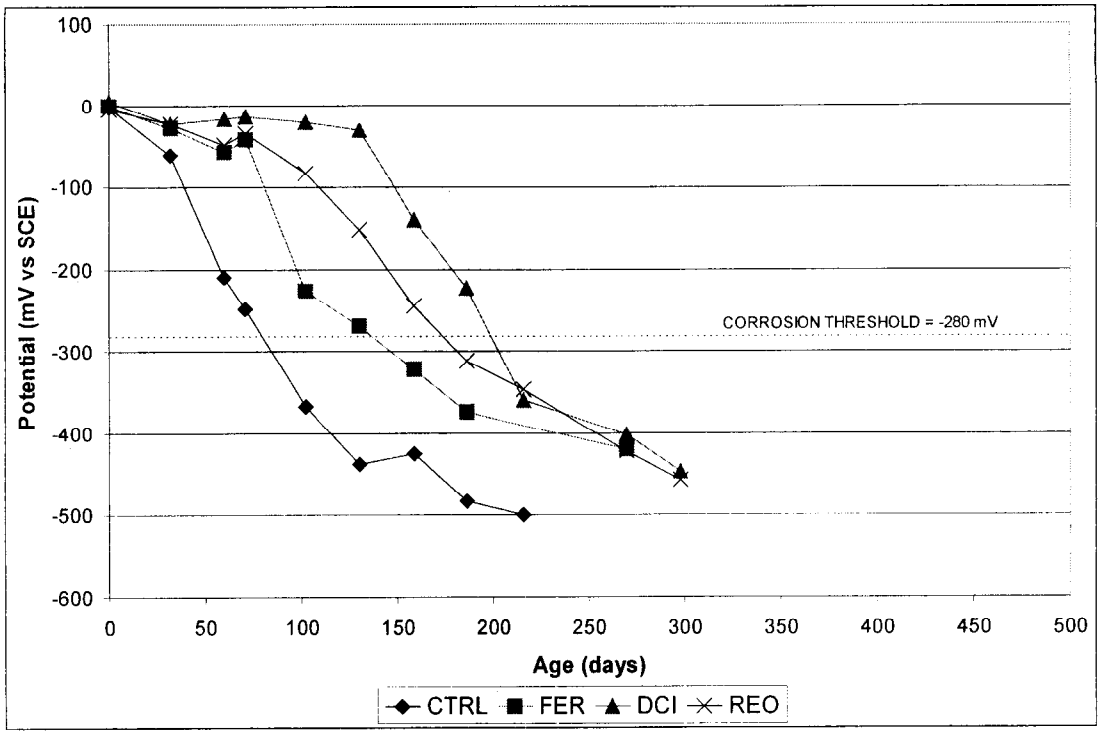

Figure 26. C2 group half-cell potentials to a SCE over time for the three-bar column specimens.

emphasized that these trends reflect early behavior in highly permeable concrete, and may be different than those that will develop for the less permeable concrete formulations.

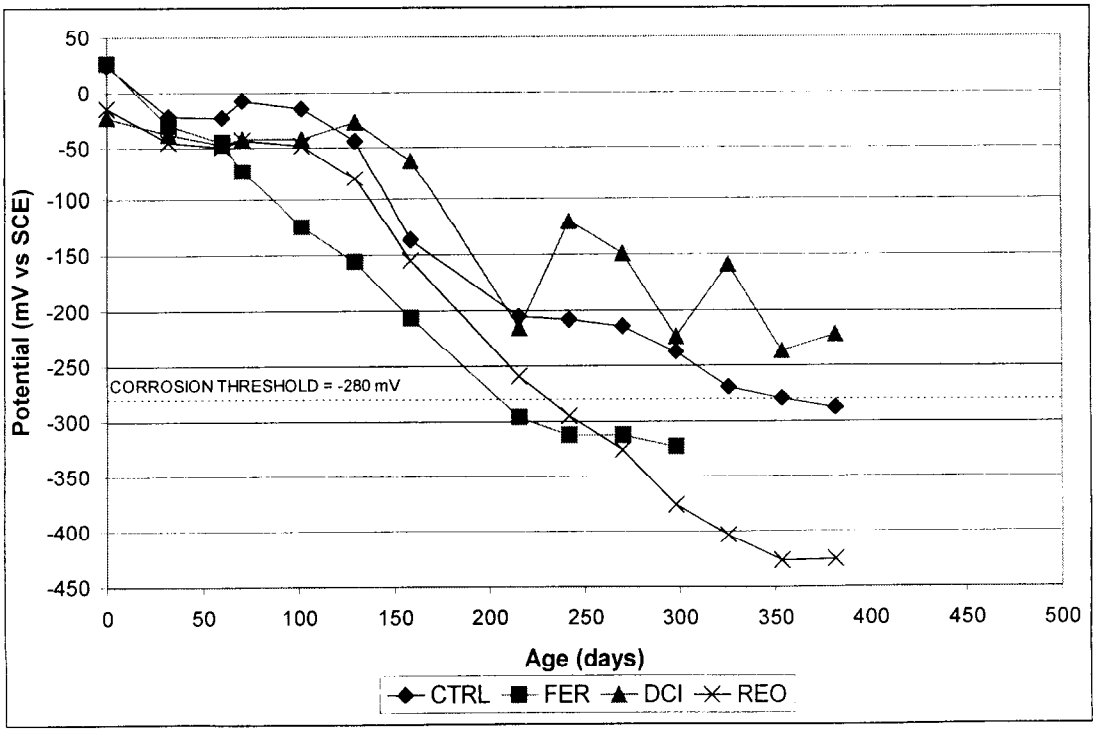

Figure 27. P3 group half-cell potentials to a SCE over time for the three-bar column specimens.

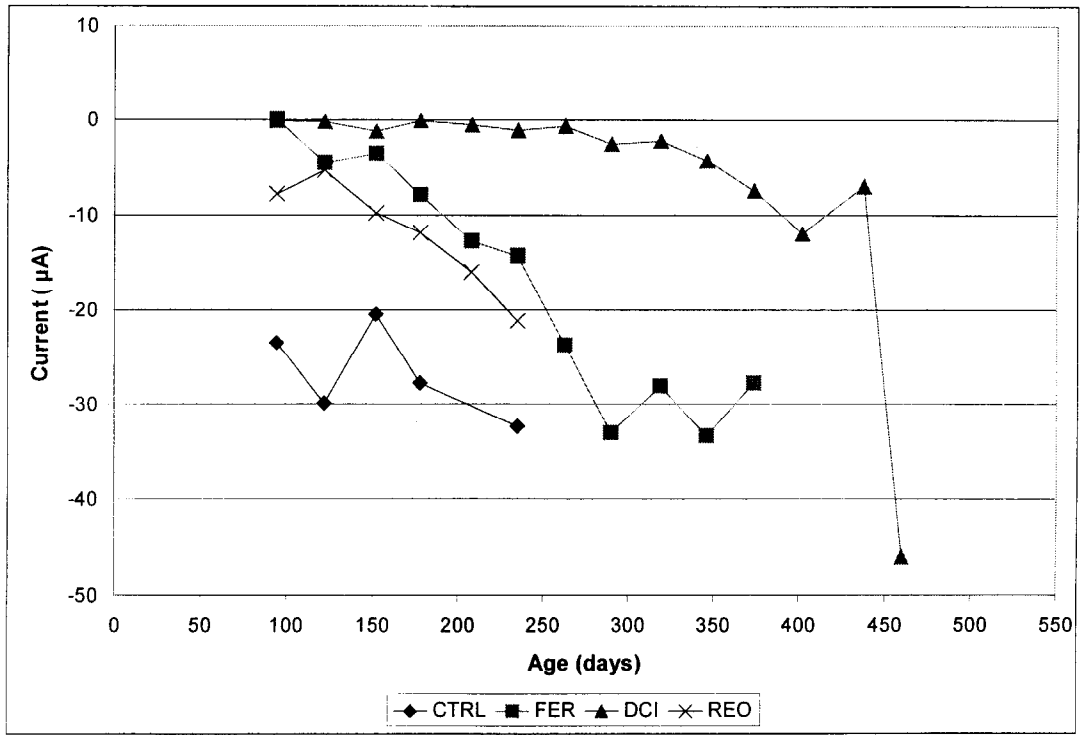

Figure 28(a). C1 group average current values over time for the three-bar column specimens.

4.2.2 Calcium Nitrite-based Inhibitor (DCI-S)

As of June 30, 1999, all C1, C2, and P3 specimens but four had failed and were removed for inspection. Comparing in Figures 25 through 27 the potential data of the DCI-S specimens with that of the respective controls, the DCI-S specimens exhibited nearly double the nominal time to

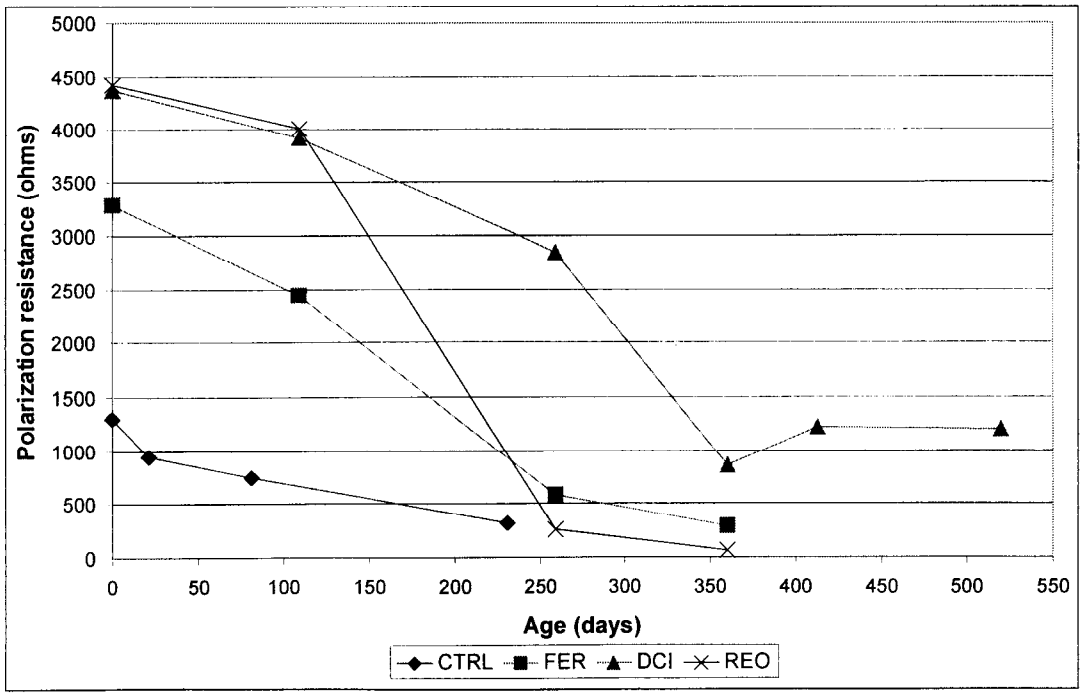

Figure 28(b). C1 group polarization values over time for a selected three-bar column specimen from each group.

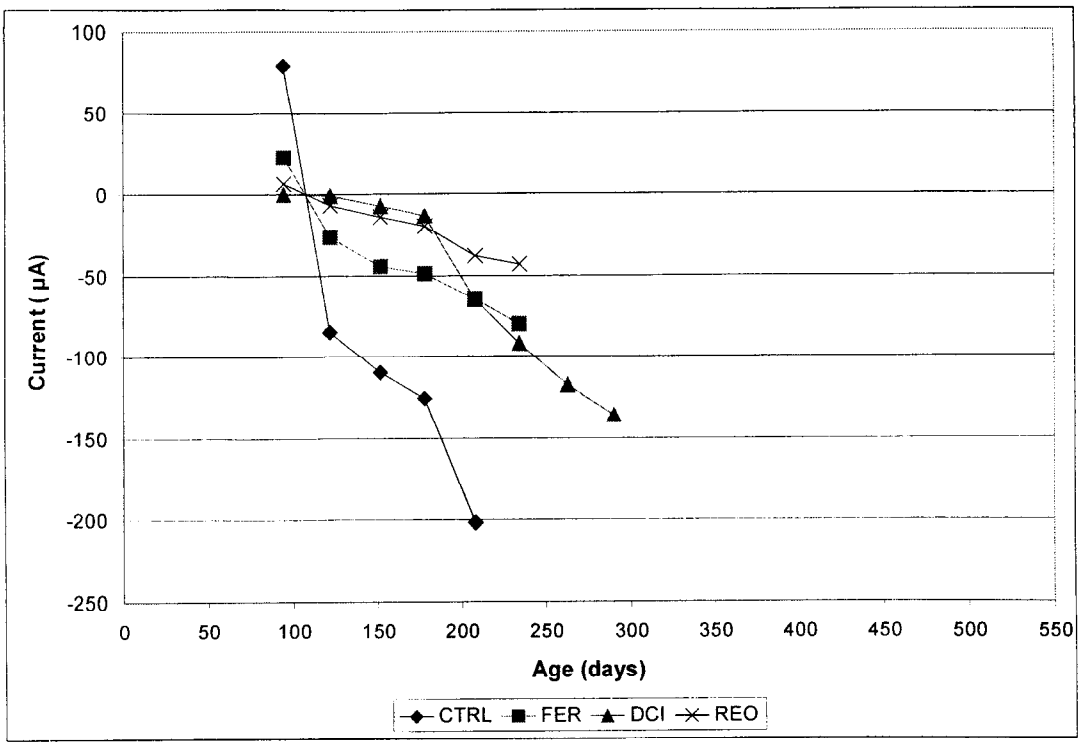

Figure 29(a). C2 group average current values over time for the three-bar column specimens.

corrosion initiation (TCI) (assigned as the time at which the average half-cell potential reached –280 mV/SCE) of the controls. From the values in Table 14, the DCI-S specimens also showed a nominal improvement of about 50 percent over the controls in observed time-to-failure values (although this figure will be updated as the complete set of specimens reaches failure). The DCI-S specimens also had before-failure macrocell currents (absolute values) lower than those of the controls and the other

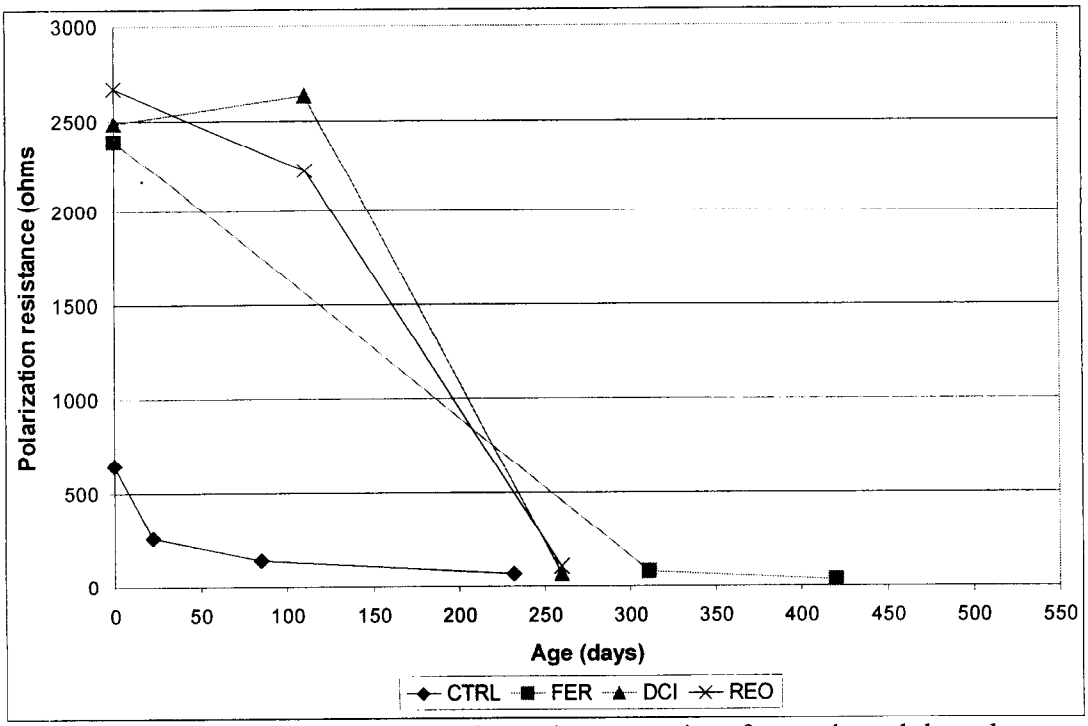

Figure 29(b). C2 group polarization values over time for a selected three-bar column specimen from each group.

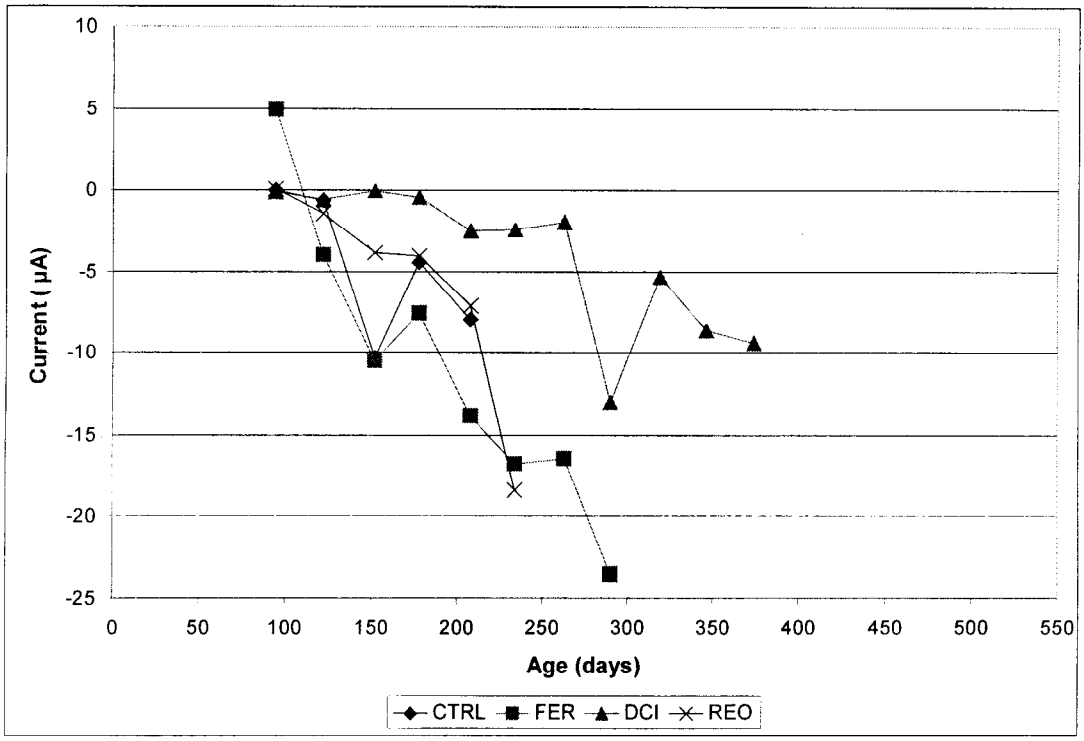

Figure 30(a). P3 group average current values over time for the three-bar column specimens.

two inhibitors in the C1 and C2 groups. The polarization resistance of the DCI-S specimens was also much higher (less corrosion) than that of the controls in all three concretes, and also higher than those of the two other inhibitors in the C1 group. Additional discussion of the macrocell and polarization resistance results of all three inhibitors and controls is presented in Section 4.2.5. Overall, the results collected from electrochemical testing agree with the generally good ranking

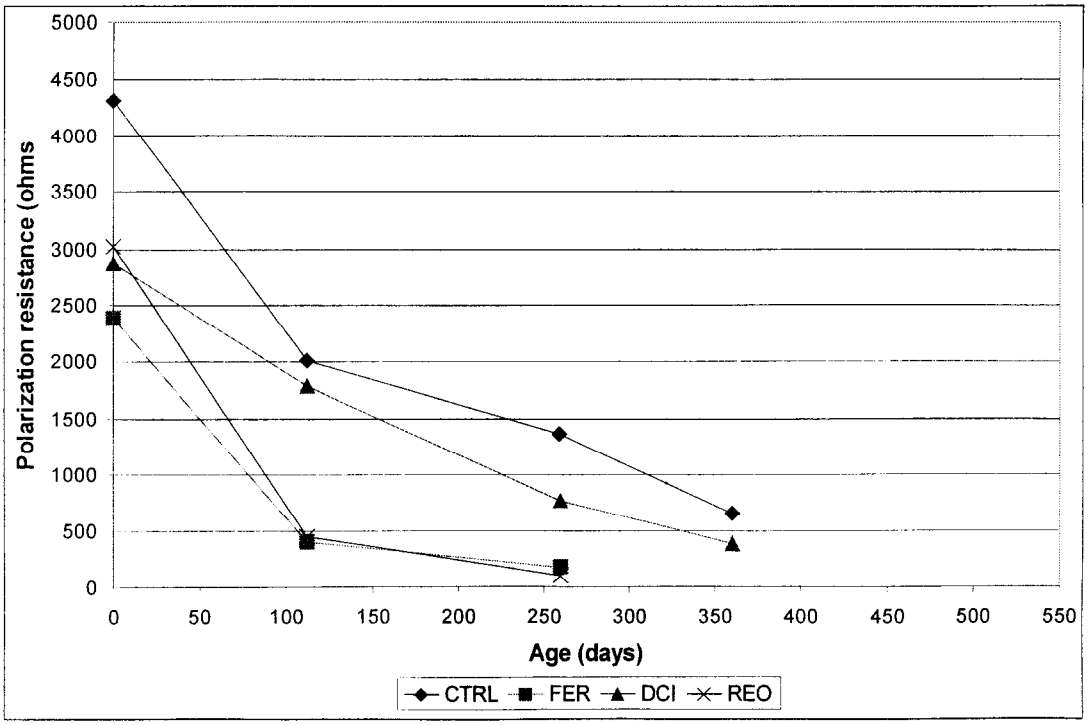

Figure 30(b). P3 group polarization values over time for a selected three-bar column specimen from each group.

indicated by the TCI and time-to-failure observations. For P3 group specimens, the controls showed lower corrosion currents and polarization resistance values when compared to the three inhibitors studied here.

4.2.3 Organic Corrosion Inhibitor F (FerroGard 901)

As of June 30, 1999, all C1, C2, and P3 specimens (except for three) had failed and were removed for inspection. Based on trends observed from half-cell potentials over time, FerroGard 901 admixed specimens provided on average only a very slight improvement in TCI over the respective control specimens. The observed time-to-failure values for FerroGard 901 indicated also only a fractional improvement over the controls (subject to update as more specimens are analyzed). The electrochemical current and polarization resistance results indicate also a relatively modest improvement over the controls to date.

4.2.4 Organic Corrosion Inhibitor R (Rheocrete 222+)

Generally, little consistent difference in TCI or time to failure was seen between the Rheocrete 222+ admixed specimens and the respective controls. In contrast, electrochemical measurements showed evidence of some protection during early exposure of the C1 and C2 groups (but not the P3 group).

4.2.5 Additional Comments

The macrocell current and polarization resistance measurements are relative indicators of corrosion intensity. Accurate evaluation of corrosion rates from those measurements is not possible because of numerous complicating factors detailed elsewhere.[28] However, rough estimates can be made using simplifying assumptions.

For macrocell current measurements in the three-bar columns, it could be assumed that the central bar is a pure cathode and that the cathodic current generated at that bar is 1/3 of the total cathodic current (the upper portion of the other two bars would contribute the remaining 2/3). The precise size of the anodic region that developed after corrosion initiation is unknown and was probably increasing with time as chloride penetration progressed. Nevertheless, based on the overall appearance of damage in selected autopsied specimens (results to be detailed in a subsequent report), the length of the corroding region in bars 1 and 3 was typically on the order of 10 cm, corresponding to a total corroded area ~80 cm^2. Approximating steel corrosion as if it were that of pure Fe forming Fe^{++} ions, a uniform anodic current density of 1 $\mu A/cm^2$ corresponds by Faradaic conversion[29] to a corrosion penetration rate of 11.7 μm/y. Thus for these specimens a macrocell current of 10 μA would correspond to an apparent uniform corrosion penetration rate (in the corroding region) of 10 x 3 x 11.7 / 80 = 4.4 μm/y (~0.2 mpy). Average macrocell currents after corrosion initiation in these specimens ranged from ~10 μA to ~200 μA so apparent average penetration rates were in the order of ~4 μm/y to ~80 μm/y (individual bars or portions of bars may have experienced rates significantly higher than the average). The critical corrosion penetration for cracking the concrete cover, when the cover to rebar diameter is comparable to that present in these specimens, has been reported to be in the order of ~10 μm to ~100 μm.[30] This range roughly agrees with the estimated rates and the observation of cracking in the three-bar specimens within about 1 year of testing.

The available polarization resistance measurements for the three-bar specimens are few in number, but after corrosion initiation fall in the range from 1,200 Ω down to ~50 Ω. Assuming as before

Faradaic conversion and a corroding surface area ~80 cm^2, and a Stearn-Geary constant of 0.026 V,[29] these results correspond again to apparent corrosion penetration rates in the order of ~4 μm/y to 80 μm/y in good agreement with the macrocell current results. Detailed analysis of continuation testing will be performed to assess the validity of these preliminary corrosion rate estimates.

OBJECTIVE 5 - DETERMINE POSSIBLE NEGATIVE SIDE EFFECTS – PERFORMANCE TESTS

5.1 Estimated Time to Failure

Expected TCI is based on several factors including concrete permeability, chloride concentration, corrosion current, half-cell potential, and polarization resistance. As samples are removed from the

Table 15. Average Days to Failure for Three-bar Columns

SAMPLE NAME	MIX DATE	PLACEMENT IN SALTWATER	AVERAGE DAYS TO FAILURE*	FAILED SAMPLES / TOTAL
CTRL-C1	01/28/97	10/15/97	298	2/2
FER-C1-0.5	02/17/97	10/15/97	428	6/6
FER-C1-1.0	01/22/97	10/15/97	414	5/5
DCI-C1-0.5	02/17/97	10/15/97	>492	1/2
DCI-C1-1.0	12/16/96	10/15/97	>533	2/3
REO-C1-0.5	02/20/97	10/15/97	362	3/3
REO-C1-1.0	01/30/97	10/15/97	279	4/4
CTRL-C2	01/09/97	10/15/97	187	4/4
FER-C2-1.0	12/26/96	10/15/97	279	4/4
DCI-C2-1.0	12/18/96	10/15/97	306	5/5
REO-C2-1.0	12/19/96	10/15/97	317	5/5
CTRL-P1	02/10/97	10/22/97	>564	2/5
FER-P1-0.5	02/24/97	10/22/97	>519	2/5
FER-P1-1.0	02/13/97	10/22/97	>586	0/2
DCI-P1-0.5	02/24/97	10/22/97	>586	0/6
DCI-P1-1.0	03/05/97	10/22/97	>586	0/6
REO-P1-0.5	02/27/97	10/22/97	>547	2/5
REO-P1-1.0	02/27/97	10/22/97	>564	2/5
CTRL-P2	04/14/97	10/30/97	>557	1/6
FER-P2-0.5	04/17/97	10/30/97	>578	0/6
FER-P2-1.0	04/17/97	10/30/97	>578	0/6
DCI-P2-0.5	04/22/97	10/30/97	>578	0/6
DCI-P2-1.0	04/22/97	10/30/97	>578	0/6
REO-P2-0.5	04/28/97	10/30/97	>578	0/6
REO-P2-1.0	04/28/97	10/30/97	>578	0/6
CTRL-P3	04/01/97	10/15/97	>442	4/5
FER-P3-1.0	03/27/97	10/15/97	>397	5/6
DCI-P3-1.0	03/24/97	10/15/97	471	4/4
REO-P3-1.0	03/20/97	10/15/97	369	4/4
CTRL-P4	04/01/97	10/22/97	>586	0/6
FER-P4-1.0	03/27/97	10/22/97	>586	0/6
DCI-P4-1.0	03/24/97	10/22/97	>586	0/6
REO-P4-1.0	03/20/97	10/22/97	>586	0/6
CTRL-G1	05/08/97	10/30/97	376	6/6
FER-G1-1.0	05/20/97	10/30/97	456	6/6
DCI-G1-1.0	05/12/97	10/30/97	>578	0/6
REO-G1-1.0	05/15/97	10/30/97	>570	2/5

* "FAILURE" is considered the first visual sign of corrosion-induced cracking.

tank, all of the factors are taken into consideration to formulate a time to failure for the remaining samples. The addition of nitrite raises the repassivation potential to increase the time to failure, even at high chloride concentrations.

Preliminary results from a limited number of three-bar specimens show poor correlation between chloride concentrations and actual time to failure. Possible sources causing this behavior may include the lowering of concrete pH by added pozzolans resulting in a lower critical chloride threshold, and non-uniform chloride penetration ("chloride bunching," multidimensional chloride penetration, and the chosen location of sampling for chloride testing as per Figure 24). Work to be done in these areas includes retrieving chloride samples from the three-bar specimens at the outer edge of the active bar to investigate the effects of non-uniform chloride penetration, and laboratory tests to further investigate the effects of lower pH on critical chloride threshold. This work will be completed and results will be discussed in a future report.

5.2 Determine Effect of Insufficient Dosage on Corrosion Progression

This discussion concerns the effect of inhibitor dosage reduction and supplements the earlier discussion of behavior under full dosage. Table 15 lists the three-bar column average time-to-failure values for all mix groups, keyed to whether no inhibitor (control), half dosage, or full dosage was used. Thus, for those cases the reported average days to failure are only a lower limit resulting from averaging the actual failure times in the failed specimens with the total test time to date for the unfailed specimens in the group. The mix groups considered in this section are limited to C1 (no pozzolans, 0.41 w/c ratio), P1 (20 percent fly ash replacement, 0.41 w/c ratio), and P2 (20 percent fly ash replacement, 8 percent microsilica replacement, 0.41 w/c ratio). Each of these mix groups includes specimens cast with half and full inhibitor doses.

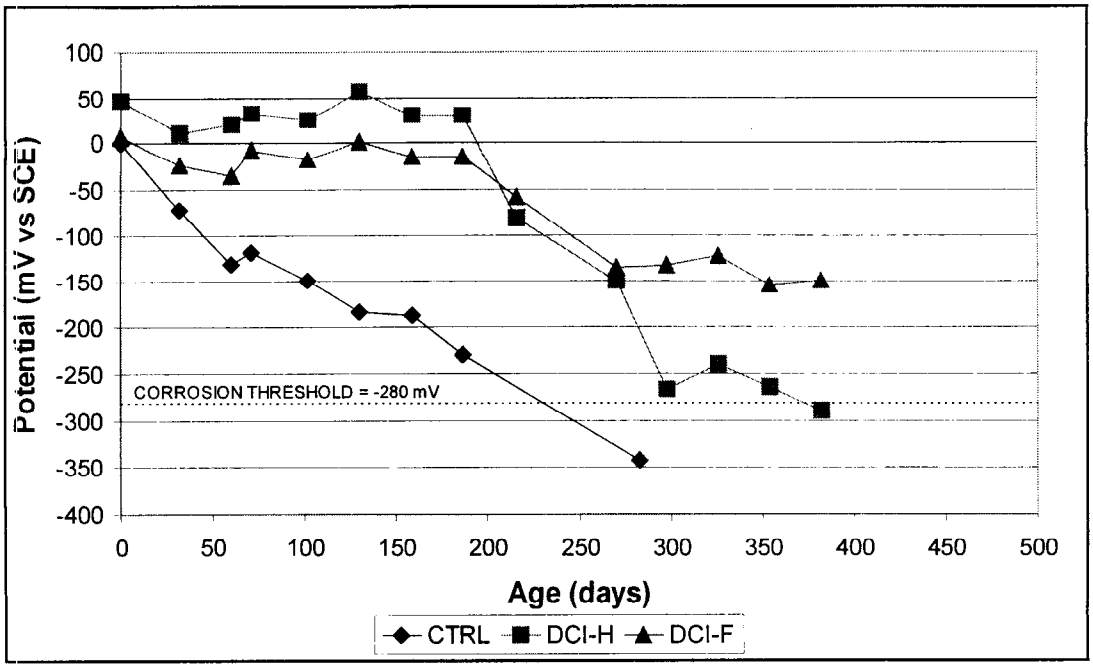

Figure 31. Comparison of the Group C1 potential histories of the full-dose DCI-S specimens, the half-dose DCI-S specimens, and the control specimens.

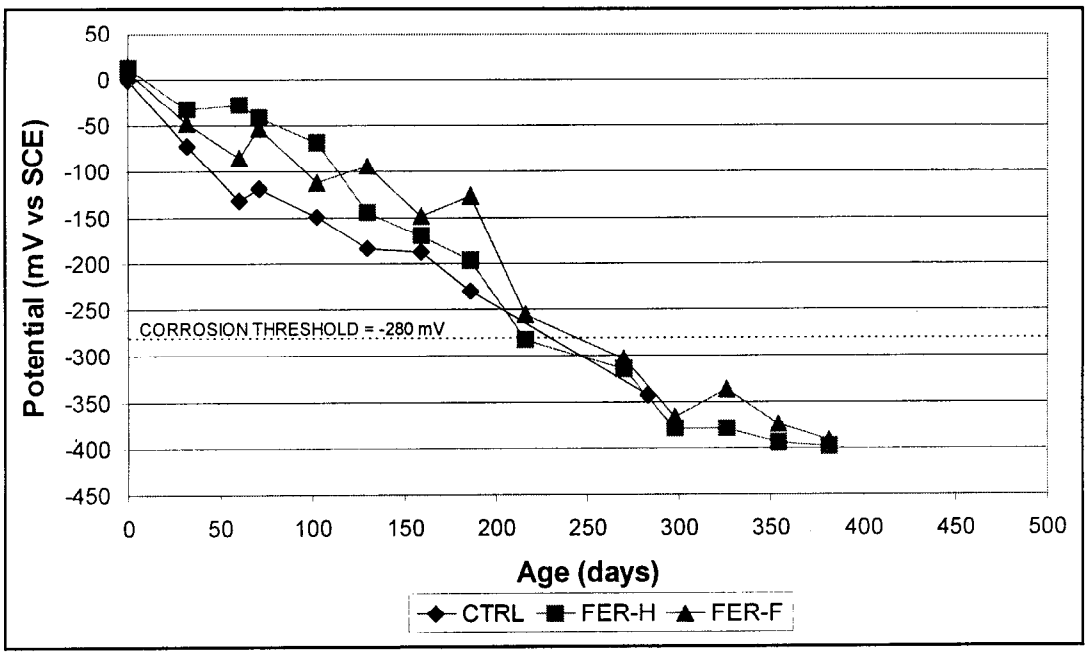

Figure 32. Comparison of the Group C1 potential histories of the full-dose FerroGard 901 specimens, the half-dose FerroGard 901 specimens, and the control specimens.

5.2.1 Calcium Nitrite-based Inhibitor (DCI-S)

Based on the data taken from ongoing testing, the TCI (defined using the same nominal potential criterion as in Section 4.2) increased as the DCI-S dosage rate increased. As an example, Figure 31 shows an increase in TCI for specimens containing half the recommended dose of DCI-S (11 L/m^3) over the control and on average nearly double the TCI for specimens containing the recommended dosage of DCI-S (22 L/m^3) compared to the TCI for the control.

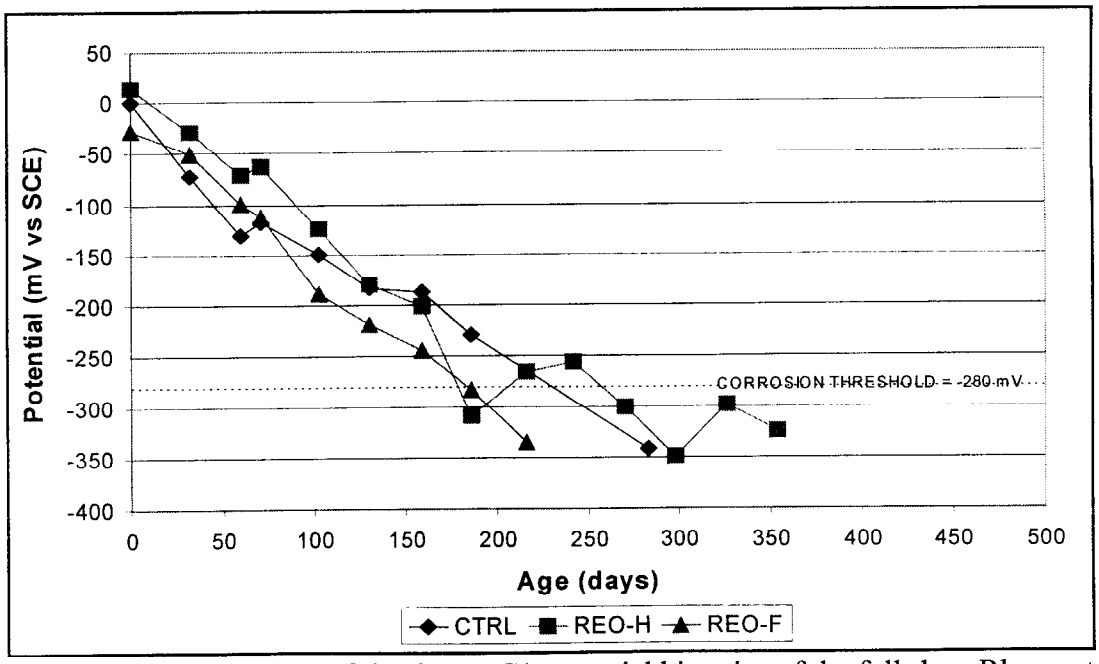

Figure 33. Comparison of the Group C1 potential histories of the full-dose Rheocrete 222+ specimens, the half-dose Rheocrete 222+ specimens, and the control specimens.

Table 16. Saltwater Exposure Time and Chloride Concentrations for Three-bar Columns.

MIX NAME	SAMPLE	SALTWATER EXPOSURE (DAYS)	INITIAL CHLORIDE (lb/yd^3)	CHLORIDE @ END OF EXPOSURE (lb/yd^3)
FER-C1-0.5	E	478	0.192	6.63
FER-C1-0.5	F	478	0.192	7.05
FER-C1-1.0	D	321	0.204	4.98
DCI-C1-1.0	F	321	0.167	7.55
REO-C1-0.5	F	321	0.194	5.78
REO-C1-1.0	F	321	N/A	11.60
CTRL-C2	E	321	0.179	14.83
FER-C2-1.0	D	279	0.082	7.55
DCI-C2-1.0	A	321	0.116	8.42
DCI-C2-1.0	B	321	0.116	11.44
REO-C2-1.0	A	321	N/A	10.44
CTRL-P1	F	546	0.182	0.81
FER-P1-0.5	D	314	0.156	2.01
REO-P1-0.5	F	454	0.201	3.52
REO-P1-1.0	D	181	0.172	2.59
CTRL-P2	C	476	0.242	3.95
CTRL-P3	E	321	0.137	1.43
FER-P3-1.0	B	321	0.15	2.46
FER-P3-1.0	F	321	0.15	1.91
DCI-P3-1.0	F	321	0.192	3.19
REO-P3-1.0	B	321	0.164	6.63
CTRL-G1	C	370	0.318	2.32
CTRL-G1	D	370	0.318	3.57
FER-G1-1.0	B	446	0.267	3.73
FER-G1-1.0	F	370	0.267	3.95

5.2.2 Organic Corrosion Inhibitor F (FerroGard 901)

As seen in Figure 32, the addition of the recommended dose (10 L/m^3) of FerroGard 901 provided on average only a marginal increase in TCI versus the control specimens. No noticeable difference was observed between the half dose and the control.

5.2.3 Organic Corrosion Inhibitor R (Rheocrete 222+)

No appreciable difference between half the recommended dose and the full recommended dose was observed. An example of the observed behavior is shown in Figure 33. Generally, the specimens admixed with Rheocrete 222+ behaved in the same manner as the control specimens.

5.3 Effect of Inhibitor on Chloride Transport

Chloride concentrations were determined according to Florida Method FM 5-516 (a wet chemistry test of acid-soluble chlorides, in triplicate with a maximum acceptable range of results being 0.08 lbs/yd^3) on 122 three-bar specimens. Of those specimens, 37 were blanks (cast without steel). Specimens containing reinforcing steel were allowed to crack before terminating saltwater exposure and sampling for chlorides. Table 16 lists the initial chloride concentrations of the three-bar specimens before saltwater exposure, and chloride concentrations at the end of saltwater exposure

Table 17. Saltwater Exposure Time and Chloride Concentrations for Intentionally Cracked Three-bar Columns

MIX NAME	SAMPLE	SALTWATER EXPOSURE (DAYS)	INITIAL CHLORIDE (lb/yd³)	CL⁻ @ END OF EXPOSURE (lb/yd³)	MIX NAME	SAMPLE	SALTWATER EXPOSURE (DAYS)	INITIAL CHLORIDE (lb/yd³)	CL⁻ @ END OF EXPOSURE (lb/yd³)
CTRL-C1	A	279	0.148	7.24	FER-P2-1.0	A	279	0.279	0.57
CTRL-C1	C	279	0.148	9.56	FER-P2-1.0	C	370	0.279	0.78
FER-C1-1.0	B	279	0.204	7.21	DCI-P2-1.0	A	468	0.282	1.26
FER-C1-1.0	C	279	0.204	5.87	DCI-P2-1.0	C	279	0.282	0.77
DCI-C1-1.0	A	279	0.167	7.87	REO-P2-1.0	B	370	0.243	0.58
DCI-C1-1.0	B	321	0.167	10.25	REO-P2-1.0	C	370	0.243	1.31
REO-C1-1.0	A	279	N/A	7.05	CTRL-P4	A	454	0.245	1.30
REO-C1-1.0	C	279	N/A	8.76	CTRL-P4	B	272	0.245	1.15
CTRL-P1	A	272	0.182	0.75	FER-P4-1.0	B	454	0.244	1.06
CTRL-P1	B	272	0.182	2.39	FER-P4-1.0	C	454	0.244	1.12
FER-P1-1.0	A	272	0.175	1.82	DCI-P4-1.0	B	314	0.277	0.61
FER-P1-1.0	C	314	0.175	0.95	DCI-P4-1.0	C	454	0.277	2.26
DCI-P1-1.0	B	272	0.175	4.87	REO-P4-1.0	B	272	0.253	0.81
DCI-P1-1.0	C	314	0.175	1.55	REO-P4-1.0	C	314	0.253	1.56
REO-P1-1.0	A	454	0.172	2.56	CTRL-G1	A	279	0.318	6.51
REO-P1-1.0	B	314	0.172	1.60	CTRL-G1	C	370	0.318	5.40
REO-P1-1.0	C	314	0.172	1.21	FER-G1-1.0	B	279	0.267	4.43
CTRL-P2	A	279	0.242	1.72	FER-G1-1.0	C	279	0.267	2.25
CTRL-P2	C	279	0.242	0.91	DCI-G1-1.0	A	279	0.253	0.49
					DCI-G1-1.0	B	279	0.253	1.30

(from the location indicated in Figure 24). These locations between the bars were chosen to minimize any multidimensional effects of chloride intrusion, also to try to avoid any chloride bunching around the rebar. Any bunching would skew the results. Likewise, Table 17 lists chloride information for 39 pre-cracked specimens. From the cores extracted, the specimens tested for chloride content consisted of 6.3 mm slices taken corresponding to the minimum concrete cover over the reinforcement, 25 mm. On blank control specimens, chloride concentrations were determined at ten separate elevations as shown in Figure 34 to map a general profile of chloride transport. The blank control specimens were all sampled at approximately 550 days of exposure. The chloride concentration values obtained from the water line (150 mm from the bottom of the specimen, and corresponding to the region shown in Figure 24) are also presented in Table 18. As mentioned in Section 5.1, further investigation is planned.

Table 18 also shows the ratio of chloride content in the specimens containing inhibitors (average in a given

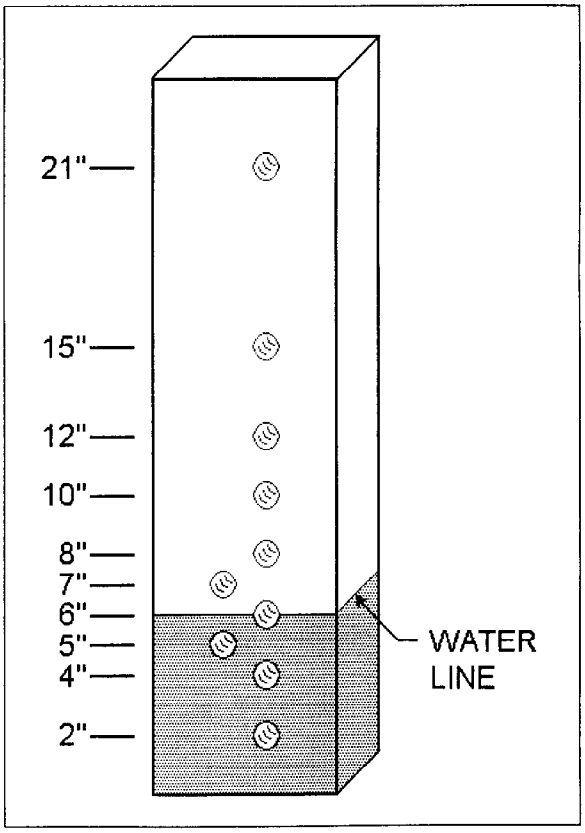

Figure 34. Core locations for chloride testing on blank specimens.

Table 18. Saltwater Exposure Time and Chloride Concentrations for Blank Lab Columns

SAMPLE NAME	SALTWATER EXPOSURE (DAYS)	INITIAL CHLORIDE (lb/yd^3)	Cl^- @ END OF EXPOSURE (lb/yd^3)	Cl^- RATIO INHIB VS. CONTROL	SAMPLE NAME	SALTWATER EXPOSURE (DAYS)	INITIAL CHLORIDE (lb/yd^3)	Cl^- @ END OF EXPOSURE (lb/yd^3)	Cl^- RATIO INHIB VS. CONTROL
CTRL-C1	552	0.148	3.43	1.00	CTRL-P2	537	0.242	0.64	1.00
FER-C1-0.5	552	0.192	3.06	0.89	FER-P2-0.5	537	0.255	0.23	0.36
FER-C1-1.0	552	0.204	2.80	0.82	FER-P2-1.0	537	0.279	1.79	2.80
DCI-C1-0.5	552	0.206	2.40	0.70	DCI-P2-0.5	537	0.25	0.60	0.94
DCI-C1-1.0	552	0.167	6.53	1.90	DCI-P2-1.0	537	0.282	0.39	0.61
REO-C1-0.5	552	0.194	3.35	0.98	REO-P2-0.5	537	0.26	1.61	2.52
REO-C1-1.0	552	N/A	6.09	1.78	REO-P2-1.0	537	0.243	0.43	0.67
CTRL-C2	552	0.179	8.92	1.00	CTRL-P3	552	0.137	1.45	1.00
FER-C2-1.0	552	0.082	9.26	1.04	FER-P3-1.0	552	0.15	1.22	0.84
DCI-C2-1.0	552	0.116	7.74	0.87	DCI-P3-1.0	552	0.192	2.37	1.63
REO-C2-1.0	552	N/A	5.98	0.67	REO-P3-1.0	552	0.164	7.50	5.17
CTRL-P1	545	0.182	1.39	1.00	CTRL-P4	545	0.245	0.87	1.00
FER-P1-0.5	545	0.156	1.16	0.83	FER-P4-1.0	545	0.244	1.19	1.37
FER-P1-1.0	545	0.175	0.49	0.35	DCI-P4-1.0	545	0.277	0.68	0.78
DCI-P1-0.5	545	0.173	0.82	0.59	REO-P4-1.0	545	0.253	0.53	0.61
DCI-P1-1.0	545	0.175	0.92	0.66	CTRL-G1	537	0.318	5.40	1.00
REO-P1-0.5	545	0.201	0.23	0.17	FER-G1-1.0	537	0.267	2.05	0.38
REO-P1-1.0	545	0.172	1.51	1.09	DCI-G1-1.0	537	0.253	2.30	0.43

group including both the full- and half-dosage specimens) to chloride content in the corresponding control. Table 19 shows the average chloride content ratios of the three inhibitor mixes compared to that of the corresponding control mixes. Since all the analyses for the blanks were made after nearly the same time of exposure (about 550 days), these ratios of chloride content at the same depth might reveal differences in chloride ingress. However, the ratios showed a great deal of variability from group to group. On average, the chloride penetration when comparing concrete with different inhibitors versus concrete without inhibitor differed by less than a factor of two. Thus, the results to date have not revealed any well-defined effect in chloride penetration from the presence of any of the inhibitors examined. Chloride penetration data from ongoing tests with the G-109 specimens may provide more decisive information. Because the times to failure varied widely, an analysis similar to that of the blank specimens could not be reliably performed on the specimens. The results in Table 16 do indicate typically higher chloride contents at the rebar depth for the failed specimens than for the blanks, even though the latter were exposed for longer times. This observation likely reflects enhanced chloride ingress through distressed concrete in the failed samples, possibly resulting from extensive microcracking during the period before damage became visually apparent.

5.4 Examine Possible Adverse Effects on Concrete Physical Properties

5.4.1 Transport Effects – Rapid Chloride Permeability (RCP).

This test complies with ASTM C 1202. All testing of the mixes listed in Table 13 has been completed, and results are presented in Table 20. Generally, the 360-day RCP tests resulted in lower

Table 19. Average Chloride Content Ratios of All Specific Inhibitor Mixes versus the Corresponding Control Mixes for Blank Lab Columns

INHIBITOR	MAXIMUM RATIO	MINIMUM RATIO	AVERAGE OF RATIOS
FERROGARD	2.8	0.35	0.97
DCI-S	1.9	0.43	0.91
RHEOCRETE	5.17	0.12	1.38

Table 20. Impressed Current, RCP and Surface Resistivity at 28 and 360 Days

MIX	CAST DATE	IMPRESSED CURRENT Days (Ohms)	RCP (Coulombs)				SURFACE RESISTIVITY (kOhm-cm)		
			28 DAY RCP	28 DAY INHIBITOR VS CTRL*	360 DAY RCP	360 DAY INHIBITOR VS CTRL*	28 DAYS	360 DAYS	360 DAY INHIBITOR VS CTRL*
CTRL-C1	01/28/97	19 (445)	5689	1.00	4448	1.00	3.18	3.58	1.00
FER-C1-0.5	02/17/97	N/A	6530	1.15	5039	1.13	2.65	3.22	0.90
FER-C1-1.0	01/22/97	48 (886)	>12000	>2.11	4710	1.06	2.81	3.78	1.06
DCI-C1-0.5	02/17/97	N/A	5773	1.01	4305	0.97	2.92	3.84	1.07
DCI-C1-1.0	12/16/96	21 (540)	>12000	>2.11	6034	1.36	2.77	3.03	0.85
REO-C1-0.5	02/20/97	N/A	5124	0.90	4571	1.03	2.93	3.67	1.03
REO-C1-1.0	01/30/97	16 (383)	9821	1.73	6943	1.56	2.02	2.3	0.64
CTRL-C2	01/09/97	12 (302)	10110	1.00	7166	1.00	2.2	2.12	1.00
FER-C2-1.0	12/26/96	36 (710)	>12000	>1.19	8192	1.14	1.95	2.17	1.02
DCI-C2-1.0	12/18/96	4 (224)	>12000	>1.19	9839	1.37	1.94	2.39	1.13
REO-C2-1.0	12/19/97	16 (321)	>12000	>1.19	8000	1.12	1.99	1.88	0.89
CTRL-P1	02/10/97	21 (644)	6793	1.00	1011	1.00	3.55	14.1	1.00
FER-P1-0.5	02/24/97	N/A	6706	0.99	1056	1.04	2.62	N/A	N/A
FER-P1-1.0	02/13/97	164 (3714)	7086	1.04	1020	1.01	3.49	15.28	1.08
DCI-P1-0.5	02/24/97	N/A	6188	0.91	1257	1.24	2.65	N/A	N/A
DCI-P1-1.0	03/05/97	2 (436)	11083	1.63	1610	1.59	2.23	9.61	0.68
REO-P1-0.5	02/27/97	N/A	4478	0.66	929	0.92	2.82	N/A	N/A
REO-P1-1.0	02/27/97	30 (872)	4057	0.60	987	0.98	3.05	15.03	1.07
CTRL-P2	04/14/97	104 (2914)	959	1.00	549	1.00	18.42	24.77	1.00
FER-P2-0.5	04/17/97	N/A	1095	1.14	558	1.02	15.3	24.36	0.98
FER-P2-1.0	04/17/97	154 (3820)	1078	1.12	528	0.96	16.16	26.59	1.07
DCI-P2-0.5	04/22/97	N/A	>12000	>12.51	N/A	N/A	11.3	21.24	0.86
DCI-P2-1.0	04/22/97	33 (1839)	1662	1.73	686	1.25	8.47	19.8	0.80
REO-P2-0.5	04/28/97	N/A	1147	1.20	503	0.92	12.67	25.27	1.02
REO-P2-1.0	04/28/97	198 (3958)	1132	1.18	498	0.91	11.96	24.21	0.98
CTRL-P3	04/01/97	25 (619)	7328	1.00	1431	1.00	2.92	9.67	1.00
FER-P3-1.0	03/27/97	37 (1143)	9339	1.27	1763	1.23	2.49	8.53	0.88
DCI-P3-1.0	03/24/97	14 (455)	9194	1.25	2722	1.90	2.35	5.77	0.60
REO-P3-1.0	03/20/97	19 (605)	10351	1.41	1781	1.24	2.55	8.15	0.84
CTRL-P4	04/01/97	119 (2642)	1149	1.00	895	1.00	16.67	14.91	1.00
FER-P4-1.0	03/27/97	106 (2496)	1269	1.10	984	1.10	15.27	15.02	1.01
DCI-P4-1.0	03/24/97	103 (2386)	1818	1.58	1393	1.56	10.36	9.94	0.67
REO-P4-1.0	03/20/97	71 (1935)	1419	1.23	1013	1.13	15.35	13.95	0.94
CTRL-G1	05/05/97	38 (764)	3461	1.00	3172	1.00	5.14	5.09	1.00
FER-G1-1.0	05/20/97	56 (1350)	4413	1.28	4438	1.40	5.25	4.53	0.89
DCI-G1-1.0	05/12/97	20 (577)	4992	1.44	4131	1.30	5.3	4.7	0.92
REO-G1-1.0	05/15/97	35 (939)	4116	1.19	3712	1.17	6.34	4.95	0.97

* Value represents the ratio of inhibitor versus corresponding control mix within each respective mix group.

(improved) values compared to the corresponding 28-day results, which is in agreement with the compressive strength results showing that the specimens continued to cure. The addition of corrosion inhibitors (FerroGard 901, Rheocrete 222+) resulted in small or moderate increases in RCP (see next section) of wet-cured concrete. RCP values were lower for those mixes using granite as the coarse aggregate. The addition of fly ash yielded results indicating a slower curing time, but a less permeable concrete at 360 days. When microsilica was admixed, the RCP results indicated that the curing process was accelerated.

Several tests with air-cured concrete resulted in very high (about 12 kC or larger) RCP values. Those results are being examined for possible experimental artifacts.

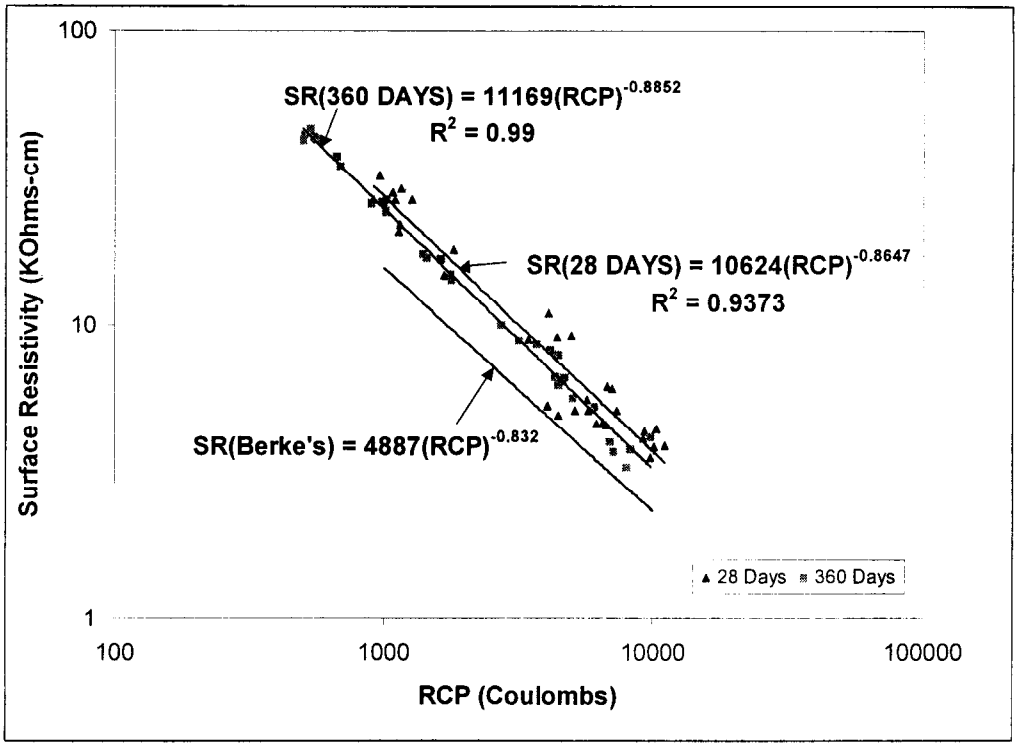

Figure 35. Surface resistivity versus RCP using concrete cylinders from all mix groups at 28 and 360 days.

5.4.2 Transport effects – Wet Surface Resistivity (WSR)

The WSR readings were taken at 28 and 360 days on the surface of the same specimens used for RCP, after moisture conditioning, using a CNS Wenner array probe and the procedure described by Morris et al.[31] WSR measurements have been conducted for all groups per the testing schedule, at 28 and 360 days. The results are presented in Table 20.

Table 20 also compares the ratio of 360 day WSR of concrete with each inhibitor to that of the inhibitor-free controls. An average of the corresponding ratios for all mixtures is presented in Table 21. The addition of inhibitor resulted in only modest reductions in WSR in the more permeable concretes. For the less permeable concretes (P1 to P4) the DCI-S caused about 1/3 WSR reduction at full dosage while the effect for the other inhibitors was smaller. These effects were also reflected by increases in RCP in the corresponding specimens.

As expected, the WSR results correlate well with the RCP results, as shown in Figure 35. Both 28 and 360 day test results have been plotted on the same graph for comparison to the equation developed by Berke[32] for correlation between WSR and RCP.

5.4.3 Transport Effects – Impressed Current

This test complies with Florida Method FM 5-522.[33] Reinforced concrete "lollipop" specimens are subjected to anodic impressed current (from a constant potential source) in 5% saltwater solution. Generally, the longer the specimen lasts under test, the lower the permeability. Information obtained from this test is indirectly related to the concrete permeability, which in turn affects resistivity. Testing for all groups has been completed. All reported readings (Table 20) are an average of three

Table 21. 360 Day RCP and Surface Resistivity Ratio Averages of All Specific Inhibitor Mixes versus Corresponding Control Mixes.

INHIBITOR	RCP 360 DAY AVERAGE OF RATIOS	Surface Resistivity 360 DAY AVERAGE OF RATIOS
FERROGARD	1.11	0.99
DCI-S	1.39	0.84
RHEOCRETE	1.10	0.93

test specimens. Generally, FerroGard 901 mixes lasted longer than the respective control mixes. Also, due to the ionic contribution from calcium nitrite, mixes containing DCI-S generally cracked more quickly than their corresponding controls. No noticeable tendencies were observed between the Rheocrete 222+ mixes and the respective controls. Specimens also generally took longer to fail when either microsilica was admixed, or when granite was used as the coarse aggregate instead of limestone.

5.4.4 Compressive Strength

This test is conducted in accordance with ASTM C 39. Compressive strength tests were conducted at 28 and 360 days after batching on each of the mix groups (Table 22). All compressive strength information reveals little difference between the mixes containing corrosion inhibitors and their respective control mixes. Rheocrete 222+ mixes were the only mixes to consistently show a small loss of compressive strength compared to the controls for corresponding mix groups. Generally, 360 day test results were higher than 28 day test results, which indicates that the specimens continued to cure during that time. The curing of the cylinders in open air (as opposed to saturated Limewater) appeared to result in increased early compressive strength. The addition of fly ash extended the

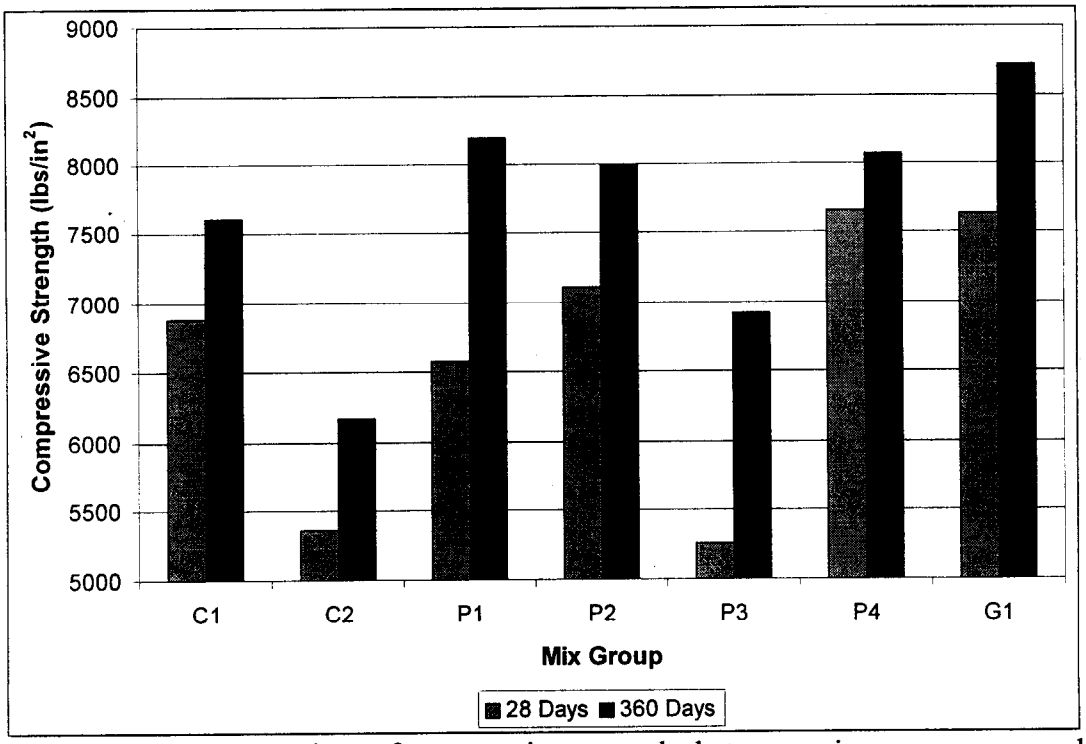

Figure 36. Comparison of compressive strengths between mix groups measured at 28 and 360 days.

Table 22. Compressive Strength and Sulfate Exposure Properties of All Mixes

MIX	CAST DATE	COMPRESSIVE STRENGTH (psi)				SULFATE EXPOSURE			
		28 DAYS		360 DAYS		28 DAYS		360 DAYS	
		TANK CURED	AIR CURED	TANK CURED	AIR CURED	% LENGTH CHANGE	% MASS CHANGE	% LENGTH CHANGE	% MASS CHANGE
CTRL-C1	01/28/97	6937	N/A	7693	N/A	-0.0027	-0.6417	-0.0096	-0.7391
FER-C1-0.5	02/17/97	7707	N/A	8257	N/A	N/A	N/A	N/A	N/A
FER-C1-1.0	01/22/97	7483	N/A	8328	N/A	-0.0001	-0.7106	0.0019	-0.6232
DCI-C1-0.5	02/17/97	7703	N/A	8505	N/A	N/A	N/A	N/A	N/A
DCI-C1-1.0	12/16/96	6186	N/A	6980	N/A	0.0013	-0.9726	0.0097	-0.4322
REO-C1-0.5	02/20/97	6781	7004	7396	8544	N/A	N/A	N/A	N/A
REO-C1-1.0	01/30/97	5356	N/A	6057	N/A	0.0054	-0.3624	-0.0059	0.8135
CTRL-C2	01/09/97	5245	N/A	6112	N/A	N/A	N/A	N/A	N/A
FER-C2-1.0	12/26/96	5678	N/A	6290	N/A	N/A	N/A	N/A	N/A
DCI-C2-1.0	12/18/96	6062	N/A	6948	N/A	N/A	N/A	N/A	N/A
REO-C2-1.0	12/19/97	4472	N/A	5342	N/A	N/A	N/A	N/A	N/A
CTRL-P1	02/10/97	6214	N/A	8223	N/A	-0.0016	-1.2129	-0.0083	-0.8708
FER-P1-0.5	02/24/97	7174	7577	8587	7813	N/A	N/A	N/A	N/A
FER-P1-1.0	02/13/97	6636	N/A	8341	N/A	-0.0036	-0.9057	-0.0160	-0.5683
DCI-P1-0.5	02/24/97	6582	7234	8203	7943	N/A	N/A	N/A	N/A
DCI-P1-1.0	03/05/97	6630	7377	8388	N/A	-0.0050	-0.6131	-0.0092	-0.6078
REO-P1-0.5	02/27/97	6697	7179	7981	7706	N/A	N/A	N/A	N/A
REO-P1-1.0	02/27/97	6147	6474	7633	N/A	-0.0030	-0.8502	-0.0040	-0.3925
CTRL-P2	04/14/97	7119	7637	7943	8794	-0.0028	-0.8752	-0.0084	-0.7903
FER-P2-0.5	04/17/97	6838	7437	7600	7956	N/A	N/A	N/A	N/A
FER-P2-1.0	04/17/97	7321	7586	8015	8497	N/A	N/A	N/A	N/A
DCI-P2-0.5	04/22/97	N/A	N/A	8085	N/A	N/A	N/A	N/A	N/A
DCI-P2-1.0	04/22/97	7365	8200	8461	8771	0.0054	0.7448	0.0076	0.8350
REO-P2-0.5	04/28/97	6943	7340	7930	N/A	N/A	N/A	N/A	N/A
REO-P2-1.0	04/28/97	7043	7420	7908	8703	-0.0067	-1.1454	-0.0168	-1.1197
CTRL-P3	04/01/97	5536	5654	7314	6898	N/A	N/A	N/A	N/A
FER-P3-1.0	03/27/97	5237	5351	6833.5	5850	N/A	N/A	N/A	N/A
DCI-P3-1.0	03/24/97	5310	5766	7114	6327	N/A	N/A	N/A	N/A
REO-P3-1.0	03/20/97	4961	5356	6392.5	6048	N/A	N/A	N/A	N/A
CTRL-P4	04/01/97	8312	8624	8549	9322	N/A	N/A	N/A	N/A
FER-P4-1.0	03/27/97	7228	7658	7616	8586	N/A	N/A	N/A	N/A
DCI-P4-1.0	03/24/97	7478	8282	8235	8212	N/A	N/A	N/A	N/A
REO-P4-1.0	03/20/97	7610	7872	7886	8947	N/A	N/A	N/A	N/A
CTRL-G1	05/05/97	7718	7003	9026	N/A	-0.0047	0.2657	-0.0020	0.3553
FER-G1-1.0	05/20/97	7095	6357	8068	N/A	-0.0021	0.3771	0.0035	0.5258
DCI-G1-1.0	05/12/97	8732	8499	9729	N/A	-0.0006	0.1218	0.0029	0.2368
REO-G1-1.0	05/15/97	6988	6615	8025	N/A	-0.0037	0.2932	-0.0023	0.4521

overall curing time for the specimens, with compressive strength increasing considerably from 28 day tests to 360 day tests. The addition of microsilica resulted in specimens achieving high early strength, with little change in strength from 28 to 360 day tests. Of the various coarse aggregate groups, the group using granite coarse aggregate exhibited the highest compressive strengths for all mix groups (Figure 36).

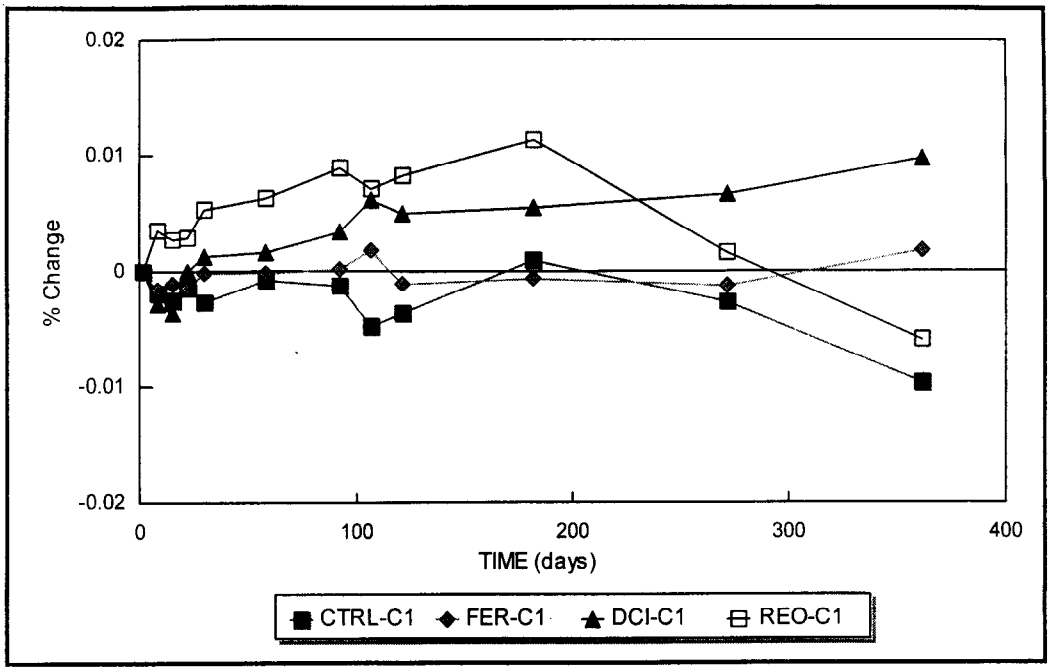

Figure 37(a). Length change due to sulfate exposure over time for the C1 group.

5.4.5 Sulfate Exposure (Length Change and Mass Change)

This test is conducted in compliance with ASTM C 490. All testing has been completed, and results are shown in Table 22. A complete set of figures showing length change and mass change over time

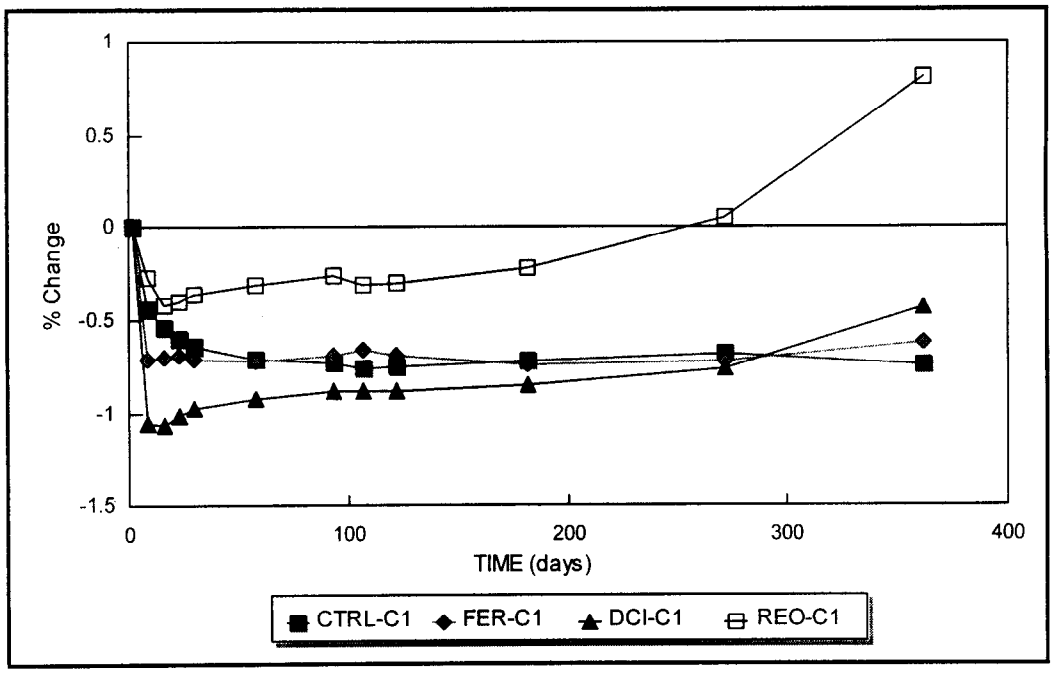

Figure 37(b). Mass change due to sulfate exposure over time for the C1 group.

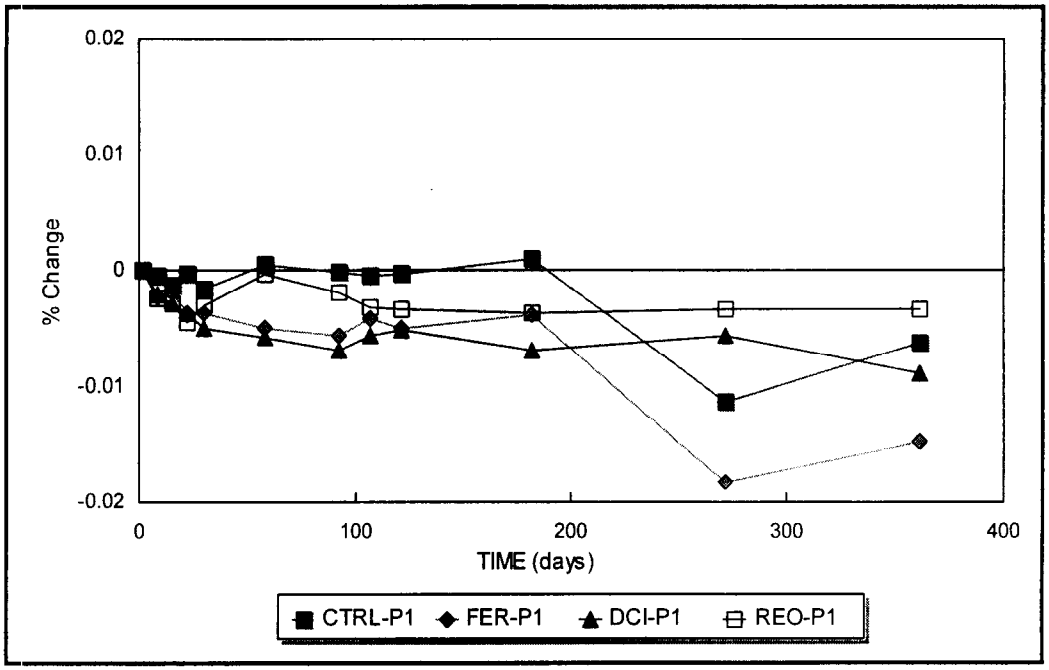

Figure 38(a). Length change due to sulfate exposure over time for the P1 group.

is shown in Figures 37 to 40. There appears to be no appreciable difference between inhibitor mixes and their respective controls for either length change or mass change. There appears to be no appreciable difference between specimens containing limestone or granite aggregate. Generally, the addition of fly ash and fly ash with microsilica appears to result in a decrease in length and mass change compared to the control group.

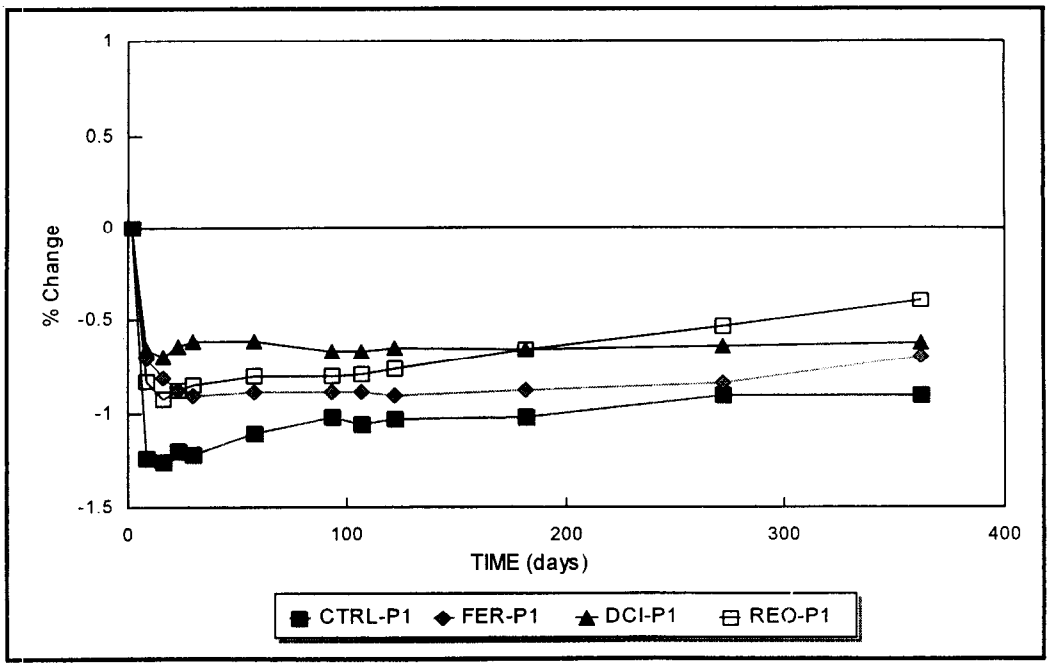

Figure 38(b). Mass change due to sulfate exposure over time for the P1 group.

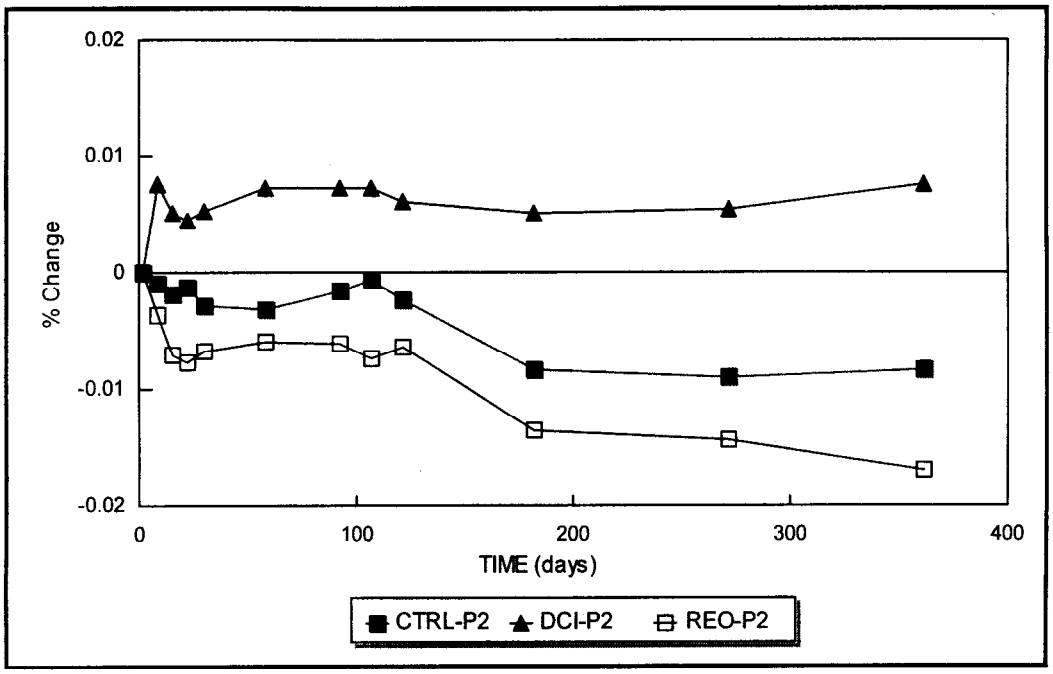

Figure 39(a). Length change due to sulfate exposure over time for the P2 group.

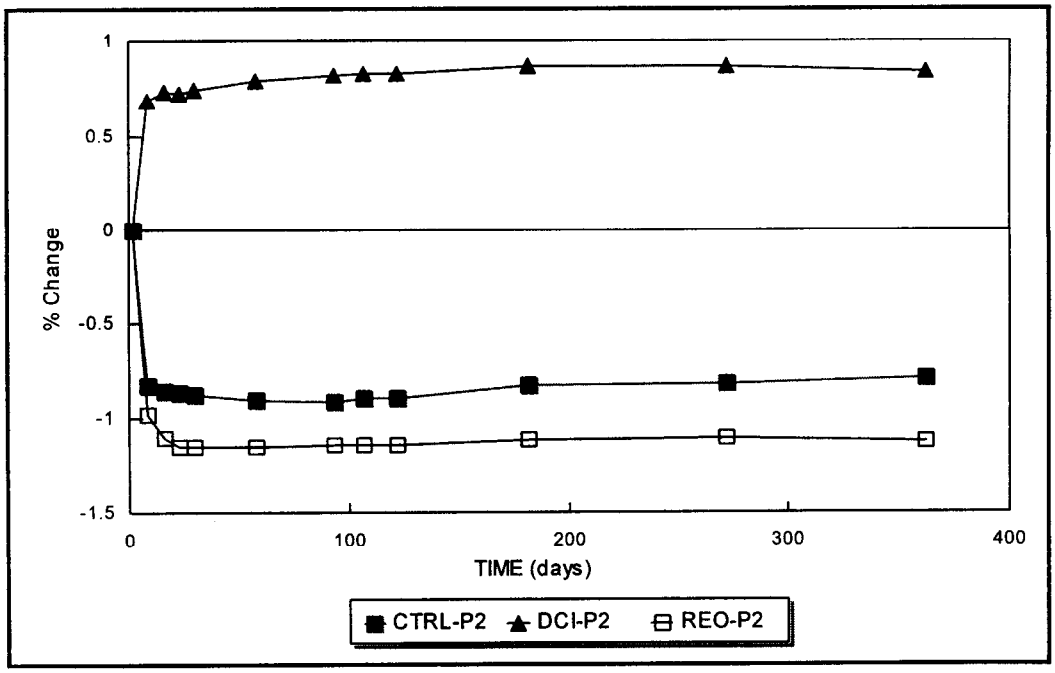

Figure 39(b). Mass change due to sulfate exposure over time for the P2 group.

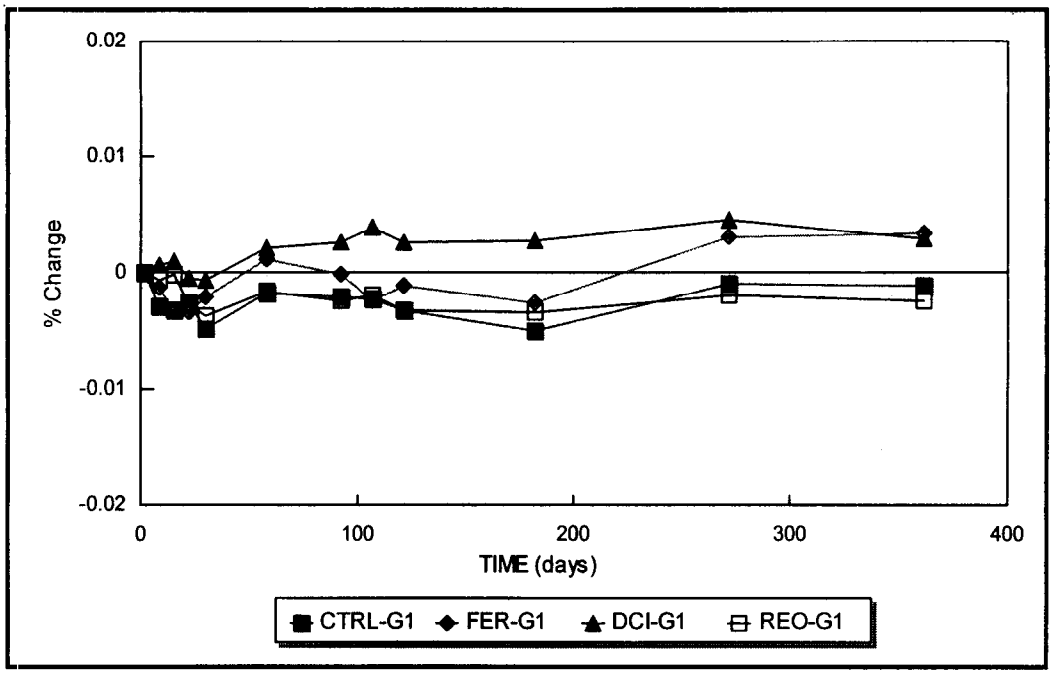

Figure 40(a). Length change due to sulfate exposure over time for the G1 group.

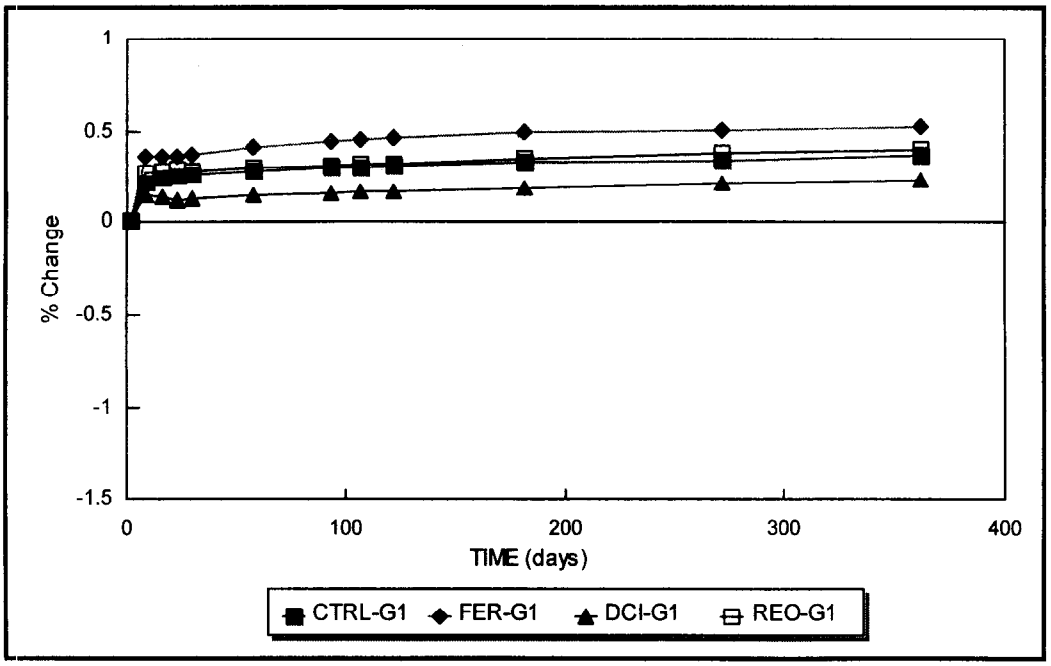

Figure 40(b). Mass change due to sulfate exposure over time for the G1 group.

OBJECTIVE 6 - ESTABLISH SUITABILITY FOR REHABILITATION APPLICATIONS

6.1 Evaluate Alternative Repair Strategies

Twelve specimens were cast using concrete from the P1 group control mix. All specimens are located in the outdoor exposure facility so as to experience the effects of differing temperatures and humidities indigenous to Gainesville, Florida (Figure 41(a)). The object is to pond the specimens with 3 percent sodium chloride solution as shown in Figure 41(b) and allow them to corrode and spall naturally as part of their conditioning. Once all specimens have spalled, they will be repaired using concrete batched with the original mix design. However, four specimens will be repaired with calcium nitrite-based inhibitor (DCI-S) admixed, four specimens will be repaired with organic vapor-phase corrosion inhibitor (FerroGard 903) admixed, and the remaining four specimens will be repaired as controls. Testing will begin as saltwater ponding resumes. Currently, all specimens are still in the conditioning stage, with approximately 50 percent of specimens showing signs of corrosion.

6.2 Test Field Repairs and Long-Term Assessment

Testing performed on an experimental bridge cap located on State Road 60 over Tampa Bay revealed that no active corrosion was in progress at the time. Further studies of this site are planned.

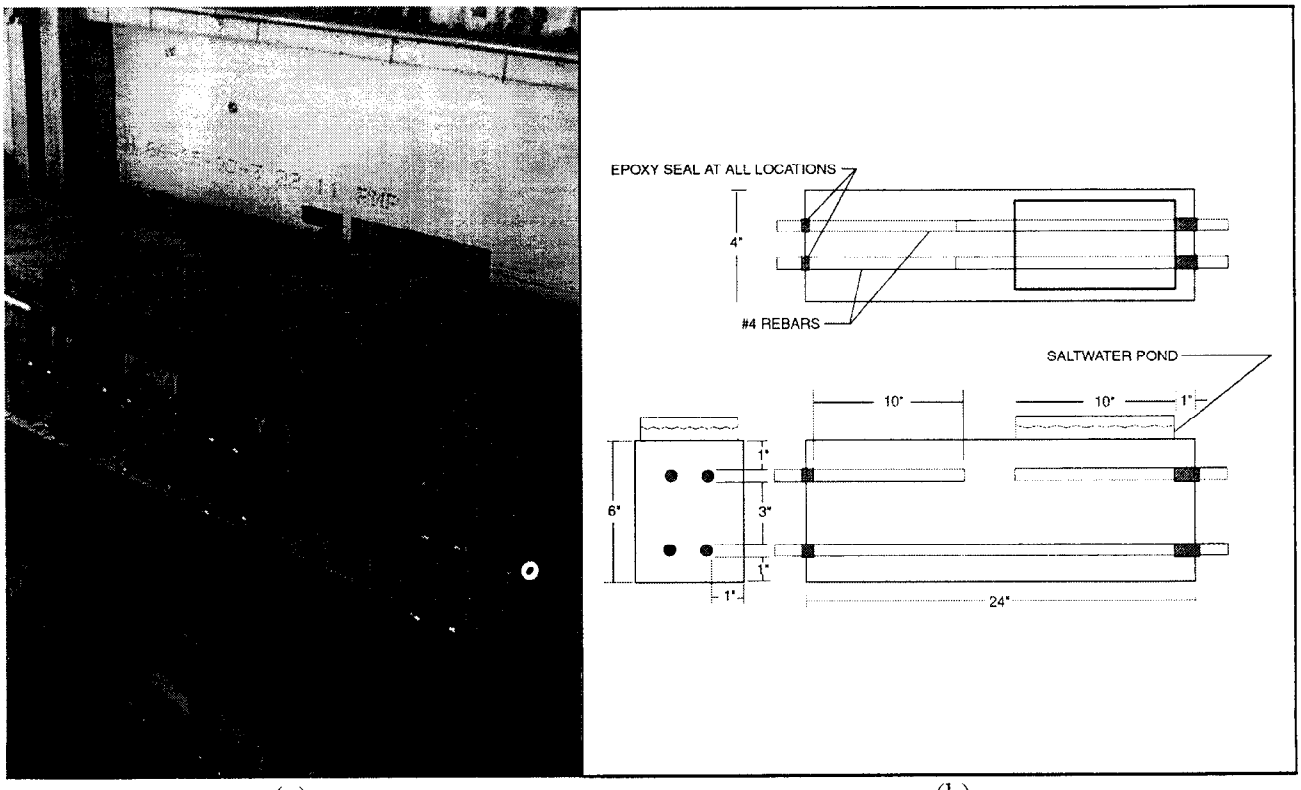

(a) (b)

Figure 41. Sheltered outdoor specimens.

CONCLUSIONS

1. The procedure to determine nitrite content in hardened concrete has been well established; nearly 100 percent nitrite recovery was achieved.

2. A 70- percent to 80- percent recovery of FerroGard 901 using UV absorption at 224 nm from concrete and mortar samples has been achieved.

3. Autopsy of 17-year-old reinforced concrete slabs prepared in a former FHWA investigation and exposed to weathering indicated that calcium nitrite is chemically stable in the concrete environment, as expected also from theoretical calculations. In slabs that retained physical integrity, there was spatial internal redistribution of the nitrite but much of it remained in place. There was significant nitrite loss in some high-chloride content slabs where crumbling of the concrete cover took place due to corrosion damage. That condition is thought to have facilitated nitrite loss by leaching during weathering.

4. The apparent diffusion coefficient of nitrite in OPC concrete (w/c=0.41) was ~2.0 x 10^{-8} cm^2/sec. The diffusivity of nitrite decreased with a lower w/c ratio of concrete, extended curing, fly ash addition as cementitious replacement, or lower temperature.

5. Preliminary results showed that the apparent diffusivity of the detectable species within FerroGard 901 was on the order of 5 x10^{-9} cm^2/sec.

6. Both the ISL and the PWE methods indicated that nitrite experienced approximately linear binding in concrete and mortar. When admixed as calcium nitrite, the ratio between bound nitrite to free nitrite was ~7. The ratio was much lower for nitrite when admixed as sodium nitrite.

7. For a typical DCI-S dosage of 22 L/m^3 in concrete, free nitrite in pore water was ~0.2 M.

8. Addition of DCI-S into concrete lowered the pore solution pH. The reduction was roughly proportional to the total nitrite content. Precipitation of calcium hydroxide upon introduction of calcium nitrite (from DCI-S) quantitatively explained this phenomenon.

9. Cyclic polarization tests were performed on reinforcing steel in simulated concrete pore solution containing chloride in excess of nitrite, to reveal behavior under low-dosage conditions. Addition of nitrite as calcium nitrite (DCI-S) under those conditions modestly raised the pitting and repassivation potentials. Addition of sodium nitrite to similar molar levels resulted in a strong increase of both potentials. The difference was ascribed to reduction of pH upon addition of the calcium salt, but not of the sodium salt.

10. In open-circuit immersion tests in calcium hydroxide solutions containing chloride, DCI-S provided better corrosion inhibition than the other products examined.

11. Three-bar reinforced concrete specimens with DCI-S, exposed to chloride, showed extended TCI and time to cracking, compared to controls without inhibitor. This observation was in agreement with non destructive electrochemical measurements during exposure.

12. Three-bar specimens with FerroGard 901 exposed similarly as the DCI-S specimens showed only modest indications of corrosion protection. Under the test conditions used the Rheocrete 222+ specimens showed little evidence of effective corrosion protection.

13. No conclusions can be determined from the chloride concentrations.

14. Tests with three-bar specimens indicated significant reduction in protection when the DCI-S dosage was reduced by 1/2. No appreciable changes from the full-dosage performance were observed for the other two inhibitors when the dosage was reduced by 1/2.

15. There was poor correlation between concrete chloride contents determined in selected three-bar specimens and the onset and development of corrosion in peer group specimens. Sources of uncertainty, to be examined in subsequent work, may include variability in the location of corrosion initiation and non-uniform chloride penetration. The results available to date are not sufficient to discern any effect on chloride penetration from the presence of any of the three inhibitors tested.

16. The addition of corrosion inhibitors resulted in small (FerroGard 901, Rheocrete 222+) to moderate (DCI-S) increases in RCP charge measurements in wet-cured concretes.

17. The presence of inhibitor resulted in only modest reductions of concrete resistivity (in wet concretes) in the higher permeability concrete tested. For the less permeable concretes (those with pozzolanic additions), the presence of DCI-S caused about 1/3 resistivity reduction at full dosage while the effect of the other inhibitors was smaller.

18. Impressed current tests at constant driving potential in "lollipop" specimens showed lower times to cracking in the DCI-S specimens than in those of the other inhibitors. It is expected that this behavior reflects the lower resistivity of the concrete with DCI-S.

19. There was little difference between the compressive strengths of concrete mixes containing any of the three corrosion inhibitors and their respective inhibitor-free controls. Rheocrete 222+ mixes were the only ones showing a consistent but small loss of compressive strength compared to that of the controls.

20. There appears to be no appreciable difference between the sulfate resistance of mixes containing any of the inhibitors and their respective controls.

REFERENCES

1. A. M. Rosenberg and J. M. Gaidis, *Materials Performance*, Vol. 18, No. 11, pp. 45-48, 1979.
2. R. Pyke and M. Cohen, *J.Electrochem. Soc*, Vol. 93, No. 3, pp. 63-78, 1948.
3. APHA-AWWA-WPCF, *Standard Methods for the Examination of Water and Wastewater*, 17th Ed., L. Clesceri et al., Eds., American Public Health Association., Washington DC, 1989.
4. W. Medford and M. Leming, "Results of Testing Calcium Nitrite Content in Hardened Concrete," State of North Carolina Department of Transportation and North Carolina State University, 1994.
5. R. Powers, A. A. Sagüés, W. Cerlanek, C. Kasper, and L. Li, "Time to Corrosion of Reinforcing Steel in Concrete Containing Calcium Nitrite," U.S. Department of Transportation, FHWA Publication No. FHWA-RD-99-145, McLean, VA, October 1999.
6. L. Li, A. A. Sagüés, and N. Poor, *Cement and Concrete Research,* Vol. 29, pp. 315-321, 1999.
7. A. A. Sagüés, E. I. Moreno, and C. Andrade, *Cement and Concrete Research,* Vol. 27, p. 747, 1997.
8. Canadian Patent #1258473. CORTEC Corporation filed on 1-5-1989.
9. A. Welle, J.D. Liao, K. Kaiser, M. Grunze, U. Mader, and N. Blank, *Applied Surface Science*, Vol. 119, pp. 185-198, 1997.
10. C.R. Brundle, M. Grunze, U. Mader, and N. Blank, "Detection and Characterization of Dimethylethanolamine-Based Corrosion Inhibitors at Steel Surfaces. I. The Use of XPS and ToF-SIMS," *Surface and Interface Analysis*, Vol. 24, pp. 549-563, 1996.
11. D. Bjegovic, L. Sipos, V. Ukrainczyk, and B. Miksik, "Diffusion of the MCI 2020 and 2000 Corrosion Inhibitors into Concrete" in *Corrosion and Corrosion Protection of Steel in Concrete*, Vol. 2. R. N. Swamy, Ed., Sheffield Academic Press Ltd., Sheffield, pp. 865-877, 1994.
12. U. Maeder, "A New Class of Corrosion Inhibitors" in *Corrosion and Corrosion Protection of Steel in Concrete*, Vol. 2. R. N. Swamy, Ed., Sheffield Academic Press Ltd., Sheffield, pp. 851-864, 1994.
13. J. Goschnick,"Investigations of the Transport of Amino Alcohol-Based Corrosion Inhibitors Through Concrete – A Final Report," Forschungszentrum Karlsruhe, Institut fur Radiochemie, 20 October 1995.
14. I. L. Rosenfeld, *Corrosion Inhibitors*, McGraw-Hill Inc., New York, p. 167, 1981.
15. American National Standard Institute, "Measurement of the Leachability of Solidified Low-Level Radioactive Wastes by a Short-Term Test Procedure," ANSI/ANS-16.1-1986, American Nuclear Society, La Grange Park, IL, 1986.
16. H. Liang, Master's Thesis, University of South Florida, Tampa, FL, April 1999.
17. P. B. Bamforth, *Magazine of Concrete Research*, Vol. 51, pp. 87-96, 1999.
18. S. Goni, M. Hernandez, A. Guerrero, and M. P. Lorenzo, *Construction and Building Materials*, Vol. 10, p. 171, 1996.
19. J. W. Mellor, *Supplement to Mellor's Comprehensive Treatise on Inorganic and Theoretical Chemistry*, Vol. VIII, Suppl. II, Nitrogen (Part II), p. 353, J. Wiley, NY, 1967.
20. J. Seinfeld and S. Pandis, *Atmospheric Chemistry and Physics*, p. 340, J. Wiley, NY, 1998.
21. W. L. Jolly, *The Inorganic Chemistry of Nitrogen*, p. 69, W. A. Benjamin, NY, 1964.
22. N. Berke and K. Sundberg, "The Effects of Calcium Nitrite and Microsilica Admixtures on Corrosion Resistance of Steel in Concrete," SP 122-15, Paul Klieger Symposium, p. 265, American Concrete Institute, Detroit, MI, 1989.

23. A. M. Rosenberg, J. M. Gaidis, T. G. Kossivas, and R. W. Previte, "A Corrosion Inhibitor Formulated with Calcium Nitrite for Use in Reinforced Concrete," in *Chloride Corrosion of Steel in Concrete*, ASTM STP 629, D. E. Tonini and S. W. Dean, Eds., American Society for Testing and Materials, pp. 89-99, 1977.
24. L. Li and A. A. Sagüés, "Effect of Chloride Concentration on the Pitting and Repassivation Potentials of Reinforcing Steel in Alkaline solutions," Paper No. 99567, *Corrosion/99*, NACE International, Houston, TX, p. 11, 1999.
25. L. Li and A. A. Sagüés, "Chloride Corrosion Threshold of Reinforcing Steel in Alkaline Solutions - Open-Circuit Immersion Tests," *Corrosion*, Vol. 57, pp. 19-28, 2001.
26. *Handbook of Chemistry & Physics*, 56th Ed., CRC Press, Boca Raton, FL, p.B-82, 1975-1976.
27. S. S. Zumdahl, *Chemistry*, 2nd Ed., D.C. Heath and Co., Lexington, MA, p. 709, 1989.
28. A. A. Sagüés, "Corrosion Measurement Techniques for Steel in Concrete," Paper No. 353, *Corrosion/93*, NACE International, Houston, TX, p. 22, 1993.
29. D. A. Jones, *Principles and Prevention of Corrosion*, 2nd Ed., Prentice Hall, Upper Saddle River, NJ, 1996.
30. A. A. Torres-Acosta and A. A. Sagüés, "Concrete Cover Cracking with Localized Corrosion of Reinforcing Steel," in *Proceedings of the Fifth CANMET/ACI International Conference on Durability of Concrete*, SP-192, V. M. Malhotra, Ed., American Concrete Institute, Farmington Hills, MI, p. 591, 2000.
31. W. Morris, E. Moreno, and A. A. Sagüés, *Cement and Concrete Research*, Vol. 26, No. 12, pp. 1779-1787, 1996.
32. N. S. Berke and M. C. Hicks, "Estimating the Life Cycle of Reinforced Concrete Decks and Marine Piles Using Laboratory Diffusion and Corrosion Data," in *Corrosion Forms and Control for Infrastructure*, ASTM STP 1137, V. Chaker, Ed., American Society for Testing and Materials, Philadelphia, PA, pp. 207-231 1992.
33. Florida Department of Transportation, "An Accelerated Laboratory Method for Corrosion Testing of Reinforced Concrete Using Impressed Current," *Manual of Florida Sampling and Testing Methods*, FM 5-522, 1993.

APPENDIX 1

NITRITE RECOVERY CALCULATION

Nitrite, extracted from a powdered concrete sample (which has been previously drilled from a concrete specimen), is first converted to the amount of nitrite per gram of as-drilled concrete, and then further converted to the amount of nitrite per gram of oven-dry concrete. To accurately calculate recovery, this amount should be compared to the amount of nitrite admixed per gram of the same concrete if it were oven dried, as follows.

The evaporable water content of the powdered sample can be obtained by drying a known amount of the powdered sample in a 105 °C oven to a constant weight. For the purposes of these analyses the water content b is defined as the difference between the original weight and the dry weight of the powdered sample divided by the dry weight of the powdered concrete:

$$b = \frac{W_o - W_d}{W_d} \cdot 100\% \qquad \text{(A1-1)}$$

where

b = % (evaporable) water in powdered sample
W_o = original weight of the powdered sample
W_d = oven-dry sample weight

From the mix design, the amount of nitrite per gram of as-mixed concrete is known. This amount can be approximately converted to the amount of nitrite per gram of the same concrete if it were oven dried. The weight of this hypothetical oven-dry concrete expressed as a percentage a of the as-mixed concrete can be estimated by Equation A1-2, assuming that any nonhydrated water is evaporable [A1-1]:

$$a = \frac{W_t - W_w - (AC)_{CA} \cdot W_{CA} - (AC)_{FA} \cdot W_{FA} + 0.24 \cdot W_c \cdot \alpha}{W_t} \cdot 100\% \qquad \text{(A1-2)}$$

where

W_t = total weight of the as-mixed concrete
W_w = weight of water in the concrete mix
W_{CA} = weight of coarse aggregate in the concrete mix
$(AC)_{CA}$ = absorption capacity of the coarse aggregate
W_{FA} = weight of fine aggregate in the concrete mix
$(AC)_{FA}$ = absorption capacity of the fine aggregate
α = degree of cement hydration
W_c = weight of cement in the concrete mix

Finally the nitrite recovery is equal to the amount of measured nitrite per gram of oven-dry concrete (obtained from the extraction) divided by the amount of admixed nitrite per gram of hypothetical oven-dry concrete calculated from the mix design and application of Equation A1-2.

For example, using 2.00 g of a powdered concrete sample from cylinder C1 (Table 1), after extraction the final volume of extracting solution is 500.0 mL, the dilution factor is 25.0, and the

absorbance of this final dilution is measured to be 0.3462. The extracted nitrite amount in this sample is calculated by:

$$\frac{0.3462}{0.913} \cdot 25.0 \cdot 0.500 = 4.74 \text{ mg extracted } NO_2^-$$

where

0.913 = spectrophotometric calibration factor, L/mg

A 1.0453-g sample of the same powdered concrete is oven dried, and the measured dry weight of this sample is 1.0200 g. The water content of this sample can be calculated by:

$$\frac{1.0453 - 1.0200}{1.0200} \cdot 100\% = 2.48\%$$

and the measured amount of nitrite per gram of oven-dry concrete can be calculated by:

$$\frac{4.74}{2.000 \cdot (1 - 0.0248)} = 2.43 \text{ mg of } NO_2^-/\text{g of oven-dry concrete}$$

For the calculations shown below, the absorption capacities of the limestone coarse aggregate and sand fine aggregate were assumed to be 4.5% and 0.5%, respectively, based on the properties of the typical materials used in this laboratory. The degree of hydration was assumed to be 0.65, and is consistent with values reported by Mindess and Young.[A-1] (Substituting 0.50 or 0.75 as the degree of hydration changes the result of average recovery to 99% and 101%, respectively, less than one standard deviation). The weight of the hypothetical oven-dry concrete expressed as a percentage of the as-mixed concrete is obtained by:

$$a = \frac{2390 - (167 + 29.14 \cdot 65\% + 1045.5\% + 735 \cdot 0.5\%) + 0.24 \cdot 414 \cdot 0.65}{2390} \cdot 100\%$$

$$= 92.8\%$$

As noted in Table 1, the amount of admixed nitrite was 2.46 mg of NO_2^-/g of as-mixed concrete, so the amount of nitrite per gram of hypothetical oven-dry concrete is calculated by:

$$\frac{2.46}{92.8\%} = 2.65 \text{ mg of } NO_2^-/\text{g of hypothetical oven-dry concrete}$$

Finally the nitrite recovery is calculated by:

$$\frac{2.43}{2.65} \cdot 100\% = 91.7\%$$

Reference:

A-1. S. Mindess and J. F. Young, *Concrete*, Prentice-Hall, Inc.,Upper Saddle River, NJ, p. 103 1981.

APPENDIX 2

APPARENT DIFFUSION COEFFICIENT CALCULATIONS

Value of D1:

The calculation based on the slope of the CFL vs. $t^{1/2}$ curve at early times (yielding the value D1) is illustrated for the data for specimen of DCI-C2-1, test #2 in Figure 3.

The slope for $0.02 < CFL < 0.2$ was calculated by least-square-error fit of the data for that interval, yielding:

$k \sim 1.17 \times 10^{-4}\ s^{-1/2}$

The specimen dimensions were 15.2 cm diameter, 4.6 cm height.

Surface area $S = 2 \times \pi \times (15.2)^2/4 + \pi \times 15.2 \times 4.6 = 583\ cm^2$
Volume $V = \pi \times (15.2)^2 / 4 \times 4.6 = 833\ cm^3$
$S/V = 0.7\ cm^{-1}$

Per Eq. (2): $D1 = \pi \times (1.17 \times 10^{-4}\ sec^{-1/2}/2)^2 \times (1 / 0.7\ cm^{-1})^2 = 2.19 \times 10^{-8}\ cm^2/s$

(reported as $2.2 \times 10^{-8}\ cm^2/s$)

Value of D2:

This calculation is illustrated for the data from specimen 6 (DCI-P1-1 in synthetic seawater) in Figure 4. In this case CFL > 0.2, and the result is obtained using Eq.(3) and designated as D2.

Specimen dimensions were 7.6 cm diameter (d), 2.5 cm height (l).

Ratio l/d = 0.33

at $t = 7.8 \times 10^6$ s, CFL = 0.208

Value of G from Table 1 in Reference 15, for l/d=0.33 and CFL = 0.208 (rounded off to 0.21), obtained by interpolation: $G \sim 3.8 \times 10^{-4}$

Per Eq. (3): $D2 = 3.87 \times 10^{-4} \times (7.6)^2 / (7.8 \times 10^6)\ cm^2/s = 2.8 \times 10^{-9}\ cm^2/s$

APPENDIX 3

PORE WATER NITRITE CONTENT EXAMPLE CALCULATION

Evaluations of nitrite content in the pore water were made by assuming that in specimens equilibrated to a nearly 100% RH environment the capillary pores were completely filled with water. Of the total nitrite admixed, only a fraction was found to be present in the pore water. Concrete specimens with admixed 5.8 kg of nitrite ion per m^3 of concrete were found to contain pore water with a nitrite concentration of 0.2 M. The molar concentration in the pore water was found to be approximately proportional to the total admixed amount, an indication that nitrite binding is approximately linear in nature.

If one assumes that the capillary porosity of concrete is $\varepsilon = 0.1$, then 1 m^3 of concrete would contain 100 L of pore water. As the molecular weight of the nitrite ion is 46, the 0.2 M in the above example corresponds to 0.046 kg/mol x 0.2 mol/L x 100 L/m^3 concrete = 0.92 kg nitrite / m^3 of concrete. Since the admixed amount was 5.8 kg / m^3, only (0.92/5.8) x 100 ~ 16 % or about 1/6 of the nitrite was estimated to be present as free nitrite in the pore water . The remaining 4.88 kg/m^3, or about 5/6 of the total admixed amount, is considered to be bound elsewhere in the concrete. This is only a rough calculation as it strongly depends on the assumed value for ε. Thus if ε were 0.15 instead of 0.1, the estimated fractions of free and bound nitrite would have been about ¼ and ¾ respectively.

HRDI-09/2-02(674)E